# Development of placental ultrasound markers to screen for the term, small for gestational age (SGA) baby

**Sally L. Collins**

**BSc, BMBCh, MRCOG**

Jesus College




A thesis submitted for the degree of Doctor of Philosophy

to the Faculty of Medical Sciences, University of Oxford.

Michaelmas Term 2011

# Development of placental ultrasound markers to screen for the term, small-for-gestational-age (SGA) baby

**Sally L. Collins**

Jesus College, University of Oxford

## Abstract

Fetal growth restriction is the largest single risk factor for stillbirth, one of the biggest issues in modern day obstetrics. This study aimed to identify ultrasound markers to aid the development of a screening test for growth restriction. Data were acquired from 143 pregnancies. Of these; 113 were normotensive and delivered appropriate for gestational age (AGA) babies at term; 13 women were normotensive with term small for gestational age (SGA) babies, five were hypertensive with term SGA babies and two had pre-term SGA babies.

A technique examining the jet of blood from the mouth of the spiral artery (SA) is described and validated. As predicted histologically in the literature, the size of the SA mouth increased, and the jet pulsatility decreased, with advancing gestation. The waveform developed differently in SGA pregnancies. The study also describes the novel observation of mega-jets, a potential surrogate marker for placentation.

Only before 14 weeks' gestation could the whole placental volume be reliably captured in a single sweep. A novel semi-automated method for generating placental volume (PlaV), total surface area and area of the basal plate was used in a study for the first time. The dimensionless standardized placental volume (*s*PlaV) was explored and shown to predict SGA, independent of PAPP-A. A model developed by combining *s*PlaV and PAPP-A performed well, especially in a low risk population, (50% sensitivity for a 10% false positive rate).

The 3 dimensional (3-D) power Doppler data gathered in this study enabled the effect of gain on calculated Virtual Organ Computer-aided AnaLysis II (VOCAL II™) indices to be examined *in vivo.* This suggested that the use of the sub-noise gain setting might help to standardise the information gained for each subject, which should improve between patient comparisons.

We conclude that the development of a screening test for SGA including *s*PlaV may be possible. Development of other markers may further improve the test. This should ensure appropriate antenatal care for 'at risk' pregnancies whilst keeping the normal ones, 'normal'.

# Acknowledgements

So many people have helped to make the last three years an enjoyable experience that I am not sure where to start, but I think it should be with my two ever-patient supervisors, Lawrence Impey and Alison Noble. Without their encouragement, good-humour and hard work this project would never have happened. A special mention has to go to Lawrence not only for remaining patient and helpful when I hunted him down with questions and problems, but for never taking offence when receiving 'one of those looks'.

I am grateful to the Oxford Biomedical Research Centre and Stephen Kennedy, Head of the NDOG, for funding my research, and also to my NDOG mentor, Aris Papageorghiou, for all his help and advice.

The work contained in this thesis would not have been possible without the image analysis research carried out by my partner in crime, Gordon Stevenson. His relentless positivity, superb ideas and down right hard work brought the tools needed into being, making much of this research possible. I remain very much in his debt and look forward to our next project together.

I appreciate the patience of all the staff of the ultrasound department and fetal medicine unit at the John Radcliffe Hospital who helped me to learn to scan and recruit my participants. A special mention must go to Katie Blissett and Libby Searle. A huge thank you to Jacqueline Birks for all her statistical input and considerable patience, and Robert Whittaker for his emails clearly explaining maths to an obstetrician. Thank you also to; Annie Roberts for always receiving the long lists of names so cheerfully; Bronwen Meredith for her fabulous secretarial (and emotional) support and Alec Welsh for generously offering help and advice to a D.Phil. student who cornered him at a conference.

Last, but never least, thank you to all the friends and family who have supported me and given me so much encouragement including; Rebecca Black, Alex Brooks, Lisa Buck, Pat Collins, Ann Collins, Ana De La Concepcion Fernandez, Christos Ioannou, Ingrid Granne and Geraldine Thimbleby. The biggest thank you of all must go to my wonderful family; my husband, David Reynard, who has helped with everything from maths to proof reading, and my daughters Lexi & Bea, who haven't complained about the time Mummy has spent locked away with a laptop. As promised girls, Mummy's finished.

# Table of contents

**ABSTRACT** ..... **2**

**ACKNOWLEDGEMENTS** ..... **3**

**TABLE OF CONTENTS** ..... **4**

**LIST OF FIGURES** ..... **10**

**LIST OF TABLES** ..... **14**

**LIST OF ABBREVIATIONS** ..... **16**

**1 INTRODUCTION** ..... **18**

**1.1 The significance of fetal growth restriction (FGR)** **18**

1.1.1 Implications, definition and diagnosis of FGR ..... 18

1.1.2 The definition of growth restriction chosen for this study ..... 22

1.1.3 Causes of growth restriction ..... 22

1.1.4 Utero-placental insufficiency leading to FGR ..... 23

**1.2 Screening for growth restriction** **24**

1.2.1 Why screen for FGR? ..... 24

1.2.2 Current methods for assigning risk of FGR ..... 25

1.2.3 Potential methods for assigning risk of FGR ..... 26

1.2.4 Screening for FGR: The future ..... 29

**2 HYPOTHESES AND AIMS OF THE THESIS** ..... **30**

**2.1 Hypotheses 30**
2.1.1 Inadequate spiral artery conversion ..... 30
2.1.2 Placental volume (PlaV) ..... 31
2.1.3 Abnormal placental morphology ..... 31
2.1.4 3-D Power Doppler ..... 32

**2.2 Aims of this thesis 33**

**2.3 Publications arising from this work 34**
2.3.1 Publications in peer-reviewed journals ..... 34
2.3.2 International Research Awards ..... 35
2.3.3 Oral presentations at international conferences ..... 35
2.3.4 Poster presentations at international conferences ..... 36

**3 THE 'SPIRAL 3-D' STUDY ..... 37**

**3.1 Aims of this chapter 37**

**3.2 Ethical review 37**

**3.3 Methods: Data Collection – Phase I 37**
3.3.1 Participants ..... 37
3.3.2 Ultrasound data collected: 2-D ..... 38
3.3.3 Uterine artery measurement ..... 39
3.3.4 Ultrasound data collected: 3-D ..... 47
3.3.5 Post delivery data collection ..... 49

**3.4 Methods: Data Collection – Phase II 49**
3.4.1 Participants ..... 50
3.4.2 Ultrasound data collected: 2-D ..... 50
3.4.3 Ultrasound data collected: 3-D ..... 50

3.4.4 Post delivery data collection ..... 50

**3.5 Methods: Statistical analyses 51**

**3.6 General results and patients outcomes 52**

3.6.1 Phase I ..... 52

3.6.2 Phase II ..... 56

3.6.3 Complete results (Phase I and II) ..... 57

**4 OBSERVATIONS IN PLACENTAL ANATOMY AND SGA ..... 61**

**4.1 Introduction, background and aims 61**

4.1.1 Histological anatomy of the utero-placental interface ..... 61

4.1.2 Characterising the spiral artery blood flow *in vivo* ..... 63

4.1.3 Aims of this chapter ..... 68

**4.2 Methods 69**

4.2.1 General methods for measurement of the jets and uterine arteries .. 69

4.2.2 Jets: Intra- and inter-observer variability analysis ..... 69

4.2.3 Statistical methods ..... 70

**4.3 Results 74**

4.3.1 Measurement of the jets ..... 74

4.3.2 Jets: Intra-observer and inter-observer variability analysis ..... 75

4.3.3 Spiral artery jet and uterine artery waveforms ..... 76

4.3.4 Spiral artery jet waveform differences in SGA pregnancies ..... 80

4.4.1 Changes in size and velocity of the jets ..... 86

4.4.2 Mega-Jets ..... 91

4.4.3 Placental lakes ..... 94

**4.5 Discussion 99**

4.5.1 Intra-observer and inter-observer variability ..... 100

4.5.2 Spiral artery jet and uterine artery waveforms ..... 101

4.5.3 Spiral artery jet waveform differences in SGA babies ..... 102

4.5.4 Changes in size and velocity of the jets ..... 105

4.5.5 Mega-jets ..... 107

4.5.6 Placental lakes ..... 108

**5 PLACENTAL SHAPE AND VOLUME ..... 110**

**5.1 Introduction, background and aims 110**

5.1.1 Placental volume ..... 110

5.1.2 Morphometric measurements ..... 112

5.1.3 Previously employed methods for placental volume estimation ..... 114

5.1.4 A new semi-automated placental segmentation technique ..... 116

5.1.5 Aims of this chapter ..... 120

**5.2 Methods 121**

5.2.1 Placental volume with advancing gestation ..... 121

5.2.2 Placental volume in SGA pregnancies ..... 121

5.2.3 Morphometric measurements in SGA pregnancies ..... 122

5.2.4 Combined screening model for SGA ..... 125

**5.3 Results 126**

5.3.1 Placental volume with advancing gestation ..... 126

5.3.2 Placental volume in SGA pregnancies ..... 129

5.3.3 Morphometric measurements in SGA pregnancies ..... 131

5.3.4 Combined screening model for SGA ..... 133

**5.4 Discussion 138**

5.4.1 Novel, semi-automated process ..... 138

5.4.2 Optimal gestation for a placental volume screening test ..... 138

5.4.3 Controlling for gestation in the potential screening test ..... 139

5.4.4 The use of a dimensionless index - *s*PlaV ..... 140

5.4.5 Early placental morphology ..... 141

5.4.6 Calculating a model to predict SGA ..... 141

5.4.7 Limitations ..... 143

**6 3-D POWER DOPPLER STUDIES ..... 146**

**6.1 Introduction and background 146**

6.1.1 Factors affecting power Doppler results ..... 147

6.1.2 Power Doppler gain setting ..... 148

6.1.3 Fetal and maternal circulations ..... 149

6.1.4 Aims of this chapter ..... 150

**6.2 Methods 150**

6.2.1 Data collection ..... 150

6.2.2 Data analysis - the whole placenta ..... 151

6.2.3 Data analysis – separate fetal and maternal samples ..... 152

6.2.4 Data analysis – calculations and statistics ..... 154

**6.3 Results 155**

**6.4 Discussion 160**

**7 GENERAL DISCUSSION ..... 164**

**7.1 Summary of principal new findings 164**

**7.2 Limitations 165**

7.2.1 Definition of fetal growth restriction ..... 165

7.2.2 Study size ..... 166

7.2.3 Vessel selection ..... 167

7.2.4 Recruitment strategy ..... 167

7.2.5 Measurements with Doppler ..... 168

**7.3 Future work 168**

7.3.1 Confirmation of technique ..... 168

7.3.2 Vascular volume ..... 168

7.3.3 Development of a screening test ..... 169

**REFERENCES ..... 171**

**8 APPENDICES ..... 186**

**8.1 Patient information leaflet provided 186**

**8.2 Ultrasound machine settings used 191**

**8.3 Segmentation Protocol 192**

**8.4 Assessment of Normality 195**

# List of figures

Figure 1: Placement of the Doppler gate at the mouth of the spiral artery where the jet enters the intervillous space. ..... 40

Figure 2: Typical jet waveform, unidirectional flow. ..... 40

Figure 3: Correct placement of the calipers for jet width and length ..... 43

Figure 4: Incorrect placement of the calipers for jet width and length. ..... 43

Figure 5: An example of a placental lake. ..... 44

Figure 6: A mega-jet terminating in a placental lake. ..... 45

Figure 7: Showing the decreasing velocity and pulsatility of a mega-jet with placing the pulse wave gate at increasing distances from the opening into the IVS. ..... 46

Figure 8: Pregnancy outcomes for Phase I of the study. ..... 53

Figure 9: Distribution of the customised birth weight centiles ..... 56

Figure 10: Pregnancy outcomes for all participants in the study (Phase I and II). ..... 57

Figure 11: Reconstruction of the spiral arteries at various stages of pregnancy. ..... 63

Figure 12: Diagram demonstrating the anatomy of the spiral artery jets. ..... 64

Figure 13: Percentage of participants with three jets measured at each visit. . 78

Figure 14: Percentage of participants with pulsatile jets at each visit. ..... 78

Figure 15: The relationship between the RI of the jets and gestation. ..... 79

Figure 16: The relationship between a) the mean RI and b) the minimum value for RI of the uterine arteries, and gestation.[13] ..... 79

Figure 17: The change in PI and RI for the jets of SGA pregnancies compared with AGA. ..... 82

Figure 18: The change in PI and RI for the uterine arteries of SGA pregnancies compared with AGA. ..... 83

Figure 19: Difference in the mean PI and RI of the jets between the first and last visit. ..... 85

Figure 20: Jet mouth width for women with normal pregnancy outcomes. ..... 87

Figure 21: Jet length in mm, for women with normal pregnancy outcomes. .... 87

Figure 22: Jet peak systolic velocity in cm/s, for women with normal pregnancy outcomes..... 88

Figure 23: Percentage difference in the mean mouth width and peak systolic velocity of the jets between the first and last visit. ..... 89

Figure 24: The change in size of the jet mouths, lengths and velocity of SGA compared with AGA pregnancies. ..... 90

Figure 25: Breakdown of phase I patients for analysis of mega-jets. ..... 91

Figure 26: Frequency distribution of the length measured of the most prominent jets measured at 23 to 24 weeks' gestation ..... 92

Figure 27: Percentage of women with mega-jets and placental lakes. ..... 93

Figure 28: Kaplan-Meir survival function for the appearance of mega-jets in SGA and AGA babies. ..... 94

Figure 29: Breakdown of phase I patients included in analysis placental lakes. ..... 95

Figure 30: Breakdown of phase I and II participants included in analysis of placental lakes. ..... 95

Figure 31: Percentage of women seen to have placental lakes in phase I and II. ..... 97

Figure 32: The number of women with mega-jets and lakes (n=47). ..... 98

Figure 33: Example of generating a placental volume in VOCAL™. ..... 114

Figure 34: Illustration of Random Walker segmentation of a placenta. ..... 118

Figure 35: Bland Altman plots – (a) new method vs. manual for Observer 1 (b) – new method vs. Manual for Observer 2. ..... 119

Figure 36: Demonstrating a) the masking process to generate b) the area of the basal plate. ..... 122

Figure 37: Percentage of participants in whom the whole placenta could be captured in a single volume. ..... 127

Figure 38: Kaplan-Meier for capture of the whole placenta. ..... 127

Figure 39: Placental volume for each participant between 11 and 13+6 weeks. ..... 128

Figure 40: Screening receiver-operating characteristics curves for prediction of all cases of SGA in the whole population. ..... 130

Figure 41: Screening receiver-operating characteristics curves for prediction of all cases of SGA in the whole population. ..... 132

Figure 42: Screening receiver-operating characteristics curves to predict all SGA in the whole population. ..... 136

Figure 43: Screening receiver-operating characteristics curves to predict term, normotensive SGA babies. ..... 137

Figure 44: Screening receiver-operating characteristics curves to predict SGA in a population deemed to be ‘low risk’ at booking. ..... 137

Figure 45: Screening receiver-operating characteristics curves to predict all severe SGA (<5th centile) in the whole population. ..... 145

Figure 46: The sphere used to ensure identical regions of interest (ROI) are sampled for each volume at different gain settings. ..... 153

Figure 47: Influence of gain on the fetal vascular image. ..... 156

Figure 48: The effect of changing the PD gain on VOCAL™ indices. ..... 158

Figure 49: Demonstrating the correlation between BMI and the individualised SNG setting. ..... 159

Figure 50: Two different seedings of the same 2D image. ..... 192

Figure 51: Seeding when the fetus is close to the placenta. ..... 193

Figure 52: Two different seedings of the same 2D image (poorly demarcated interface). ..... 194

## List of equations

Equation 1: Sphericity. ..... 124

Equation 2: Models generated to predict SGA babies ..... 134

# List of tables

Table 1: Baseline patient demographics of normotensive Phase I participants who delivered at term ..... 54

Table 2: Delivery details of Phase I participants ..... 55

Table 3: Baseline patient demographics of *all participants* (phases I & II) ..... 58

Table 4: Delivery details for *all participants* (phases I & II) ..... 59

Table 5: Baseline patient demographics of *all normotensive participants who delivered at term* (phases I & II) ..... 60

Table 6: Results for Inter-observer reproducibility sub-group analysis of measurement of the three most prominent jets (n=14) ..... 75

Table 7: The correlation coefficients at each visit comparing the mean jet PI/RI to both the mean uterine artery (*meanUt A*) PI/RI and the minimum uterine artery (*minUt A*) PI/RI ..... 77

Table 8: The results for the linear mixed model coefficients with 95% confidence interval for PI and RI over gestation for SGA babies compared to normally grown babies ..... 81

Table 9: Comparison of SGA and AGA pregnancies at the first and last visits for jet PI and RI ..... 84

Table 10: Log rank testing results for the appearance of lakes before 26 weeks in both Phases I and II ..... 97

Table 11: Intra-observer & inter-observer variability by measurement type[19] 119

Table 12: The four dimensionless parameters generated by Buckingham π theorem for the available physical variables ..... 124

Table 13: Log rank testing for the survival functions of the placentas becoming too large to be included in a single volume ..... 128

Table 14: Differences in placental volume and its derived indices between SGA and AGA pregnancies ..... 129

Table 15: Screening performance of PQ, *s*PlaV and Ut A PI ..... 130

Table 16: The results for univariate regression against birth weight for the four dimensionless parameters and sphericity ..... 133

Table 17: Results of univariate linear regression against customised birth weight ..... 134

Table 18: The linear regression analysis comparing the VI, FI & VFI with different gain settings ..... 157

Table 19: Results of the normality analysis for the continuous variables explored to predict SGA ..... 195

# List of abbreviations

| | | | |
|---|---|---|---|
| 2-D | Two-dimensional | IVS | Intervillous space |
| 3-D | Three-dimensional | LI | Lawrence Impey |
| AC | Abdominal circumference | MAP | Mean arterial pressure |
| | | MCA | Middle cerebral artery |
| AFP | Alpha fetoprotein | Mean Ut A | Calculated mean value of uterine arteries |
| AGA | Appropriate for gestational age | Min Ut A | Minimum value of the two uterine artery values |
| APO | Adverse pregnancy outcome | | |
| AUC | Area under the curve in ROC curve analysis | MI | Mechanical index |
| | | NICE | National Institute for Health and Clinical Excellence |
| BMI | Body mass index | | |
| BPA | Basal plate area | | |
| BPD | Bi-parietal diameter | NICU | Neonatal intensive care unit |
| HCG | Human chorionic gonadotropin | | |
| | | OR | Odds ratio |
| CI | Confidence interval | OXMAT | Oxford maternity records database |
| CRL | Crown-rump length | | |
| ECL | Echogenic cystic lesion | PAPP-A | Pregnancy associated plasma protein-A |
| *s*FA | Standardised functional area | | |
| | | PD | Power Doppler |
| FL | Femur length | PET | Pre-eclampsia (Pre- eclamptic Toxaemia) |
| FMBV | Fractional moving blood volume | | |
| | | PI | Pulsatility index |
| FGR | Fetal growth restriction | PIH | Pregnancy-induced hypertension |
| GS | Gordon Stevenson | | |
| HC | Head circumference | PlaV | Placental volume |
| IBME | Institute of Biomedical Engineering | *s*PlaV | Standardised placental volume |
| IUGR | Intrauterine Growth Restriction | PLR | Positive likelihood ratio |
| | | PQ | Placental quotient |

| | | | |
|---|---|---|---|
| PPV | Positive predictive value | SNG | Sub-noise gain |
| PSV | Peak systolic flow velocity | TI | Thermal index |
| | | TSA | Total (placental) surface area |
| RI | Resistance index | | |
| ROC | Receiver-operating characteristics (analysis) | Ut A | Uterine artery |
| | | UK | United Kingdom |
| | | VOCAL™ | Virtual Organ Computer-Aided anaLysis™ |
| SA | Spiral artery | | |
| SC | Sally Collins | | |
| SGA | Small for gestational age | | |

# 1 Introduction

## *1.1 The significance of fetal growth restriction (FGR)*

### 1.1.1 Implications, definition and diagnosis of FGR

Every fetus has an inherent growth potential which, under ideal conditions, will produce a healthy baby the appropriate size given its genetic legacy. Attaining this relies on such factors as a healthy mother, well functioning utero-placental unit and the absence of pathology. If the *in utero* circumstances are less than ideal, this growth potential may not be achieved and fetal well-being may be compromised. The consequences of this are far-reaching. Fetal growth restriction is associated with an increased risk of still-birth (Froen et al. 2004; Gardosi et al. 2005), perinatal mortality (McCowan et al. 2005; Ego et al. 2006; Figueras et al. 2007), pre-term delivery (Morken et al. 2006), cerebral palsy (Jacobsson et al. 2008) and increased morbidity in pre-term neonates (Garite et al. 2004). The health effects can continue into adolescence and adulthood and have been linked with neurological and cardiovascular sequelae (Barker 2006; Barker et al. 2009; Chan et al. 2010).

Since the concept of fetal growth restriction (FGR) was introduced by Lubchenco in the early 1960's (Lubchenco et al. 1963) research into its cause has been fraught with difficulties. This is partly due to the definition, which to this date remains contentious (Resnik 2007; Zhang et al. 2010; Figueras et al. 2011). Historically, authors have incorrectly used the terms fetal growth restriction (FGR), intra-uterine growth restriction (IUGR) and small for gestational age (SGA) synonymously making accurate retrospective studies

and meta-analyses difficult. Growth restriction (FGR or IUGR) implies an underlying pathology 'restricting' the potential of the fetus. Small for gestational age (SGA) may be used to simply allude to birth weight being below a selected threshold. The benchmark used is vitally important when attempting to separate the constitutionally small baby from the pathologically small one. Most epidemiological research has traditionally used 'birth weight for gestational age' references derived from very large population samples (Brenner et al. 1976; Zhang et al. 1995; Kramer et al. 2001). This may be flawed. For example, pre-term babies are more likely to be growth restricted than full-term babies (Zeitlin et al. 2000; Bukowski et al. 2001; Morken et al. 2006). Consequently, the recorded birth weight of a pre-term baby may not be a true reflection of the actual weight of healthy babies remaining *in utero* at that gestation. This could lead to under-diagnosis of pathologically small babies. Currently, a large, international study is underway (Intergrowth-21st), part of which is aimed at producing standards based on a population of pre-term infants born to low-risk women without evidence of impaired fetal growth (Villar et al. 2010).

Other solutions have been proposed for refining growth references including the individualised birth weight ratio (Sanderson et al. 1994), hybrid cross-sectional growth charts (Bernstein et al. 1996) and a multivariable linear regression model to predict birth weight based on maternal and fetal physiological factors (Bukowski et al. 2008). The most investigated individually standardised birth weight model is that produced by Gardosi at the West Midlands Perinatal Institute (Gardosi et al. 1992; Gardosi et al. 2011). The reference range is customised to the current pregnancy taking into account previous pregnancies and maternal characteristics, such as weight and

ethnicity. Known risk factors including diabetes, hypertension and smoking are excluded from the model in an attempt to estimate the optimal weight in the absence of pathology. The calculated weight is then projected backwards, using an ultrasound derived proportionality curve, to predict the expected optimal weight at all gestations. This method is not without criticism. It has been argued that maternal characteristics only account for a small proportion of the factors influencing birth weight and it is the Hadlock-based proportionality curve which improves the identification of the at risk neonate (Hutcheon et al. 2011). This is possibly demonstrated by the work of Clausson and colleagues (Clausson et al. 2001) who compared SGA defined by both a population based reference range and a customised one. In this study the rates of stillbirth and neonatal death were higher in the group classed as SGA by customised reference ranges only compared to the cohort defined as SGA by both. Explanations for this apparent paradox include that this group had more pre-term deliveries which would have been inappropriately classed as AGA on population based references and the projected proportionality curve rather than any other factor in the customised calculation demonstrated that these babies were sub-optimally grown. However, as evidence is mounting that the use of these customised birth weight centiles reduces the rate of constitutionally small babies being classed as growth restricted (false positive rate) whilst helping to increase detection of pathologically small babies (Clausson et al. 2001; McCowan et al. 2005; Ego et al. 2006; Figueras et al. 2007; Gardosi et al. 2009a; Gardosi et al. 2009b; Figueras et al. 2011; Law et al. 2011) it is probably the most clinically relevant standard for growth restriction available at this time. This is confirmed by the findings that SGA based on the customized

growth potential is more strongly associated with abnormal antenatal Doppler findings, fetal distress, caesarean section, admission, and prolonged stay in neonatal intensive care as well as stillbirths and neonatal deaths than centiles based on population standards (Clausson et al. 2001; McCowan et al. 2005; Ego et al. 2006; Figueras et al. 2007; Gardosi et al. 2009b). It has also been demonstrated that use of this definition decreases the number of unexplained stillbirths from 60-75% by the Wigglesworth classification to 15% (Gardosi et al. 2005). This finding was confirmed by a later independent study (Vergani et al. 2008). SGA defined with these customised growth charts may put the child at a five to seven fold increased risk of developing cerebral palsy (Jacobsson et al. 2008). The results also appear to be consistent across the developed world with similar results seen in the United Kingdom (UK), Australia and the United States of America (Mongelli et al. 2007; Gardosi et al. 2009c; Gardosi et al. 2011).

It has been suggested that as the diagnosis of growth restriction implies underlying pathology the definition should not solely rely on birth weight. It should also include markers for utero-placental insufficiency such as abnormal umbilical artery Doppler findings (Cruz-Martinez et al. 2009). This does not allow for the apparent differences between early-onset (<34 weeks) and late-onset (≥34 weeks) FGR. In early onset FGR, Doppler abnormalities of the umbilical arteries are a common finding (Miller et al. 2008). This is important as abnormal umbilical artery Doppler findings are associated with adverse perinatal and neurodevelopmental outcomes (McCowan et al. 2000) (Valcamonico et al. 1994; Figueras et al. 2008) and progression may help to guide difficult decisions regarding delivery in cases of extreme prematurity.

However, late-onset FGR often occurs in the absence of umbilical artery abnormalities, although waveform changes may be seen in the middle cerebral artery (MCA) and amniotic fluid volume (Miller et al. 2008). Consequently, a diagnosis requiring Doppler abnormalities may potentially under diagnose much of the late onset FGR. Some regard this as unimportant, reporting that these babies represent the normal end of the growth spectrum and so are not at risk (Bobrow et al. 1999; Soothill et al. 1999). However, evidence is growing that they are at increased risk of adverse perinatal outcomes (McCowan et al. 2000; Doctor et al. 2001; Severi et al. 2002; Figueras et al. 2008) and growth restriction contributes disproportionately to the number of term stillbirths (Clausson et al. 1999).

### 1.1.2 The definition of growth restriction chosen for this study

For the purposes of this study, FGR has been defined as <10$^{th}$ centile on the Gardosi, gestation adjusted optimal weight (GROW), customised antenatal growth charts[1]. As this definition does not take into account any other markers of pathology such as Doppler abnormalities, it has been referred to as SGA in the study results, instead of FGR or IUGR, although it has been claimed that using these customised centiles they can be used interchangeably (Figueras et al. 2011). Babies who are ≥10$^{th}$ centile are defined as appropriate for gestational age (AGA).

### 1.1.3 Causes of growth restriction

Many factors can lead to a growth restricted fetus, these include; chromosomal abnormalities (Cox et al. 2009), maternal illness (Dombrowski et al. 2010;

[1] Gardosi J, Francis A. Customised Antenatal Growth Charts - GROW-CAC software v 7.1, 2006. Gestation Network, www.gestation.net

Dadhwal et al. 2011; Gelson et al. 2011), malnutrition (Belkacemi et al. 2010), drugs (Bayliss et al. 2002; Pinto et al. 2010) and toxins (including smoking (McCowan et al. 2010)). Suboptimal functioning of the utero-placental unit leading to placental insufficiency is by far the commonest cause (Sankaran et al. 2009). It is the early detection of impaired placentation, leading to growth restriction, which is the central focus of this research.

### 1.1.4 Utero-placental insufficiency leading to FGR

Inadequate conversion of the spiral arteries has long been implicated in the pathogenesis of pre-eclampsia and growth restriction (Brosens et al. 1977; De Wolf et al. 1980; Khong et al. 1986; Brosens et al. 2002; Burton et al. 2009b; Khong et al. 2011) as well as other adverse pregnancy outcomes (APO) such as placental abruption (Tikkanen 2010), pre-term labour (Kim et al. 2003) and second trimester miscarriage (Romero et al. 2011). Histopathology studies have demonstrated significant changes in spiral artery morphology by 10 weeks' gestation with the process continuing throughout the second trimester (Pijnenborg et al. 2006; Khong et al. 2011). There is debate about the pattern and rate of change of the vessels, with controversy regarding whether it occurs progressively or in two distinct waves (Pijnenborg et al. 1983; Robertson et al. 1986; Robson et al. 2001; Lyall 2002) and uncertainty still remains as to when the process is complete.

Failure of trophoblastic invasion (leading to the myometrial segment of the spiral arteries retaining its musculo-elastic wall) is seen in pregnancies complicated by normotensive FGR (Brosens et al. 1977; De Wolf et al. 1980; Khong et al. 1986) as well as pre-eclampsia (Khong et al. 2011). What remains uncertain is whether the two conditions represent different clinical

manifestations of the same pathology possibly due to variation in the number of affected vessels, the degree of vessel change or the maternal response to the pathology itself (Khong et al. 1986; Burton et al. 2009b).

The often quoted story that deficient spiral artery conversion causes poor placental perfusion is greatly over simplified. The precise mechanism linking the histological observations with the clinical manifestation remains highly controversial. Theories proposed include vessel occlusion with atheromatous plaques (Sheppard et al. 1976; Pijnenborg et al. 1991), repeated ischaemic-reperfusion insults leading to oxidative stress (Hung et al. 2001; Redman 2011) and the spiral artery's jet into the intervillous space (IVS) causing mechanical destruction of the villi (the 'jet-hose' effect) (Burton et al. 2009a). Irrespective of the underlying mechanism, retention of the musculo-elastic nature of the vessel wall will change the characteristics of the blood flow from the spiral artery into the IVS. This may be further exacerbated by a continued response to circulating vaso-active compounds. Therefore, differences in the characteristics of blood flow from the spiral artery into the IVS may indicate poor placentation.

## *1.2 Screening for growth restriction*

### 1.2.1 Why screen for FGR?

The UK National Institute for Health and Clinical Excellence (NICE) guideline states that pregnancy is a normal physiological process (NICE 2008a). In the UK, there is undoubtedly a drive towards 'normalising' pregnancy and childbirth. NICE also acknowledges that growth restriction is a cause of serious perinatal mortality and morbidity and that available methods for antenatal detection are poor. The methods currently used in routine clinical practice to assign risk of FGR perform so badly that as many as three-quarters of growth-

restricted fetuses are not diagnosed as such before delivery (Hepburn et al. 1986). An early screening test should prove cost-effective, as it would appropriately target antenatal surveillance and intervention. This should not only improve perinatal morbidity in the previously undiagnosed cases but also reduce the false-positive rate thereby preventing the medicalisation of normal pregnancies.

### 1.2.2 Current methods for assigning risk of FGR

The UK antenatal care system involves making a risk assessment at the booking visit (usually at 10 to 14 weeks). The risk of FGR is mainly based on past medical history, including factors such as maternal age, maternal illnesses including diabetes (Stratton et al. 1995; Rowan et al. 2009), renal disease or hypertension, smoking (Lindley et al. 2000), alcohol (Mills et al. 1984) and drugs (prescribed or recreational). Caffeine has also been linked to growth restriction (CARE-Study-Group 2008) although questioning about caffeine intake has yet to form part of routine antenatal care in the UK.

Past obstetric history is also important. A woman with a history of a previous FGR baby has a one in five recurrence risk (20%) in a subsequent pregnancy (Breeze et al. 2007). This must be interpreted with caution as the cause of FGR may be multi-factorial and risk factors such as smoking, drug use and maternal weight can be modified between pregnancies (Mills et al. 1984).

Obesity used to be regarded as a protective factor against growth restriction (Cnattingius et al. 1998; Nohr et al. 2008). Evidence is now building that obesity may increase the risk of an SGA baby by as much as 50% (Gardosi et al. 2009b). It could be argued that this is merely a result of the algorithm used to calculate customised birth weight charts as this includes maternal body

mass index (BMI). However, the clinical relevance was demonstrated by a large population-based study, which reported a higher perinatal mortality associated with SGA defined by customized growth charts in obese women (Gardosi et al. 2009). Importantly, these are the women in whom abdominal palpation has been shown to be less reliable than ultrasound biometry for predicting birth weight (Farrell et al. 2002). A low BMI has also been associated with lower birth weight in the UK (Sebire et al. 2001) and maternal malnutrition is one of the commonest causes of FGR in the developing world (Belkacemi et al. 2010).

For women assessed to be 'low risk', NICE recommend surveillance consisting of the measurement of symphysis-fundal height at each antenatal visit from 24 weeks onwards (NICE 2008a). A detection rate of FGR as low as 15% has been reported for these pregnancies (Backe et al. 1993).

### 1.2.3 Potential methods for assigning risk of FGR

#### 1.2.3.1 Biochemical markers

Studies have demonstrated that several biochemical markers may be linked to impaired placentation including placental protein 13 (PP13)(Cowans et al. 2008), ADAM12s (Spencer et al. 2008) and cystatin C (Thilaganathan et al. 2009). In the UK research has focused on the serum analytes used for Trisomy 21 screening (pregnancy associated plasma protein-A (PAPP-A), human chorionic gonadotropin (HCG), alpha fetoprotein (AFP), Inhibin-A and unconjugated oestriol). A large cohort study showed a link between low PAPP-A and low birth weight (Smith et al. 2002) with another demonstrating that low PAPP-A at 10 weeks is strongly associated with stillbirth related to placental dysfunction (Smith et al. 2004). A meta-analysis published in 2008 (Gagnon et

al. 2008) demonstrated that of these five analytes, an AFP of >2.0MoM was the best predictor of severe growth restriction (positive likelihood ratio 27.96 (CI 95% 8.02-97.48) and negative likelihood ratio 0.78 (CI 95% 0.55 -1.11). However, no biochemical marker has yet proved either sensitive or specific enough to be used on its own as a screening test for FGR.

#### 1.2.3.2 Ultrasound markers

Measurement of the uterine artery waveform is an important but imperfect component of screening for pre-eclampsia and FGR. A recent study has shown that the first trimester uterine artery waveform is significantly related to SGA babies (Melchiorre et al. 2009). However, a large, meta-analysis of 61 studies (including data from 41,131 patients) (Cnossen et al. 2008) showed that the uterine arteries gave a more accurate prediction when used in the second trimester with a positive likelihood ratio (PLR) of 9.1 for FGR and a PLR of 14.6 for severe FGR among low-risk patients. This suggests that whilst unlikely to prove a useful screening tool for FGR in isolation, uterine artery Doppler may well form part of a future test.

The major pathology linked with FGR is utero-placental insufficiency. The placenta and much of its vasculature is readily identifiable with ultrasonography at 11 to 14 weeks' gestation. It is somewhat surprising, therefore, that currently there are few placenta-based ultrasound screening markers. This may be due in part to the technical difficulties associated with many of the newer ultrasound tools including power Doppler and 3-D ultrasonography (discussed in Chapter 6 pg146). Much of the accepted histological evidence regarding the underlying pathology within the placental bed has yet to be fully explored with standard ultrasound techniques let alone, the newer, more controversial ones. The uterine artery waveform is consequently used as a surrogate marker for the actual pathology. This thesis seeks to explore the possibility of visualizing the underlying pathology at the utero-placental interface and expanding the use of new automated to tools to develop placental based ultrasound markers capable of being used as part of a screening test.

### 1.2.4 Screening for FGR: The future

A recent study combined uterine artery Doppler waveform and nuchal translucency, with five biochemical analytes and mean arterial pressure (MAP) (Karagiannis et al. 2011). This demonstrated that half of pregnancies resulting in SGA neonates could be identified at 11-13 weeks. This is very encouraging. If a novel placenta-based ultrasound marker can also be found, it is reasonable to hypothesise that a 'combined' test for FGR may be possible in the future.

# 2 Hypotheses and aims of the thesis

## *2.1 Hypotheses*

### 2.1.1 Inadequate spiral artery conversion

Histological evidence suggests that growth restriction is correlated with inadequate conversion of the spiral arteries. Hypotheses related to this statement and investigated by this thesis are:

- A reliable method can be developed to measure the jet of blood from the spiral arteries into the intervillous space.
- The characteristics of this jet will alter with gestation.
- This jet will have different flow characteristics when the pregnancy results in a SGA baby relative to a normal pregnancy.
- The waveform of the uterine artery is thought to be a direct reflection of the flow of blood through the spiral arteries and will therefore correlate with the waveform characteristics of the jets.
- There will be observable anatomical differences in the general appearance of the vasculature in pregnancies resulting in SGA babies.
- There will be a difference in the overall vascularity of the placental basal plate[2], in an SGA pregnancy relative to a normal pregnancy, which can be visualised with ultrasound.

  *(See Chapter 4)*

[2] The 'basal plate of the placenta' refers to the maternal-fetal interface, which is effectively the floor of the IVS and the plane along which the placenta separates from the uterus Benirschke, K., et al. (2000). Pathology of the human placenta; 4th Edition. New York, Springer-Verlag.

### 2.1.2 Placental volume (PlaV)

Placental volume (PlaV) from the early second trimester has been suggested to correlate to birth weight. Hypotheses related to this statement and investigated by this thesis are:

- A low PlaV at 11-13+6 weeks, estimated using a novel, semi-automated, time-efficient technique, will predict an increased risk of SGA.
- The effect of gestation between 11 and 13+6 weeks can be corrected for by using a dimensionless index relating PlaV to fetal growth.
    - The prediction of SGA can be improved by using this index.
    - This index is a risk factor for SGA, which is independent of other known markers such as PAPP-A.

*(See Chapter 5)*

### 2.1.3 Abnormal placental morphology

Abnormal placental morphology has been suggested to correlate with growth restriction. Hypotheses related to this statement and investigated by this thesis are:

- Placental morphology can be visualized in, and quantified using, semi-automated image analysis and visualization tools.
- Poor placentation will result in different physical characteristics compared with a ‘normal’ placenta (different shape, surface area of the basal plate, thickness etc.).
    - These differences can be explored by relating the different morphological measurements to each other

*(See Chapter 5)*

### 2.1.4 3-D Power Doppler

It has been suggested that the relatively new 3-D power Doppler (PD) ultrasound can be used to study the vasculature of the placenta. However, some PD indices have been shown in phantom models to depend on the machine settings and beam path. Hypotheses, related to this statement, which were planned to be investigated in this thesis are:

- The settings, including PD gain, can be standardised to allow appropriate inter-participant comparison.
    - The effect of PD gain can be demonstrated *in vivo.*
    - The PD gain setting can then be optimised to allow inter-participant comparison.
- Once adequately standardised, 3-D PD ultrasound can be used to sample the placental basal plate, producing the 'vascular volume'.
    - If there is a difference in the jet blood flow between SGA and AGA pregnancies demonstrable using three vessels in 2-D (2 dimensional) ultrasound (see hypothesis 2.1.1) there will be a difference seen using 3-D PD.
    - This 'vascular volume' will reflect the blood flow into the IVS from all of the spiral arteries in the placenta and, therefore, should be a more robust indicator of placentation than the sample of just three vessels.
    - The 'vascular volume' could therefore help with development of an early screening test for SGA.

*(See Chapter 6)*

## *2.2 Aims of this thesis*

- To perform a pilot study (Spiral 3-D) to prospectively explore the developing placenta with both 2-D and 3-D ultrasound *(Chapter 3)*.

- To discuss observed placental anatomy and haemodynamics of the intervillous space in an attempt to increase understanding of the underlying processes leading to normal pregnancy and fetal growth restriction *(Chapter 4)*.

- To examine potential ultrasound markers for growth restriction generated using a novel semi-automated process for estimation of placental volume and morphology *(Chapter 5)*.

- To present and discuss evidence for optimisation of 3-D information obtained from power Doppler indices *(Chapter 6).*

The thesis concludes by outlining some of the limitations of the study and discussing possible future research for developing a screening test for growth restriction.

## *2.3 Publications arising from this work*

### 2.3.1 Publications in peer-reviewed journals

Collins S.L., Grant D., Black R.S., Vellayan M., and Impey L. (2011). Abdominal pregnancy; a perfusion confusion? Placenta 32(10): 793-5.

Collins S.L., Birks J.S., Stevenson G.N., Papageorghiou A.T., Noble J.A. & Impey L. (2011). Measurement of the spiral artery jets: general principles and differences observed for small for gestational age (SGA) babies. Ultrasound in Obstetrics and Gynaecology *(In Press)*.

Collins S.L., Stevenson G.N., Noble J.A. & Impey L. (2012) Developmental changes in spiral artery blood flow in the human placenta observed with colour Doppler ultrasonography. Placenta *(In Press)*.

Collins S.L., Stevenson G.N., Noble J.A., Impey L. & Welsh A.W. (2011) Influence of power Doppler gain setting on Virtual Organ Computer AnaLysis (VOCAL™) indices in vivo: Can use of the individual sub-noise gain (SNG) level optimise information? Ultrasound in Obstetrics and Gynaecology *(In Press)*.

Bulmer, J.N., Burton, G.J., Collins, S. et al (2012) IFPA Meeting 2011 workshop report II: Angiogenic signaling and regulation of fetal endothelial function; placental and fetal circulation and growth; spiral artery remodeling. Placenta 33 Suppl A: S9-14.

Al-Khan, A., Aye, I. L., Barsoum, I., Borbely, A., Cebral, E., Cerchi, G., Clifton, V. L., Collins, S. et al. (2011). IFPA Meeting 2010 Workshops Report II: Placental pathology; trophoblast invasion; fetal sex; parasites and the placenta; decidua and embryonic or fetal loss; trophoblast differentiation and syncytialisation. Placenta 32 Suppl 2: S90-99.

### 2.3.2 International Research Awards

International Federation of Placental Associations 2011 Trophoblast New Investigator Award. IFPA Conference Geilo, Norway 2011.

### 2.3.3 Oral presentations at international conferences

Collins, S.L., Birks J.S., Stevenson G.N., Papageorghiou A.T., Noble J.A. & Impey L. (Prague 2010). OC18.04: Direct measurement of blood flow into the intervillous space and its relationship with uterine artery blood flow. Ultrasound in Obstetrics & Gynecology 36: 34.

Collins, S.L., Birks J.S., Stevenson G.N., Papageorghiou A.T., Noble J.A. & Impey L. (Prague 2010). OC18.05: Direct measurement of blood flow into the intervillous space and its relationship with the small for gestational age (SGA) baby. Ultrasound in Obstetrics & Gynecology 36: 34-35.

Collins, S.L., Birks J.S., Stevenson G.N., Papageorghiou A.T., Noble J.A. & Impey L. (IFPA Chile 2010). Spirals, spurts and the small for gestational age baby. Invited oral presentation.

Collins, S.L., Stevenson G.N., Noble J.A., Impey L. & Welsh A.W. (Los Angeles 2011). OP27.05 The need to standardise Virtual Organ Computer-aided AnaLysis (VOCAL™) power Doppler indices to the sub-bloom gain (SBG) level. Ultrasound in Obstetrics & Gynecology 38 (Suppl. 1): 135.

Collins, S.L., Stevenson G.N., Noble J.A. & Impey L. (IFPA Norway 2011). Ultrasonography to characterise the spiral artery blood flow. Invited oral presentation.

Stevenson, G.N. Collins, S.L. Impey, L. Noble, J.A. (Prague 2010). OP10.09: A novel semi-automated (SA) technique for 3D ultrasound measurement of placental volume. Ultrasound in Obstetrics & Gynecology 36 (Suppl. 1):82.

### 2.3.4 Poster presentations at international conferences

Collins, S.L., Stevenson G.N., Noble J.A. & Impey L. (IFPA Chile 2010). (P3.83) The relationship between placental volume in early pregnancy, measured using a novel semi-automated technique, and the small for gestational age (SGA) fetus. Placenta 31: A. 137.

Collins, S.L., Stevenson G.N., Noble J.A. & Impey L. (IFPA Norway 2011). (P1.89) Size is everything; Searching for an early ultrasound marker which predicts the term small for gestational age (SGA) baby.

# 3 The 'Spiral 3-D' Study General methods




## *3.1 Aims of this chapter*

This chapter describes the patient recruitment, experimental methods used and the overall patient outcomes for the two phases of the spiral 3-D study. The subsequent chapters examine the different aspects of 2-D and 3-D parts of the study in further detail. Each chapter will discuss the background, give relevant additional details and present results to support the hypotheses tested in this thesis using this general patient data set.

## *3.2 Ethical review*

Ethical approval was granted from the Oxford NREC on 17th November 2008 (REC ref 08/H0604/163) to undertake a prospective, longitudinal cohort study examining the developing placental anatomy for potential markers for adverse pregnancy outcomes using 2-D and 3-D ultrasound.

## *3.3 Methods: Data Collection – Phase I*

### 3.3.1 Participants

Recruitment was of singleton pregnancies at the time of the dating scan: women over the age of 16 years, with a BMI <35, and no significant maternal chronic illness including diabetes, or treatment with medications associated with FGR, such as beta-blockers (Bayliss et al. 2002). Women were recruited from the Feto-Maternal Medicine and ultrasound departments at the John Radcliffe Hospital, Oxford. Full details of the study were provided in patient leaflets (page

186) and written consent was obtained when they attended for the first appointment. Sociodemographic and obstetric data were collected including age, parity, family history, as well as past medical and obstetric histories. The latter two were used to classify participants as ‘high risk of SGA’ or ‘low risk of SGA’. High risk factors included; previous history of an SGA baby, pre-eclampsia in a prior pregnancy, previous pre-term birth, significant maternal chronic illness such as essential hypertension and low PAPP-A at NT screening. Women were only considered low risk if they were healthy and appropriately booked under midwifery-led care. Phase I of the study involved having seven extra ultrasound scans during their pregnancy, starting at between 11 and 13 weeks. Gestational age was calculated from crown-rump length (CRL) measurement at the first scan (Loughna et al. 2009). The next three scans were undertaken at fortnightly intervals from the first scan, with the last three at 23, 28 and 34 weeks’ gestation.

### 3.3.2 Ultrasound data collected: 2-D

The scans were undertaken by a single operator (SC) using an M6C curved array abdominal transducer and a Voluson E8™ (GE Healthcare, Milwaukee, WI, USA). The machine settings were kept constant for all participants particularly the wall motion filter was set to low 2, the colour Doppler gain was -12.0 and the pulse repetition frequency was kept at 0.9KHz (for full details of machine settings see page 191). Fetal viability was confirmed and appropriate fetal biometry measurements taken including Bi-parietal Diameter (BPD), Head Circumference (HC), Abdominal Circumference (AC) and Femur length (FL). The depth of the single deepest pool of liquor not containing umbilical cord was also recorded.

### 3.3.3 Uterine artery measurement

The uterine arteries were identified using standard techniques. Before 16 weeks' gestation this was lateral to the cervix at the level of the internal os as the artery turns cranially before it branches into the arcuate arteries (Papageorghiou et al. 2001). After 16 weeks they were identified on a longitudinal scan, lateral to the uterus, where the uterine and external iliac arteries appear to cross (Hecher et al. 2000). Pulsed-wave Doppler ultrasonography, with a gate size of 2mm, was then used to obtain at least three consecutive good quality waveforms. The angle of insonation was kept at less than 30 degrees and angle correction applied if necessary. The pulsatility index (PI) and resistance index (RI) were calculated over at least three cardiac cycles. The uterine artery indices used were calculated as the mean of the values for the left and right vessels (mean Ut A) and also the minimum value (min Ut A). The presence or absence of an early diastolic notch was also recorded (Bower et al. 1993).

#### 3.3.3.1 Spiral artery jet measurement

The blood flow from the mouth of the spiral artery into the intervillous space was identified using the following novel technique. The interface between the decidua and the basal plate of the placenta was identified in the sagittal plane, ensuring that the probe was kept at 90 degrees to the placental interface. The area was then magnified and colour Doppler signal applied. The mouth of the spiral artery is readily identifiable as the flow becomes unidirectional (single colour) at the bright deciduo-placental interface (Figure 1, page 40).

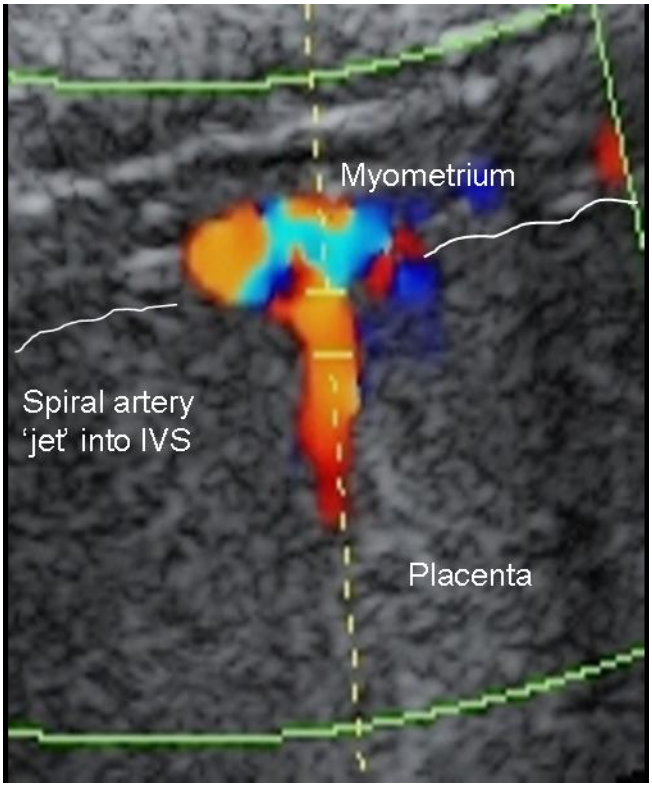



**Figure 1: Placement of the Doppler gate at the mouth of the spiral artery where the jet enters the intervillous space**

(NB image is 'inverted' with the colour red indicating flow away from the probe)

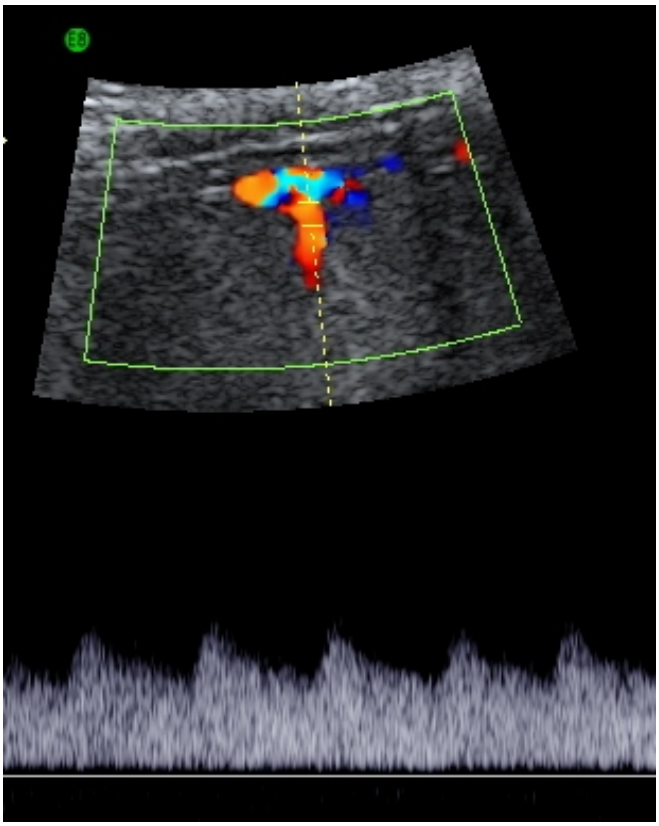


**Figure 2: Typical jet waveform, unidirectional flow.**

Pulse-wave Doppler ultrasonography, with a gate size of 2mm, was then used to obtain at least three consecutive, good quality waveforms. The angle of insonation was kept at less than 30 degrees and angle correction applied if necessary. A typical waveform is unidirectional flow (Figure 2, page 40). Both the pulsatility index (PI) and resistance index (RI) were calculated over at least three cardiac cycles using the auto-trace software provided on the Voluson E8.

*3.3.3.1.1 Pre-study jet measurements*

Before the study started all the identifiable jets were measured in three women with a BMI of <25 at between 14 and 20 weeks. The time taken to do this was between 50 and 70 minutes per participant. Twenty-nine jets were measured in one woman, with 30 and 32 in the other two. The results demonstrated that there was a difference of <0.06 between the measured maximum and minimum RI values for all the jets in each woman. Therefore, we concluded that measuring three is likely to be representative of all the jets. This maximized the number of women who could be scanned in the fixed amount of time available (20 minutes per session), whilst minimizing their exposure colour Doppler ultrasound.

*3.3.3.1.2 Phase I jet measurements*

As a result of the pre-study findings, the three most prominent spiral arteries in the central part of the placenta were measured at every visit in Phase I. The scanning time allowed for these measurements was limited to 20 minutes for safety reasons. Thermal Index (TI) was kept at <1.0 and mechanical index (MI) at <0.7 throughout. If, by 20 minutes, the jets had not been measured the procedure was abandoned.

The saved 2-D images of the three jets measured for PI and RI were examined ‘offline’. The jet image was magnified to the maximum possible on the ultrasound machine. The width of the jet at the deciduo-placental interface (presumed to be the mouth of the spiral artery) and the length of the jet (from the deciduo-placental interface to the end of the visible colour) were measured (Figure 3, page 43). As the edges of the image were often blurred care was taken to place the calipers on the area of solid colour rather than the ‘faded’ edges, which were presumed to be bloom artefact (Figure 4, page 43). The peak systolic velocity value used to calculate the PI and RI was recorded (page 39).

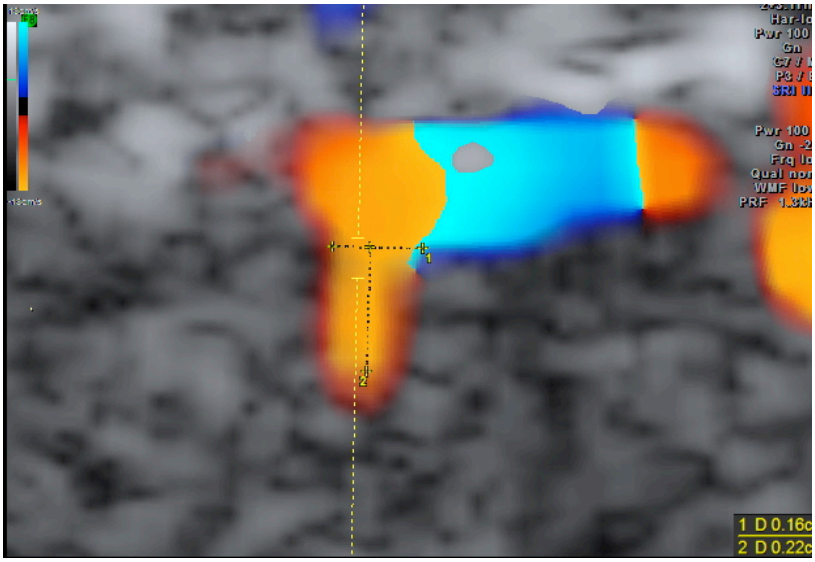



**Figure 3: Correct placement of the calipers for jet width and length**

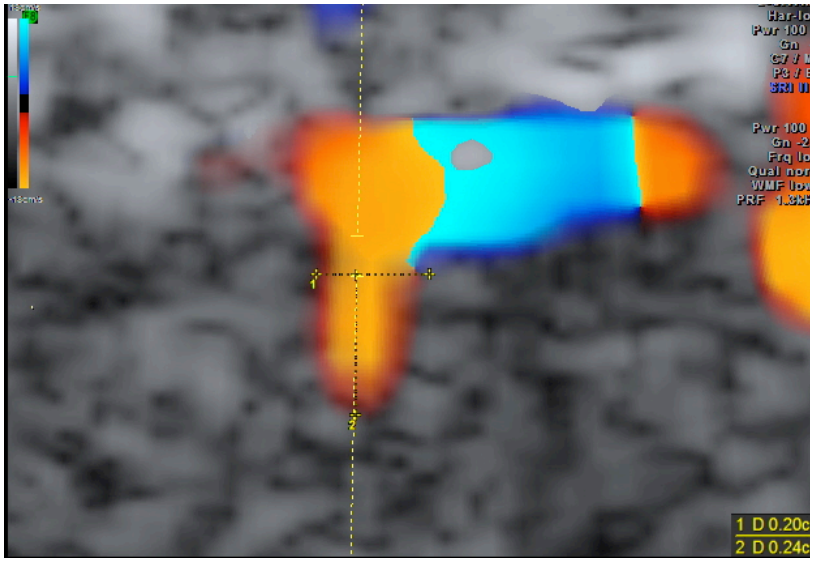



**Figure 4: Incorrect placement of the calipers for jet width and length.**
The width caliper is not at the deciduo-placental interface and both extend out into the ‘faded’ colour thereby potentially including bloom artefact.

### 3.3.3.2 Placental lakes

Placental lakes were defined as simple, hypo-echoic, cystic lesions seen within the placental tissue with a diameter in any direction of >5mm. The surrounding placental tissue was visually of normal echogenicity and texture. Their presence or absence was noted at each visit (Figure 5, page 44).

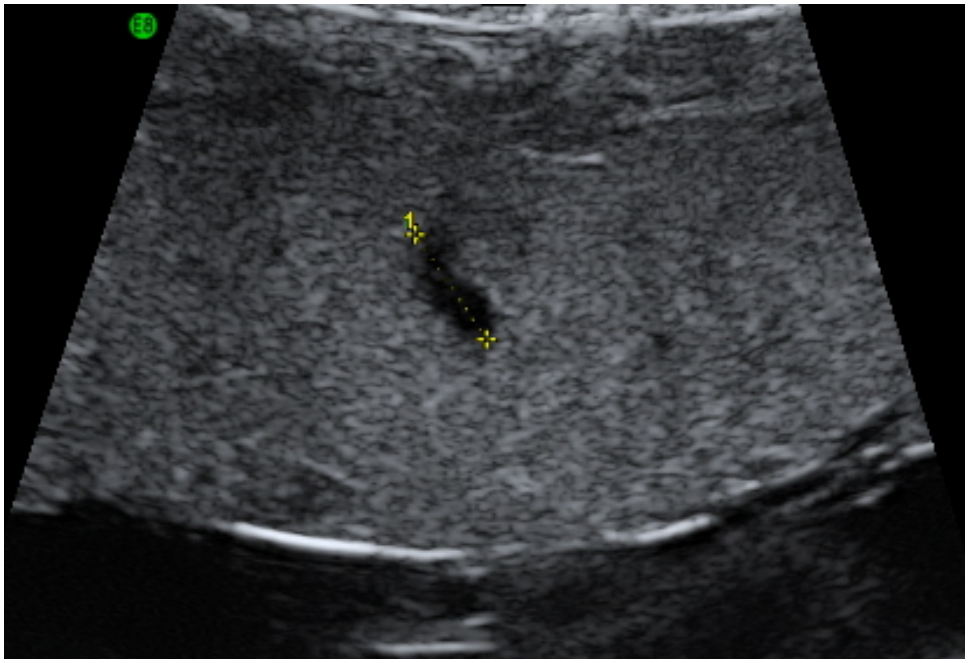


**Figure 5: An example of a placental lake.**
Simple placental lake, >5mm in diameter and normal echogenicity in the surrounding tissue.

### 3.3.3.3 Mega-jets

In the early stages of the study we observed a phenomenon for which we have found no reference to in the literature. Some women had one or two noticeably larger jets with flow travelling considerably further into the placenta than normal jets. They were termed mega-jets and objectively defined as a jet which could be seen to have blood flow travelling more than 10mm into the placental tissue (or

over 50% of the way across the placenta if it was <20mm thick). Both the velocity and pulsatility of the flow were seen to diminish in these jets as the flow travelled further away from the deciduo-placental interface into the placenta. Figure 7, page 46, shows the decrease in peak systolic velocity (PSV) and relative pulsatility in the same mega-jet when the pulse wave gate is placed along the line of flow at increasing distances from the deciduo-placental interface. These mega-jets often, but not always, terminated in a placental lake (Figure 6; page 45). Their presence or absence was noted at each visit and their dimensions measured offline.

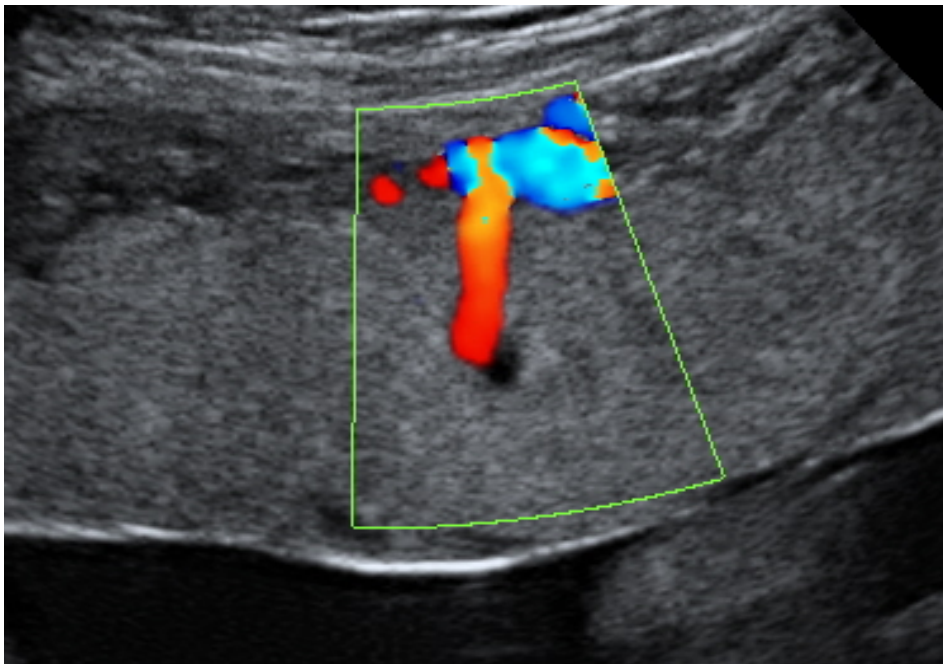


**Figure 6: A mega-jet terminating in a placental lake.** [3]

[3] The slightly hypoechoic edge of the lake is an artefact which occurred when converting the image

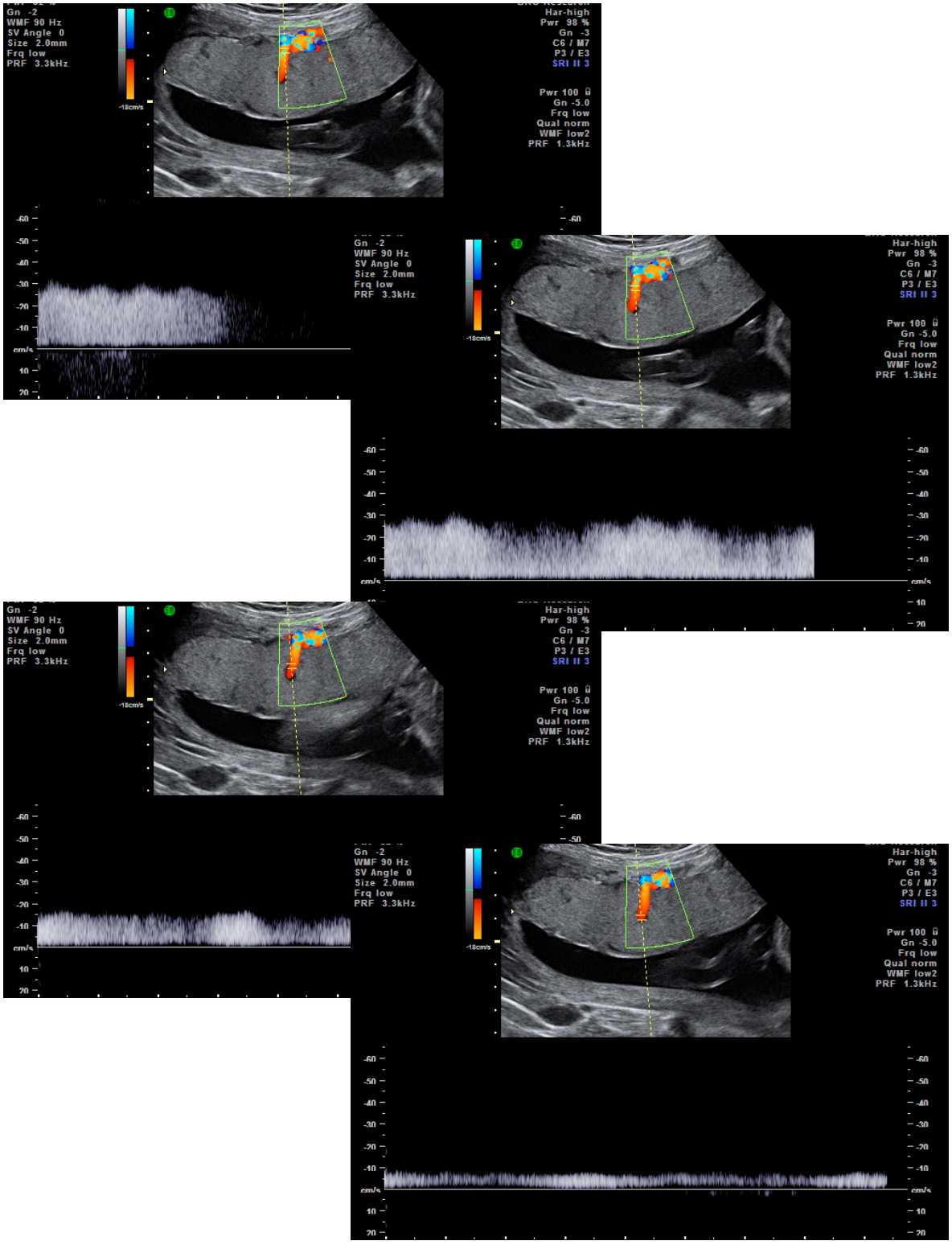



**Figure 7: Showing the decreasing velocity and pulsatility of a mega-jet with placing the pulse wave gate at increasing distances from the opening into the IVS.**

### 3.3.4 Ultrasound data collected: 3-D

Scans were undertaken by a single operator (SC) with the participant in a semi recumbent position using a RAB4-8-D 3D/4D curved array abdominal transducer (4-8.5 MHz) on a Voluson E8™ (GE Healthcare, Milwaukee, WI, USA). After identification of placental position, the optimal position for 3-D acquisition of the whole placenta was identified. This was usually a cross-sectional plane close to the centre of the placenta.

To ensure image consistency throughout the study, the machine was programmed with the '*BRC Research'* settings (8.2, Page 191). At the time only Prof. Rizzo's group in Italy were routinely publishing their full machine settings (Rizzo et al. 2008). He was kind enough to discuss this and indicated that his choice of settings was not based on experimental results but personal experience (Personal Communication). Using his settings as a starting point, the image was optimized for our population and the final agreed settings programmed into the machine (8.2, Page 191). After confirmation of viability and identification of placental position, the optimal probe placement for 3-D acquisition of the whole placenta was identified. A static, greyscale 3-D volume was captured using the pre-determined machine settings (8.2, page 191). The image was then checked to ensure that the whole placenta had been included. If not the angle was increased or the probe repositioned and the process repeated. Once a complete placental volume had been captured it was stored and analysed off-line. If the placenta was too large to capture with the maximum angle possible, this was recorded and a representative sample taken.

A static 3-D PD volume of the placenta was acquired using a previously saved machine configuration (Full details 8.2, page 191) and the PD gain set at -3dB. Without moving either the participant or the probe, the PD gain was quickly changed to -5dB and a second static 3-D image was captured. This technique was repeated for gain settings of -7dB, -9dB and the individualised ‘sub-noise’ gain (SNG) setting for that participant (five acquisitions in total). The SNG was found by increasing the gain until artefactual noise was present (seen as a PD signal scattered throughout the whole image not related to vessels) and then slowly reducing it to a level just below this threshold (i.e. to where the ‘noise’ artefact just disappeared). The volume was captured and the SNG value was recorded. Apart from the PD gain, all the machine settings were kept constant for all scans. Throughout the data acquisition the participant was asked to remain as still as possible. To ensure that all five volumes captured contained exactly the same anatomy if either the probe or the woman moved the sequence of five scans was started again. The images were then checked for ‘flash artefact’ (secondary to fetal or maternal movements). If any such artefact was detected all five scans were rejected and the full sequence of scans repeated. This was done to ensure that the same anatomical volume was captured five times, at the same time point, in the same women with the only change being in the PD gain setting. The data were stored using Sonoview and analysed off-line on a personal computer using Virtual Organ Computer-aided AnaLysis II (VOCAL II™) on 4-D View™ (GE Healthcare, Milwaukee, WI, USA). If the five volumes could not be obtained in under 20 minutes, the procedure was abandoned.

### 3.3.5 Post delivery data collection

Post delivery data was collected by reviewing the individual patient notes. This included any antenatal complications, highest recorded blood pressure, gestation at delivery, mode of delivery, intrapartum complications, gender of baby, birth weight, APGAR scores, admission to SCBU, and placental weight. The customised birth weight centile was calculated for each fetus using the Grow™ software package (version 7.5.1, West Midlands Perinatal Institute, Birmingham, UK). Small for gestational age (SGA) was defined as <10$^{th}$ centile on customised birth weight charts. Pregnancy-associated hypertensive disorders including pre-eclampsia and gestational hypertension were defined according to the International Society for the Study of Hypertension in Pregnancy (ISSHP) guidelines (Brown et al. 2001). In particular a diagnosis of pre-eclampsia required gestational hypertension with proteinuria of 300 mg or more in 24hrs or two readings of at least 2+ on urine dipstick analysis. Pregnancy-induced hypertension (PIH) was defined as the occurrence of gestational hypertension in the absence of proteinuria.

## *3.4 Methods: Data Collection – Phase II*

After analysis of the initial findings of Phase I, the protocol under went a substantial amendment on 5$^{th}$ March 2009 (REC ref 5774/08/H0604/163) to reduce the number of ultrasound scans for each participant to optimize the number of women that could be recruited in the given length of time available. We refer to this data as Phase II.

### 3.4.1 Participants

The participants recruited were the same as for Phase I (3.4.1; Participants, page 37) however, Phase II only involved five extra scans. The first was again at 11 to 13 weeks' gestation with the next three scans at fortnightly intervals and the last at 23 weeks.

### 3.4.2 Ultrasound data collected: 2-D

At each visit, viability was confirmed, fetal biometry recorded, the uterine artery waveform measured and the presence of any placental lakes noted as described in Phase I (page 38). Unlike Phase I, the waveform of the spiral artery jets was not measured in Phase II.

### 3.4.3 Ultrasound data collected: 3-D

At each visit static 3-D greyscale volumes were collected as described in Phase I (page 45). However, only a single PD volume was obtained using the individualized SNG setting rather than the five acquired for Phase I.

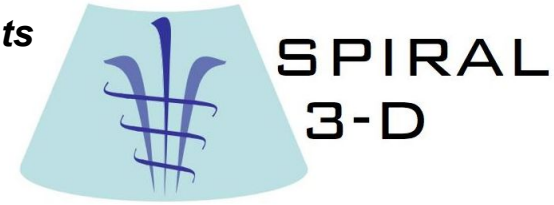
### 3.4.4 Post delivery data collection

The same data was collected from the individual patient notes as for Phase I (page 49).

## *3.5 Methods: Statistical analyses*

Statistical analyses were mostly performed using SPSS (version 16.0, IBM Corporation, NY, USA) & Excel 2004 (Microsoft Corp., Washington, USA). Results were considered to be statistically significant when $p<0.05$. However, some of the more complicated longitudinal data were analysed by Dr Jacqueline Birks of the Centre for Statistics in Medicine, Oxford University. Where this is the case, the details and an acknowledgement, are given in the relevant chapters.

## *3.6 General results and patients outcomes*




### 3.6.1 Phase I

Sixty-six women with a singleton pregnancy were recruited at between 11+0 weeks and 13+6 weeks' gestation. The majority (48/73%) of women were from an unselected population but 17 (27%) were 'higher risk' on the basis of their medical history. One participant emigrated after the first two scans and so was lost to follow up. Therefore data from 65 women were analysed.

Three women developed pregnancy-induced hypertension, two pre-eclampsia and two delivered before 37 completed weeks' gestation. Therefore 58 women were normotensive throughout pregnancy and delivered at term. Six of these were <10$^{th}$ centile on customised birth weight centiles (Figure 8, page 53).

Of the 58 included women, 55 attended for all seven extra scans; the others attended 3, 4 and 6. Delivery details were available for all 58 women. In total, data from 398 longitudinal ultrasound scans in 58 women were available for the final analysis. Baseline characteristics of the term, normotensive women are shown in Table 1, page 37 and delivery details in Table 2, page 55. There were no significant differences in the baseline demographics between the SGA group and the control group.

Figure **9** (page 56) presents the distribution of the customised birth weights of the sample population. The SGA group had significantly smaller placentas at delivery (p=0.002) despite there being no difference in the gestation at delivery (p=0.6). No babies were admitted to the neonatal intensive care unit (NICU). All the women had uterine artery Dopplers PI <95$^{th}$ centile at 23 weeks' gestation.

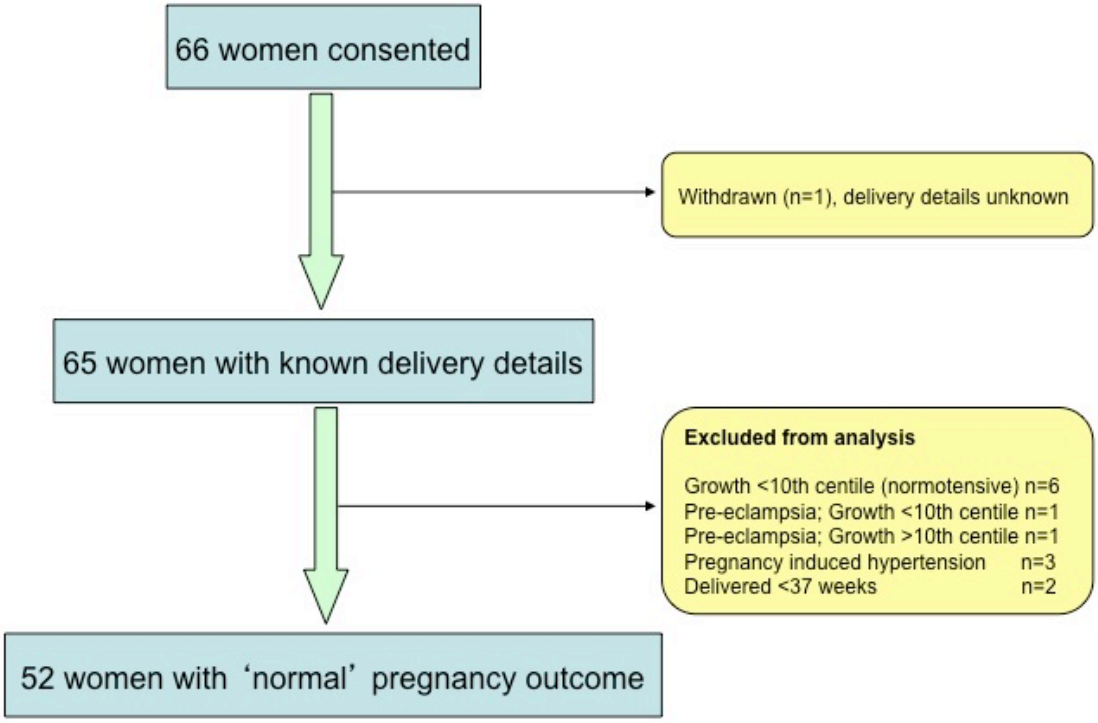



**Figure 8: Pregnancy outcomes for Phase I of the study.**

**Table 1: Baseline patient demographics of normotensive Phase I participants who delivered at term**

| | **SGA (n=6)** | **Normal pregnancy (n=52)** | **P values** |
|---|---|---|---|
| **Age** | 31 (19-44) | 28 (16-37) | 0.44* |
| **BMI at booking** | 23.2 (18-31) | 23.4 (17-35) | 0.95* |
| **Smoker** | 1 (17%) | 9 (17%) | 1.00† |
| **Multiparous** | 4 (67%) | 26 (5%) | 1.00† |
| ➢ **History of SGA** | 3 (50%) | 6 (23%) | 0.12† |
| ➢ **History of PET** | 2 (34%) | 1 (4%) | 0.06† |
| **Known obstetric family history** | | (n=51) | |
| ➢ **FHx of SGA** | 1 (17%) | 3 (6%) | 0.5† |
| ➢ **FHx of PET** | 1 (17%) | 9 (18%) | 0.6† |
| ➢ **FHx recurrent miscarriage** | 0 | 1 (2%) | |
| ➢ **FHx late IUD (>34 weeks)** | | | |
| **Self- reported ethnicity** | | | |
| ➢ **White European** | 6 | 48 | |
| ➢ **Indian** | 0 | 1 | |
| ➢ **Pakistani** | 0 | 1 | |
| ➢ **Mixed** | 0 | 2 | |
| **IVF pregnancy** | 0 | 5 | 0.7† |
| **Placental site** | | | |
| ➢ **Anterior** | 3 | 22 | |
| ➢ **Posterior** | 0 | 23 | |
| ➢ **Lateral** | 2 | 4 | |
| ➢ **Fundal** | 1 | 2 | |
| ➢ **Praevia** | 0 | 1 | |
| **P-values calculated using *t-test or † Fisher's exact test** | | | |

**Table 2: Delivery details of Phase I participants**

| | **SGA (n=6)** | **AGA (n=52)** | **P values** |
|---|---|---|---|
| **Customised birth weight centile** | 5 (0-8) | 47 (10-99) | N/A |
| **Birth weight (g)** | 2706 (2059-3010) | 3402 (2450-4730) | <0.001* |
| **Placental weight (g)** | 496 (390-647) | 637(380-872) | 0.002* |
| **Gestation at delivery (days)** | 39+2<br>(38+1 to 40+4) | 39+4<br>(35+4 to 42+2) | 0.6* |
| **Onset of labour** | | | |
| ➢ **Spontaneous** | 4 (66%) | 41 (79%) | 1.0† |
| ➢ **Induced** | 0 | 10 (19%) | |
| ➢ **Elective Caesarean** | 2 (34%) | 1 (2%) | 0.043† |
| **Mode of delivery** | | | |
| ➢ **SVD** | 2 (34%) | 39 (75%) | 0.46† |
| ➢ **Instrumental** | 2 (34%) | 8 (15%) | 0.33† |
| ➢ **Caesarean section** | 2 (34%) | 5 (10%) | 0.2† |
| **Admission to NICU** | 0 | 0 | N/A |
| **P-values calculated using *t-test or † Fisher's exact test** | | | |

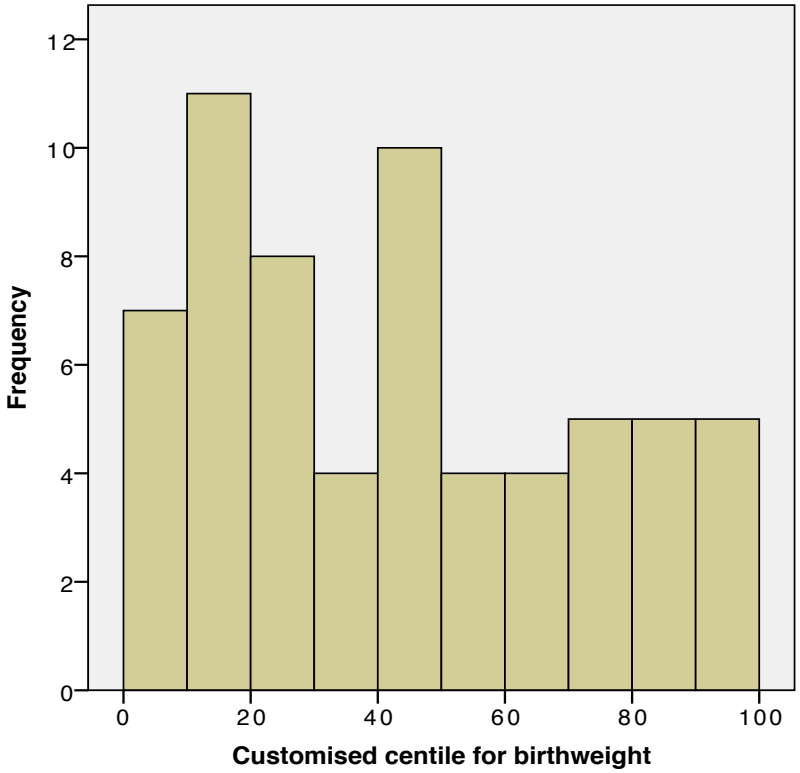



**Figure 9: Distribution of the customised birth weight centiles for the Phase I participants.**

### 3.6.2 Phase II

Seventy-nine women with a singleton pregnancy were recruited at between 11+0 weeks and 13+6 weeks' gestation. The majority (58 women) were from an unselected population but 21 were 'higher risk' on the basis of their history. One participant chose to terminate the pregnancy at 13 weeks after a diagnosis of Trisomy 21. Therefore data from 78 women were available to be analysed.

Seven women developed pre-eclampsia, three pregnancy-induced hypertension, and two delivered before 37 completed weeks' gestation. Therefore 56 women were normotensive throughout pregnancy and delivered at term. Six of these were <10$^{th}$ centile on customised birth weight centiles

### 3.6.3 Complete results (Phase I and II)

In total 145 women were recruited; one emigrated and one terminated. As a result delivery data was available for 143 women (Figure 8, page 53).

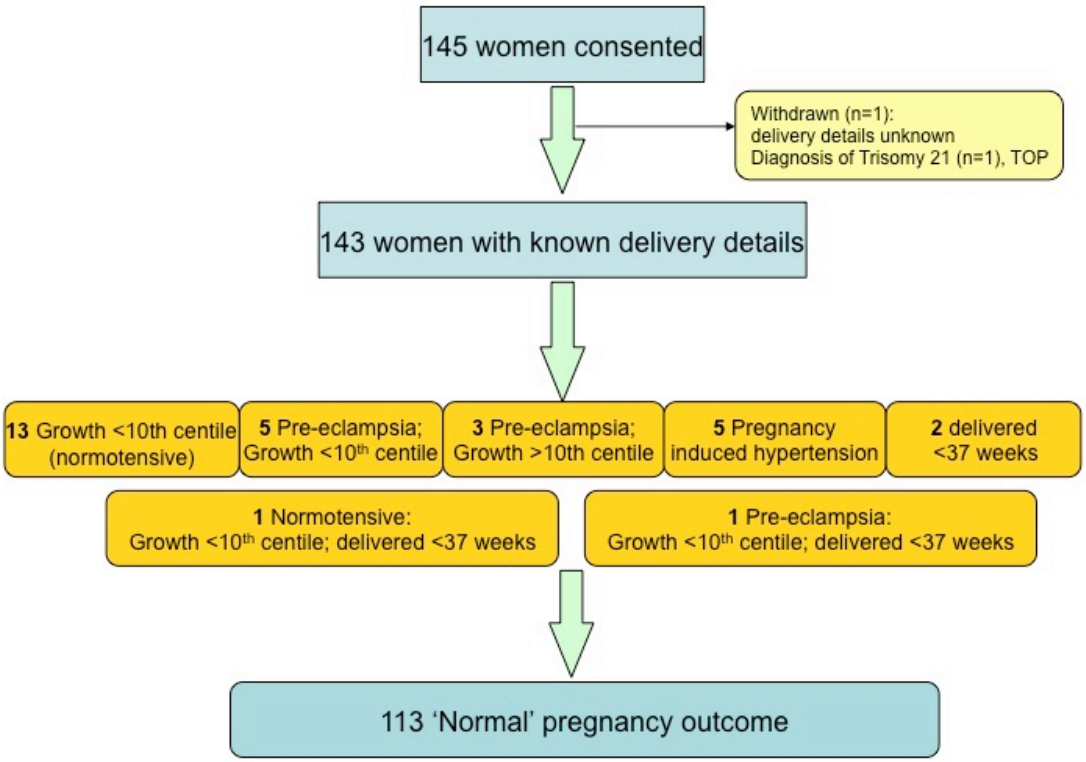



**Figure 10: Pregnancy outcomes for all participants in the study (Phase I and II).**

Baseline characteristics for all participants are shown in Table 3 (page 58) and for all normotensive participants who delivered at term in Table 5 (page 60). The pregnancy outcomes for both Phase I & II participants are given in Table 4 (page 59). There were no significant difference between the groups except for birth and placental weights.

**Table 3: Baseline patient demographics of *all participants* (phases I & II)**

| | SGA (n=20) | AGA (n=123) | P values |
|---|---|---|---|
| **Age (years)** | 31 (16-39) | 30 (18-44) | 0.45* |
| **BMI (at booking)** | 24.9 (17-35) | 24.2 (18-33) | 0.71* |
| **Smoker** | 1 (5%) | 21 (17%) | 0.93† |
| **Alcohol (units per week)** | 1.1 (0-4) | 1.3 (0-18) | 0.49* |
| **Multiparous** | 12 (67%) | 59 (48%) | 0.68† |
| ➢ **History of SGA** | 9 (75%) | 17 (29%) | 0.31† |
| ➢ **History of PET** | 5 (42%) | 6 (10%) | 0.15† |
| **Known obstetric family history** | 18 (90%) | 123 (100%) | |
| ➢ **FHx of SGA** | 2 (11%) | 8 (7%) | 0.63† |
| ➢ **FHx of PET** | 1 (6%) | 18 (15%) | 0.47† |
| ➢ **FHx recurrent miscarriage** | 0 | 2 (2%) | |
| ➢ **FHx late IUD (>34 weeks)** | 0 | 1 (1%) | |
| **Self- reported ethnicity** | | | |
| ➢ **White European** | 18 (90%) | 115 (93%) | 1.0† |
| ➢ **Indian** | 0 | 2 (2%) | |
| ➢ **Pakistani** | 0 | 1 (1%) | |
| ➢ **Mixed** | 1 (5%) | 4 (3%) | 0.54† |
| ➢ **South East Asian** | 1 (5%) | 1 (1%) | 0.3† |
| **IVF pregnancy** | 0 | 11 | 0.7† |
| **Placental site** | | | |
| ➢ **Anterior** | 13 (65%) | 50 (41%) | 0.3† |
| ➢ **Posterior** | 2 (10%) | 48 (39%) | 0.07† |
| ➢ **Lateral** | 3 (15%) | 14 (11%) | 0.71† |
| ➢ **Fundal** | 2 (10%) | 9 (7%) | 0.66† |
| ➢ **Praevia** | 0 | 2 (2%) | |
| **P-values calculated using *t-test or † Fisher's exact test** | | | |

**Table 4: Delivery details for *all participants* (phases I & II)**

| | SGA (n=20) | AGA (n=123) | p values |
|---|---|---|---|
| Customised birth weight centile | 4 (0-9) | 52 (10-99) | N/A |
| Birth weight (g) | 2629 (1780-3116) | 3478(2450-4730) | <0.001* |
| Placental weight (g) | 473 (250-647) | 611(380-920) | 0.002* |
| Gestation at delivery (days) | 39+2<br>(38+1 to 40+4) | 39+4<br>(35+4 to 42+2) | 0.6* |
| Onset of labour | | | |
| ➢ Spontaneous | 4 (66%) | 41 (79%) | 1.0† |
| ➢ Induced | 0 | 10 (19%) | |
| ➢ Elective Caesarean | 2 (34%) | 1 (2%) | 0.043† |
| Mode of delivery | | | |
| ➢ SVD | 2 (34%) | 39 (75%) | 0.46† |
| ➢ Instrumental | 2 (34%) | 8 (15%) | 0.33† |
| ➢ Caesarean section | 2 (34%) | 5 (10%) | 0.2† |
| Admission to NICU | 0 | 0 | N/A |
| p-values calculated using *t-test or † Fisher's exact test | | | |

**Table 5: Baseline patient demographics of *all normotensive participants who delivered at term* (phases I & II)**

| | SGA (n=13) | AGA (n=113) | p values |
|---|---|---|---|
| **Age (years)** | 30 (16-37) | 30 (18-44) | 0.59* |
| **BMI (at booking)** | 23.8 (17-33) | 23.9.2 (18-33) | 0.58* |
| **Smoker** | 1 (5%) | 18 (16%) | 0.93† |
| **Alcohol (units per week)** | 1.1 (0-4) | 1.4 (0-18) | 0.42* |
| **Multiparous** | 7 (54%) | 52 (46%) | 0.77 † |
| ➢ **History of SGA** | 5 (71%) | 17 (33%) | 0.09† |
| ➢ **History of PET** | 1 (42%) | 6 (5%) | 1.0† |
| **Known obstetric family history** | 12 (92%) | 113 (100%) | |
| ➢ **FHx of SGA** | 1 (11%) | 8 (7%) | 0.5† |
| ➢ **FHx of PET** | 0 (6%) | 17 (15%) | 0.6† |
| ➢ **FHx recurrent miscarriage** | 0 | 2 (2%) | |
| ➢ **FHx late IUD (>34 weeks)** | 0 | 1 (1%) | |
| **Self- reported ethnicity** | | | |
| ➢ **White European** | 11 (90%) | 106 (94%) | |
| ➢ **Indian** | 0 | 2 (2%) | |
| ➢ **Pakistani** | 0 | 1 (1%) | |
| ➢ **Mixed** | 1 (5%) | 3 (3%) | |
| ➢ **South East Asian** | 1 (5%) | 1 (1%) | |
| **IVF pregnancy** | 0 | 11 | 0.7† |
| **Placental site** | | | |
| ➢ **Anterior** | 9 (69%) | 50 (41%) | 0.34† |
| ➢ **Posterior** | 2 (15%) | 48 (39%) | 0.24† |
| ➢ **Lateral** | 1 (8%) | 14 (11%) | 1.0† |
| ➢ **Fundal** | 1 (8%) | 9 (7%) | 1.0† |
| ➢ **Praevia** | 0 | 2 (2%) | |
| **p values calculated using *t-test or † Fisher's exact test** | | | |

# 4 Observations in placental anatomy and SGA

## *4.1 Introduction, background and aims*

### 4.1.1 Histological anatomy of the utero-placental interface[4]

The gross vascular anatomy of the pelvis is well understood. The uterine arteries travel bi-laterally up the outside of the uterus supplying the arcuate arteries before anastomosing with the ovarian vessels. The arcuate arteries pass medially around the body of the uterus in the outer third of the myometrium giving off the radial arteries which plunge through the inner myometrium to terminate in the basal arteries (supplying the basal endometrium) and the spiral arteries which continue to the endometrial surface (Drake et al. 2007).

The blood supply to the endometrium has evolved to cope with the demands of very different haemodynamic situations. Massive changes are required to convert small, muscular vessels (which ensure minimal blood loss at menstruation) to high capacity, low resistance conduits needed for a term placenta. However, despite many centuries of research, the precise nature and development of the placental vasculature remains a contentious issue.

The Roman physician, Claudius Galen, first described the blood flow to the utero-placental unit in 130 AD. However, he erroneously proposed that the fetal and maternal circulations were interconnected. Leonardo Da Vinci is credited with the first accurate illustrations of a fetus inside a dissected uterus, although it appears that the placenta was of less interest to him as the one he drew was

[4] The utero-placental interface refers to the junction between the placenta and the uterus but is not limited to any particular depth of tissue on either side.

cotyledonary such as is found in cattle (Boyd et al. 1970). The renaissance anatomist, Julius Caesar Arantius, first suggested that the fetal and maternal circulations were separate. However, it was the 18th century before this was proven by the Hunter brothers injecting wax into the placental vasculature *in utero* (Hunter 1774).

Much of the early histological work to define the intricate endometrial vasculature was performed on primates (Daron 1936; Hasner 1946; Bartelmez 1957; Ramsey et al. 1967). The pattern of change throughout pregnancy in the human spiral arteries was first demonstrated by Harris and Ramsey (Harris et al. 1966). From serial histological sections, they painstakingly reconstructed representations of the 'coiled' arteries from a collection of uteri at different gestations, which had the placenta *in situ*. The normality of these changes was further confirmed by Brosens (Brosens et al. 1967) who introduced the concept of the "physiologic transformation of the spiral arteries". From this early work the theory developed that trophoblast invasion results in loss of musculo-elasticity and subsequent dilatation of the vessel walls.

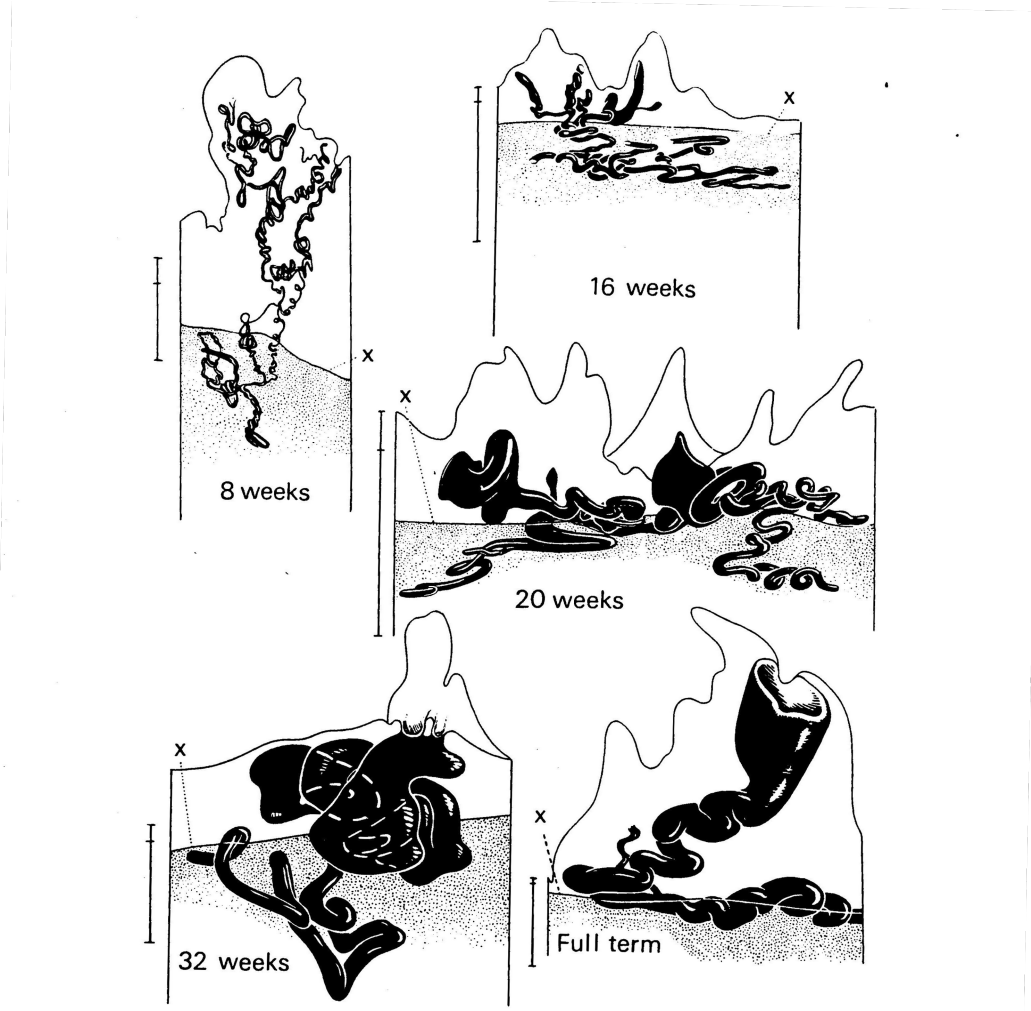



**Figure 11: Reconstruction of the spiral arteries at various stages of pregnancy.**

Drawn by Frank B Price from (Harris et al. 1966)[5].

### 4.1.2 Characterising the spiral artery blood flow *in vivo*

The vasculature of the placental bed was investigated with retrograde femoral X-ray angiography in humans in the 1950s (Borell et al. 1952). This demonstrated the presence of jets of blood spurting from a variable number of openings into the IVS. This was assumed to be the blood from the mouth of the spiral arteries Figure 12, page 64).

The nature of these jets, including the effect of uterine contractions and vaso-constrictive agents, was further investigated in primates throughout the 1960s

[5] Reproduced with permission from the Carnegie Institute

(Ramsey et al. 1960; Ramsey et al. 1963; Ramsey et al. 1967) and early 1970s (Misenhimer et al. 1972). The use of contrast agents and ionizing radiation prevented this technique from being used to study human pregnancies. Attempts at reproducing the work in primates using contrast enhanced fast scan magnetic resonance imaging (MRI) were made in the early 1990s (Panigel et al. 1993) with encouraging results. These studies were not repeated in humans either, probably due to concerns of using contrast agents and the rapid development of considerably cheaper ultrasound techniques.

The spiral arteries have been histologically shown to retain their musculo-elastic structure in pregnancies complicated by growth restriction and pre-eclampsia (Brosens et al. 1977; De Wolf et al. 1980; Khong et al. 1986; Lyall 2002; Pijnenborg et al. 2006; Khong et al. 2011). Therefore, it follows that in this pathology the functional effect should be observed as a difference in the characteristics of the jet of blood flowing into the IVS.

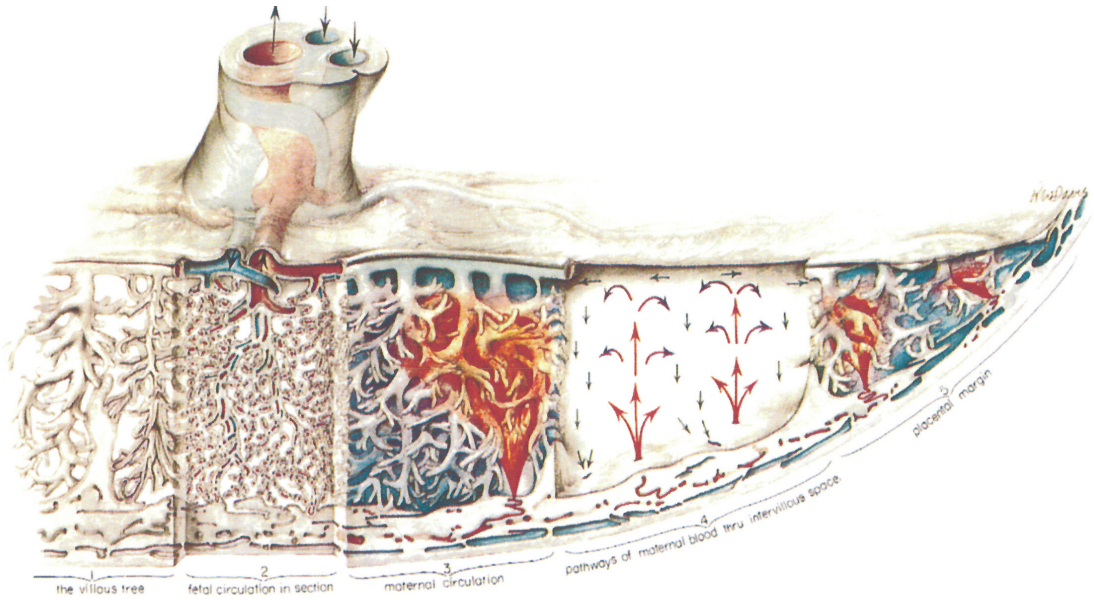



**Figure 12: Diagram demonstrating the anatomy of the spiral artery jets.** Drawing by Ranice Davis Crosby. From (Harris et al. 1966)[6].

[6] Reproduced with permission from the Carnegie Institute

#### 4.1.2.1 Spiral artery jet waveform

Doppler ultrasound examination of the spiral artery waveform has been attempted in both normal pregnancies and those with adverse outcomes (Jurkovic et al. 1991; Matijevic et al. 1995; Murakoshi et al. 1996; Kurjak et al. 1997; Hsieh et al. 2000; Chafetz et al. 2007; Ozkaya et al. 2007). The results are conflicting and the correlations with pregnancy outcome weak. The commonly employed method relies on identifying the spiral arteries by approximate location in the placental bed[7] and their 'recognisable' bi-directional waveform (Murakoshi et al. 1996). However, this method is flawed: with no fixed anatomical landmarks it is impossible to measure individual vessels at the same point; angle correction is not appropriate because of the tortuous nature of the spiral artery; and, recognition by waveform alone might inherently select 'normal' vessels, thereby missing pathology.

The decidua-placental interface is readily identifiable with B-mode ultrasound. Using colour Doppler, the single unidirectional signals seen appearing from the tangle of maternal vessels at this interface are the jets of blood discharging from the spiral arteries into the IVS. Identifying this interface allows measurement of the waveform at a fixed anatomical site: the mouth of the spiral artery. As the flow at this point is unidirectional, angle correction can be used to optimise the velocity results.

[7] The placental bed is defined as the portion of the uterus (decidua and myometrium) lying underneath the placental insertion site Benirschke, K., et al. (2000). Pathology of the human placenta; 4th Edition. New York, Springer-Verlag.

#### 4.1.2.2 Spiral artery jet size and velocity

Histological specimens may be prone to artefact due to sampling and fixing errors, and cannot fully represent the *in vivo* haemodynamics of a vessel (Boyd et al. 1970). Ideally, real time imaging should be able to provide an estimate of the size of the jet and its velocity as it enters the IVS. However, the use of colour Doppler to assess such parameters is fraught with difficulties. Phantom models have shown that the size of a lumen measured from the colour Doppler signal is linearly related to the dynamic range and gain setting used (Potter et al. 2008). That study also showed that even if the machine settings are constant, a 5 mm increase in distance between the probe and the vessel reduces measured lumen diameter by 0.04 ± 0.03 mm ($p < 0.001$). The angle of insonation affects the recorded velocity (Kremkau 1992). It is therefore not unsurprising that *in vivo* measurement of the jets has not previously been reported as the absolute values may be unreliable and not comparable between patients. Given the longitudinal nature of our data, with repeated measurements in the same participant, it is possible to crudely explore the relative change in the observed size and velocity of the jets over time.

#### 4.1.2.3 Placental lakes

One of the first reported placental abnormalities seen with B-mode ultrasound is a simple, apparently fluid-filled, hypoechoic lesion known as the placental lake (Fisher et al. 1976; Cooperberg et al. 1979) Figure 5, page 44. It is surrounded by placental parenchyma of 'normal' echogenicity which distinguishes it from echogenic cystic lesions (ECL) which have a 'halo' of hypoechoic tissue around them and a crenated border (Proctor et al. 2010). Whilst ECLs have been suggested to be a poor prognostic sign in severely growth restricted fetuses (Viero et al. 2004) their underlying pathology is not fully understood. Whilst they are most likely to represent intervillous thrombi and placental tissue infarction (Harris et al. 1990; Proctor et al. 2010) ECLs on ultrasound only have 37% sensitivity and 63% positive predictive value (PPV) for villous infarcts confirmed on histological examination (Viero et al. 2004). It has been suggested that they occur as a result of the high pressure 'jet hose' effect resulting from inadequately transformed spiral arteries (Burton et al. 2009a) disrupting the placental villous tree. However, this is yet to be demonstrated experimentally.

Placental lakes are usually reported as completely benign (Thompson et al. 2002; Viero et al. 2004; Reis et al. 2005), although a recent study has suggested a link with threatened first trimester loss (Cooley et al. 2011). This potentially implicates the early vasculature in the formation of these lakes. Having noticed the association of mega-jets with simple placental lakes their prognostic significance for our study population was explored.

### 4.1.3 Aims of this chapter

The purpose of this part of the study was to explore **Hypothesis 2.1.1, Page 30,** by investigating:

1. If the waveform of the jet of blood from the mouth of the spiral artery could be reliably and reproducibly recorded using 2-D colour Doppler.
2. Whether this waveform altered in a gestation dependent manner in concordance with histological data.
3. The nature of the relationship between the jet waveform and that of the uterine arteries.
4. Whether the waveform was different in pregnancies resulting in SGA babies compared with AGA babies.
5. If the relative size and velocity of the jet changed with increasing gestation as predicted by the observed histological changes.
6. Whether the rate of change in the size or velocity was different for SGA babies compared with AGA babies.
7. Whether the presence, or timing of appearance, of placental lakes was different for SGA babies compared with AGA babies.
8. Whether any other observed vascular phenomena were linked to adverse pregnancy outcome.

## *4.2 Methods*

### 4.2.1 General methods for measurement of the jets and uterine arteries

This was Phase I of the spiral 3-D study. The women were recruited at between 11 and 13 weeks' gestation. An extra seven scans were performed throughout their pregnancy and outcome data was retrieved from the patient notes after delivery (Full details of study in 3.3, page 37). At each visit the whole placenta was systematically examined to identify the most prominent jet which was then measured using the previously described technique chapter 2 (page 39). If this jet met the predefined criteria of having visible blood flow travelling more than 10mm into the placental tissue (or over 50% of the way across the placenta if it was <20mm thick) it was classed as a mega-jet, recorded as such and then the next most prominent vessel identified. This process was continued until all the mega-jets and then the three most prominent (non-mega) jets had been identified. The frequency distribution for all the most prominent jets recorded at each visit was plotted and examined. The waveform, peak velocity and length of the jet and the width of the mouth of the (non-mega) spiral artery jets were measured. The uterine artery waveforms were also measured using recognized, gestation appropriate, techniques (3.3.3, page 39).

### 4.2.2 Jets: Intra- and inter-observer variability analysis

A sub-group of participants were selected to assess inter- and intra-observer variability. As the range and magnitude of the variance components for each characteristic were unknown, a sample size could not be defined in advance.

Therefore ongoing statistical analysis was carried out until the parameters could be estimated and an adequate sample size defined. As participation in these sub-groups required more exposure to Doppler ultrasound, once the sample sizes were deemed to be sufficient by the statistician, recruitment was stopped.

Intra-observer variability was assessed by one observer (SC) measuring the waveform at the mouth of the same vessel in the same woman at the same time point, three times. Inter-observer variability was assessed by two different observers (SC and LI) separately identifying the three most prominent vessels and measuring them in the same woman at the same time point, each blinded to the other's results.

### 4.2.3 Statistical methods

Statistical analyses were performed with help from Jacqueline Birks at the Centre for Statistics in Medicine, University of Oxford, using SPSS (version 16.0, IBM Corporation, NY, USA), SAS (version 9, SAS Institute Inc., Cary, NC, USA) and Stata (version 10.0, Stata Corps, LP, USA).

#### 4.2.3.1 Jets: Intra-observer and inter- observer variability analysis

Inter-observer variability is often assessed using the Bland-Altman technique. However, this can only be used when there are two repeats. If the design is more complex, as in this study, a more general method must be used. Therefore, the intra-observer variability analysis was carried out using the mixed procedure of SAS[8]. Patients are considered a random effect. Gestation is considered to be a fixed effect. This results in an analysis adjusted for gestation. The 'within patient' and 'between patients' components of variance were estimated. The intra class

[8] Statistical analysis carried out by Jacqueline Birks at the Centre for Statistics in Medicine, Oxford.

correlation coefficient was derived from these variance components. Repeatability was calculated as $2\sqrt{2}$ times within subject variation. It is not dimensionless and depends on the scale of the measurement. It is defined as the upper prediction limit for the absolute difference of two measurements by the same method. Here it refers to measurement of the same vessel, at the same time by the same observer.

To analyse inter-observer variability, the data for each assessor were initially analysed separately[9]. These analyses showed that there might be a difference between assessors for within and between patient variations. Therefore the full model was designed to take this into account. The method of linear mixed models was used, which allows for the correlation between the three measurements on one patient[9]. The assessor was defined as a fixed effect term in the model and therefore the difference between assessors could be tested. The patient measurements used were the mean of measuring three different vessels per patient. As the question of interest is how the mean patient measurements of PI and RI differ between assessors, the limits of agreement were calculated as mean between patient difference ± 2 x sd (mean between patient difference).

#### 4.2.3.2 Spiral artery jet and uterine artery waveforms

The PI and RI data for both the jets and uterine arteries consisted of a series of repeated measurements in the same patient at different gestations. Therefore, to reflect the longitudinal nature of the data, a linear mixed model methodology was used[9]. The number and frequency of the dependent variables varied between

[9] Statistical analysis carried out by Jacqueline Birks at the Centre for Statistics in Medicine, Oxford.

patients. The change in a variable over gestation was modelled using a second order regression equation as this model fitted better than a linear regression. The random effects were calculated for each subject, each parameter allowed a random deviation from the population regression model. The fixed effects included a second order term to control for gestation.

Also the relationship between the mean jet PI and both mean and minimum Ut A PI separately for each visit was explored using Spearman's Rank[10]. This was repeated to compare the jet RI and Ut A RI.

#### 4.2.3.3 Spiral artery jet waveform differences in SGA babies

The methods of linear mixed models were used to analyse the data[10]. The dependent variables Jet PI, Jet RI, mean uterine artery Ut A PI and mean Ut A RI, were each measured at seven gestation time points, between 12 and 35 weeks, for each participant. The change in each variable over gestation was modelled using a second order regression equation. A random coefficient model was fitted which allows patients to differ in their rate of change of PI or RI. The random coefficients describe the fitted lines for each patient, and the random effects are the deviations of the individual random coefficients from the coefficients of the mean line. A factor, '*SGA*', describing whether the baby was <10$^{th}$ centile or not, is included in the model, as a main effect and as an interaction with gestation, as a fixed effect. These fixed effects may explain some of the variation between participants in the intercepts and gradients. Here, interest centres on the effect of the interaction of the factor with time on the rate of change. To model the correlation between measurements over time within patients, the unstructured covariance matrix was used where the

[10] Statistical analysis carried out by Jacqueline Birks at the Centre for Statistics in Medicine, Oxford

variance at each time and covariance between two times are freely estimated. There is no functional relationship imposed on the covariance between two time points.

Also the PI and RI for normally grown and SGA babies were compared at the first and last visit using linear regression analysis controlling for gestation[11]. The percentage difference in the mean PI and RI between the first and last visit was calculated for each participant and the results for SGA and AGA compared with a t-test and box-plots. As this study is exploratory, involving only a small number of participants, the level of significance at $p<0.1$ was deemed acceptable.

#### 4.2.3.4 Spiral artery jet size and velocity

To explore any difference in the rate of change of the size and velocity of the jets between SGA and AGA pregnancies the method of linear mixed models was used again[10]. The dependent variables jet mouth, jet length and jet peak systolic velocity were each measured at seven gestation time points, between 12 and 35 weeks, for each participant. The same statistical technique was used as described in 4.2.3.3. Again the interest centred on the effect of the interaction of the factor over time.

The percentage difference in the mean length, mouth width and peak systolic velocity of the jets measured at the first and last visit was calculated for each participant. The results for SGA and AGA were compared with a t-test and box-plots.

[11] Statistical analysis carried out by Jacqueline Birks at the Centre for Statistics in Medicine, Oxford.

#### 4.2.3.5 Mega-Jets and placental lakes

Once presence of either mega-jets or lakes had been noted they remained present in subsequent scans. Therefore the time of their first appearance was analysed using the Kaplan-Meier estimator. The difference in trends of appearance between normal pregnancies and those with adverse outcomes were analysed using a Log rank (Mantel-Cox) test.

## *4.3 Results*

Data from the 65 women included in Phase I were analysed. (3.6.1, page 52).

### 4.3.1 Measurement of the jets

It was possible to measure three jets in all 65 women for the first four visits, except for one participant in whom the measurements could not be obtained at the first visit in the allocated 20 minutes. At the fifth and subsequent scans, from 23 weeks, the overlying fetus occasionally obscured posteriorly sited placentas. This was most marked at the seventh scan (33 weeks), when jets could only be measured in 48 (92%) of participants (Figure 13, page 78).

All the jets were visibly pulsatile and could be measured with the 'auto-trace' feature on the ultrasound machine until the 4$^{th}$ visit (approximately 20 weeks' gestation). At this gestation one participant was found to have only jets with pulsatility so reduced that it could not be reliably measured (the waveform appeared to be turbulent with a possible suggestion of pulsatility but the auto trace feature on the E8 recorded it as continuous). The number of women with only non-pulsatile jets gradually increased with increasing gestation until at 34 weeks, 19 (37%) had no measureable jets (Figure 14, page 78).

### 4.3.2 Jets: Intra-observer and inter-observer variability analysis

Fourteen patient episodes were recorded to assess intra- and inter-observer variation. The data were analysed at this stage. For intra-observer variability the intra-class correlation co-efficient (ICC) for PI and RI was 0.9. On assessing the inter-observer variability it was seen that this sample size gave a good estimate of variance, Table 6 (page 75). There was no significant difference between the overall mean for observer 1 compared with observer 2 over the patients.

**Table 6: Results for Inter-observer reproducibility sub-group analysis of measurement of the three most prominent jets[12] (n=14)**

| | Mean (sd) for assessor 1 | Mean (sd) for assessor 2 | Mean difference (sd) assessor1 – assessor2 | Limits of agreement |
|---|---|---|---|---|
| **PI** | 0.38 (0.08) | 0.37 (0.08) | 0.008 (0.06) | -0.12 to 0.13 |
| **RI** | 0.31 (0.05) | 0.30 (0.05) | 0.008 (0.03) | -0.06 to 0.07 |

[12] Statistical analysis carried out by Jacqueline Birks at the Centre for Statistics in Medicine, Oxford.

### 4.3.3 Spiral artery jet and uterine artery waveforms

The mean RI of the jets was observed to decrease with increasing gestation (Figure 15, page 79). This follows the same pattern as both the mean and the minimum RI of the uterine arteries (Figure 16, page 79). The PI showed the same pattern for both the jets and the uterine arteries.

Although the PI and RI for the jets and the uterine arteries show a similar relationship there was no significant correlation between their trends when the strong effect of gestation was controlled for. There was also no trend observed in the correlation coefficient values with increasing gestation when they were analysed separately at each visit (Table 7, page 77).

**Table 7: The correlation coefficients at each visit comparing the mean jet PI/RI to both the mean uterine artery (*meanUt A*) PI/RI and the minimum uterine artery (*minUt A*) PI/RI[13]**

| | PI | | RI | |
|---|---|---|---|---|
| Visit | **Jet Vs. *meanUt A*** | **Jet Vs. *minUt A*** | **Jet Vs. *meanUt A*** | **Jet Vs. *minUt A*** |
| 1 | 0.03 | -0.02 | 0.02 | -0.06 |
| 2 | 0.41 | 0.52 | 0.48 | 0.55 |
| 3 | 0.01 | 0.03 | -0.03 | <0.01 |
| 4 | 0.37 | 0.19 | 0.28 | 0.23 |
| 5 | 0.29 | 0.20 | 0.24 | 0.17 |
| 6 | 0.14 | 0.35 | 0.16 | 0.34 |
| 7 | 0.30 | 0.18 | 0.29 | 0.16 |

[13] Statistical analysis carried out by Jacqueline Birks at the Centre for Statistics in Medicine, Oxford.

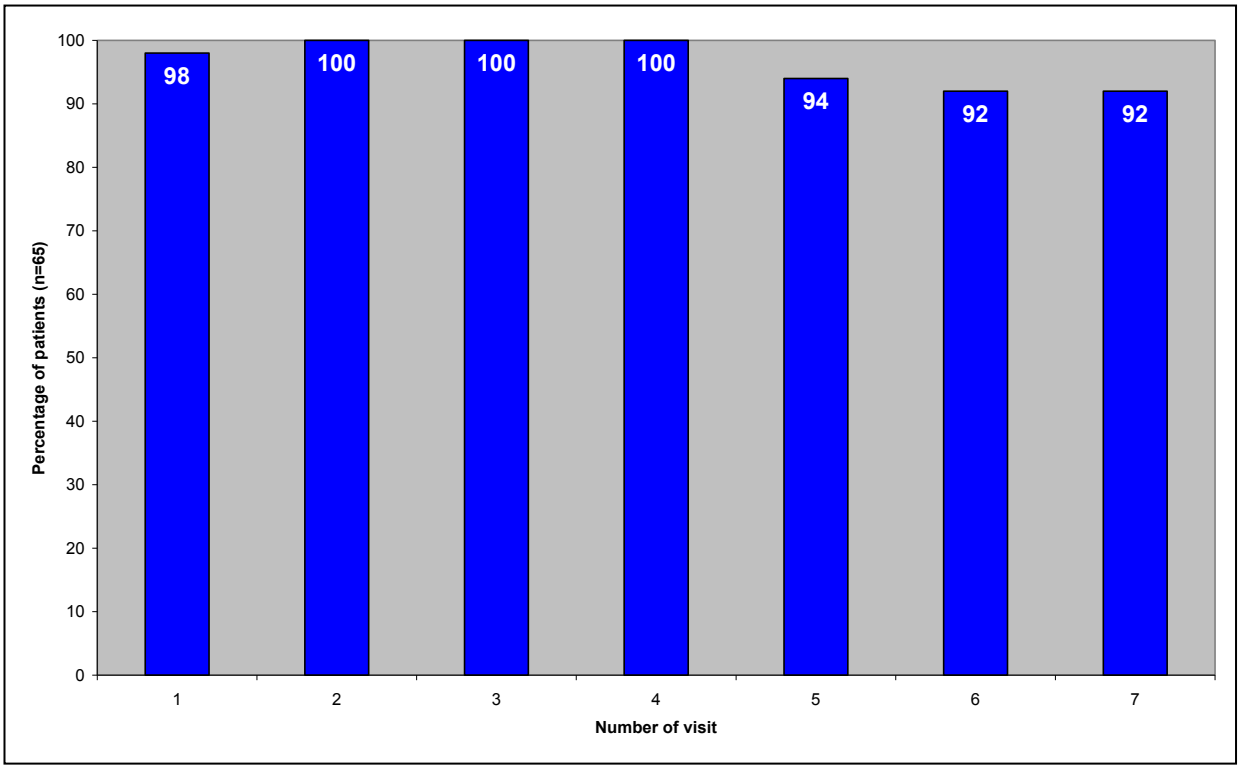



**Figure 13: Percentage of participants with three jets measured at each visit.**

(n=65)

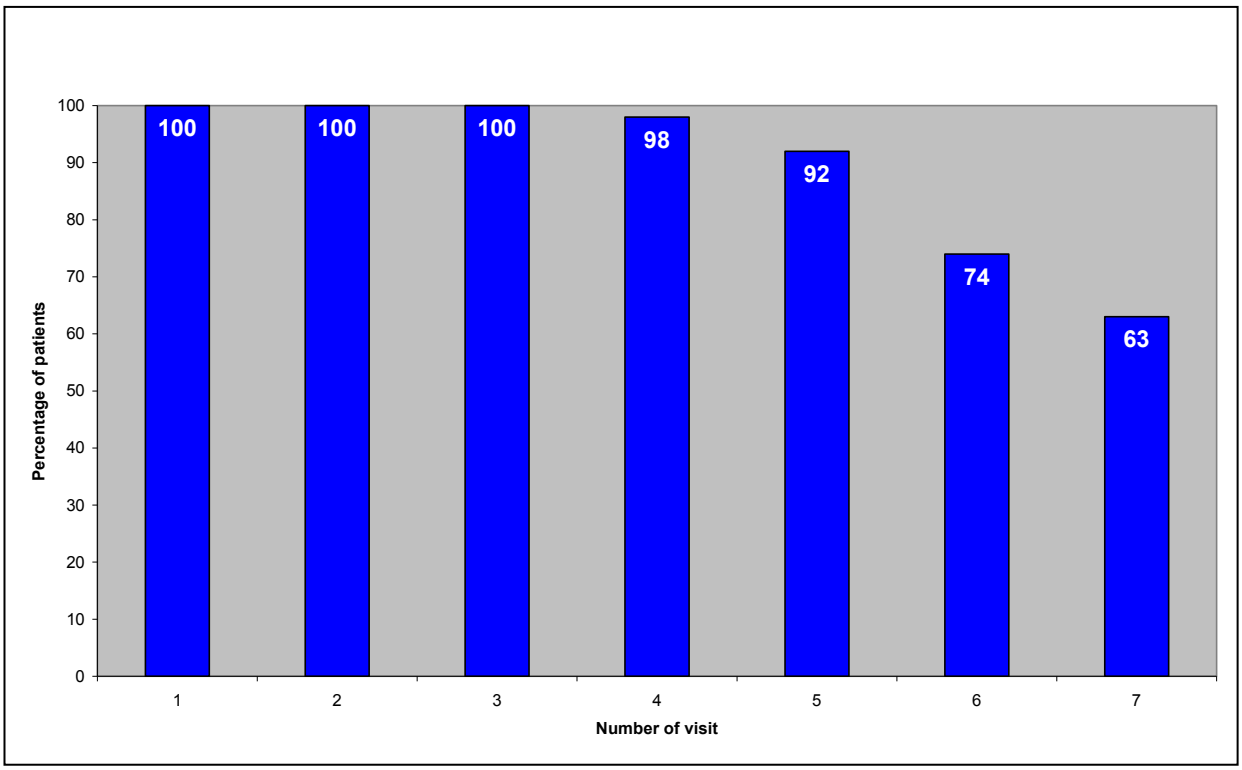



**Figure 14: Percentage of participants with pulsatile jets at each visit.**

(n=65)

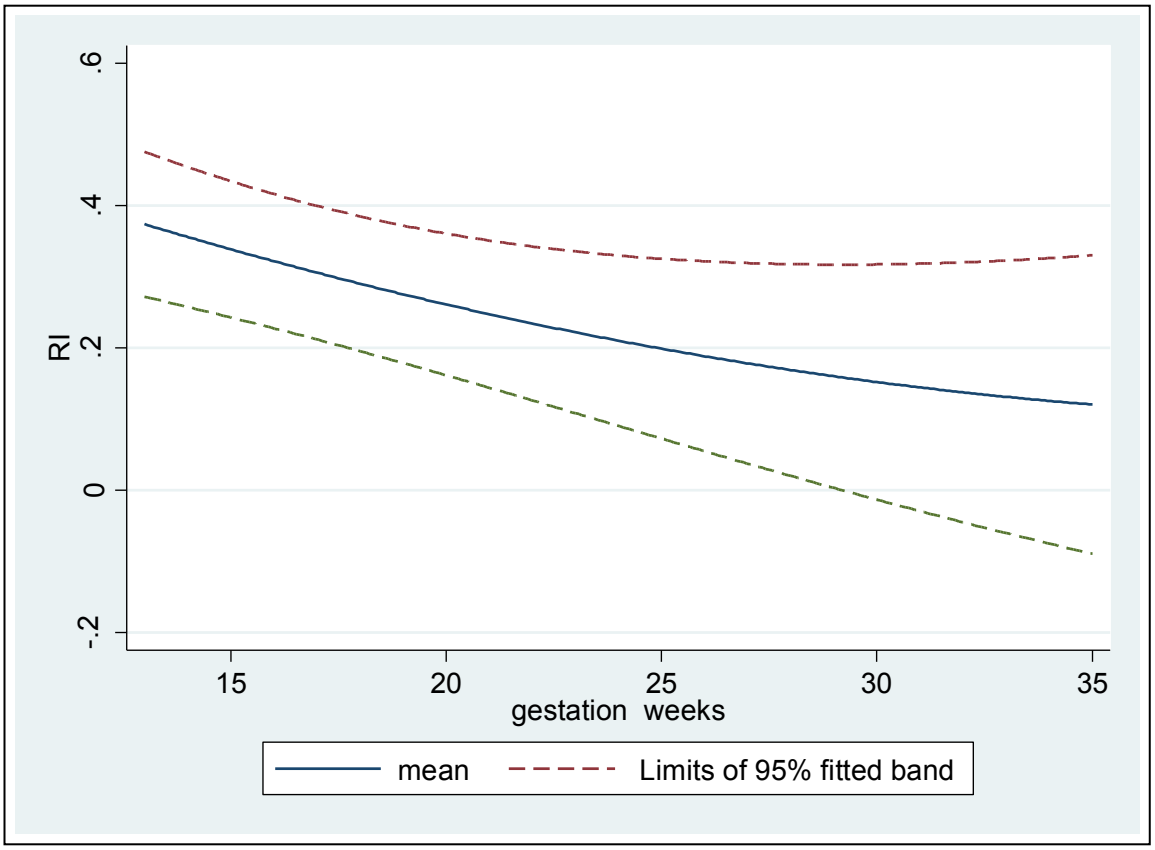



**Figure 15: The relationship between the RI of the jets and gestation.[14]**

('Limits of 95% fitted band' is equivalent to the 95% prediction interval)

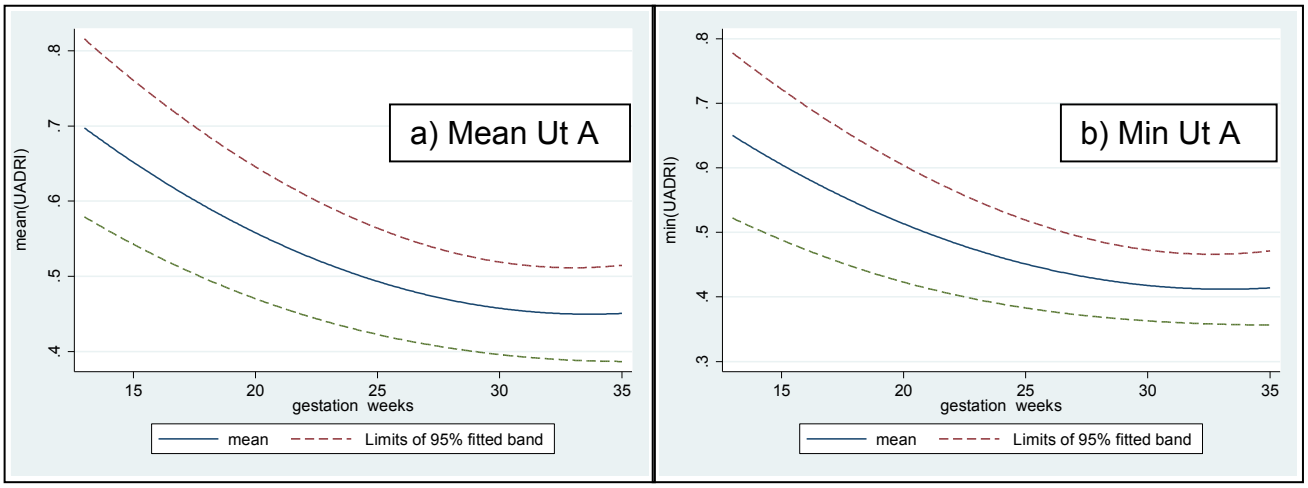



**Figure 16: The relationship between a) the mean RI and b) the minimum value for RI of the uterine arteries, and gestation.[13]**

[14] Graphs generated by Jacqueline Birks at the Centre for Statistics in Medicine, Oxford

### 4.3.4 Spiral artery jet waveform differences in SGA pregnancies

Figure 17 (page 82) shows the change in the mean PI and RI of the jets with increasing gestation for both SGA and AGA babies. The trend for both indices appears shallower in SGA babies. Figure 18 (page 83) shows the same graphs for the uterine artery PI and RI. The results of the linear mixed model are presented in Table 8 (page 81). The coefficients of both gestation and $(\text{gestation})^2$ are significant ($p<0.0001$) for both PI and RI. This indicates that the change of PI and RI over time is not linear and that a second order model is a better fit. This second order model demonstrated that at the $p<0.1$ level both the PI and RI for the jets of SGA babies were significantly different to that of the AGA babies ($p=0.06$). Neither the PI nor the RI of the uterine arteries was significantly different between SGA and normally grown babies ($p=0.8$).

When examining the first and last visits individually, there was no significant difference in the mean PI and RI between SGA and AGA babies at either of these time points ($p=0.31$ and $0.34$ respectively). When looking at the difference in the PI and RI between the first and last visit, the boxplots appear to show that both indices undergo less change in SGA pregnancies, Figure 19 (page 85). However, this is not statistically significant ($p=0.09$ and $p=0.12$).

There was no significant difference between the SGA and AGA groups for PI or RI at visit 1 or visit 7, after adjustment for gestation, Table 9 (page 84).

**Table 8**: **The results for the linear mixed model coefficients with 95% confidence interval for PI and RI over gestation for SGA babies compared to normally grown babies**[15]

| | **PI** | | |
|---|---|---|---|
| **Fixed effects** | **Coefficient (SE)** | **95% CI** | **P value** |
| **Constant baseline** | 0.97 (0.05) | 0.9 to 1.1 | |
| **Gestation** | -0.05 (0.01) | -0.05 to -0.04 | <0.0001 |
| **(Gestation)$^2$** | 0.001 (0.001) | 0.001 to 0.001 | <0.0001 |
| **SGA** | -0.12 (0.08) | -0.28 to 0.034 | |
| **SGAr*Gestation** | 0.007 (0.003) | -0.001 to 0.013 | 0.06 |
| | **RI** | | |
| **Fixed effects** | **Coefficient (SE)** | **95% CI** | **P value** |
| **Constant baseline** | 0.66 (0.04) | 0.59 to 0.74 | |
| **Gestation** | -0.03 (0.003) | -0.03 to -0.02 | <0.0001 |
| **(Gestation)$^2$** | 0.001 (0.001) | 0.001 to 0.001 | <0.0001 |
| **SGA** | -0.09 (0.05) | -0.20 to 0.01 | |
| **SGAr*Gestation** | 0.005 (0.003) | -0.0001 to 0.01 | 0.04 |

[15] Statistical analysis carried out by Jacqueline Birks at the Centre for Statistics in Medicine, Oxford.

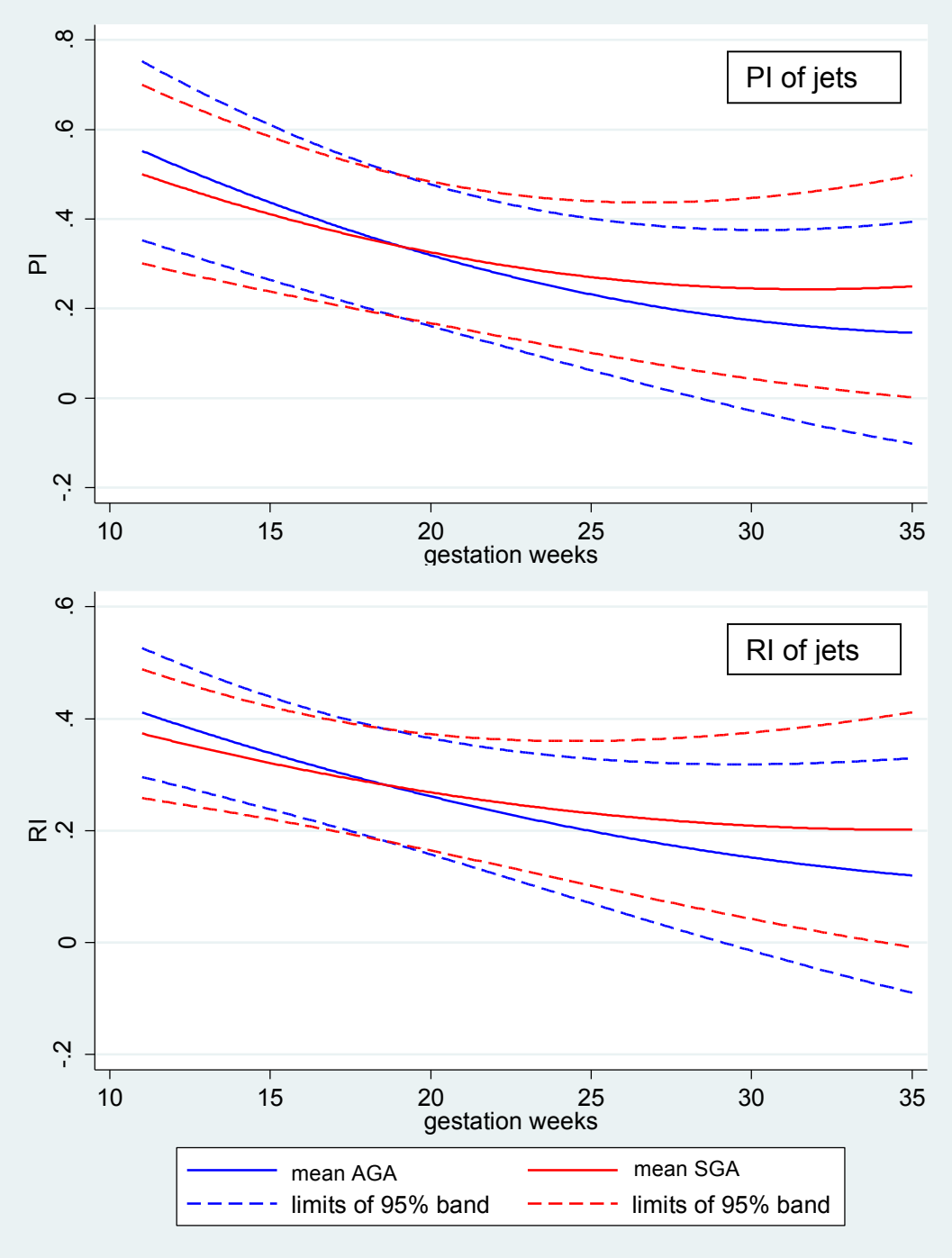



**Figure 17: The change in PI and RI for the jets of SGA pregnancies compared with AGA.**[16]

The solid blue line indicates the mean of the AGA babies (dotted lines are the 95% bands in which 95% of the measurements are predicted to lie). The solid red line indicates the mean for the SGA babies.

[16] Graphs supplied by Jacqueline Birks at the Centre for Statistics in Medicine

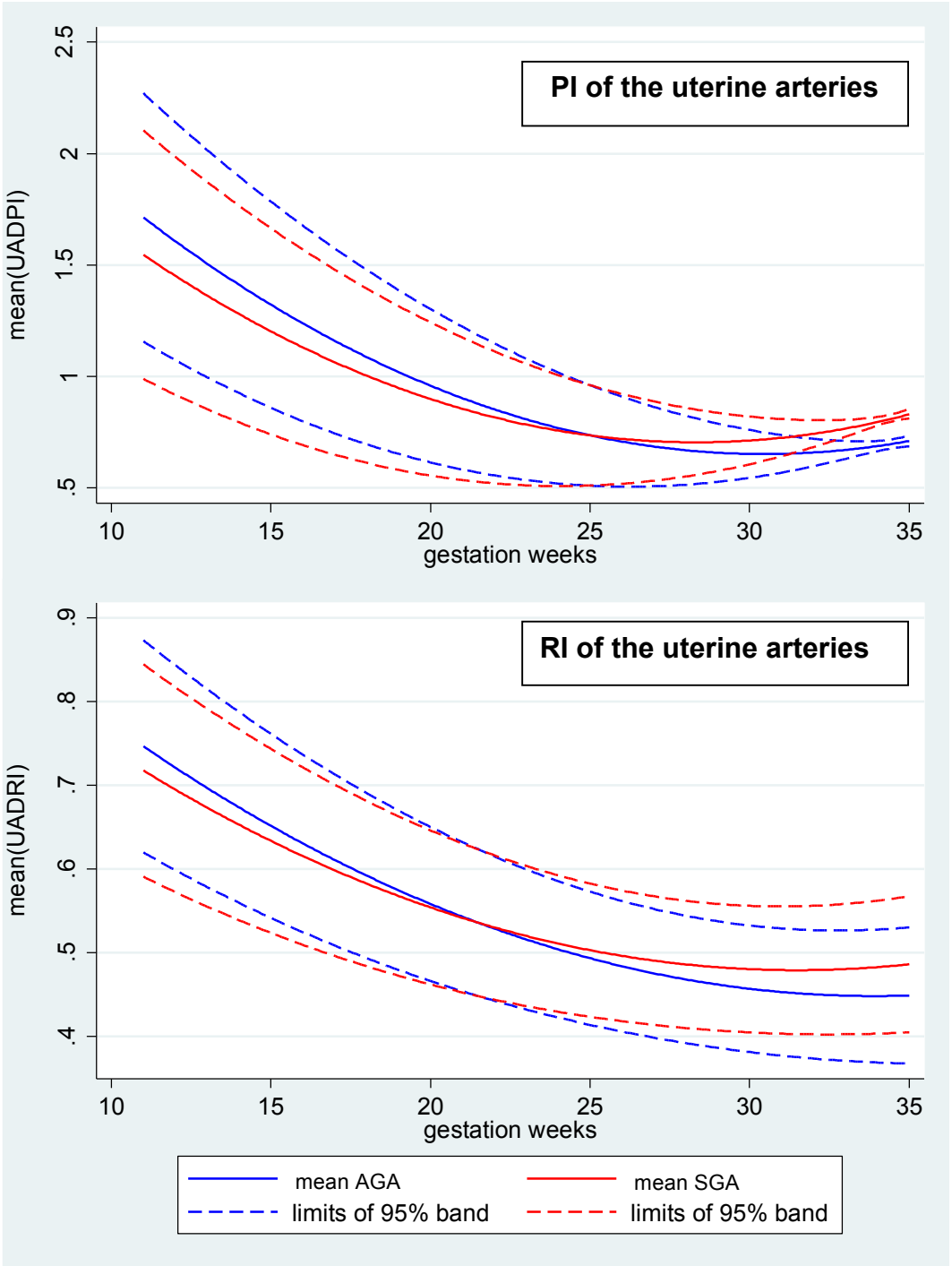



**Figure 18: The change in PI and RI for the uterine arteries of SGA pregnancies compared with AGA.**[17]

The solid blue line indicates the mean of the AGA babies (dotted lines are the 95% bands in which 95% of the measurements are predicted to lie). The solid red line indicates the mean for the SGA babies.

[17] Graphs supplied by Jacqueline Birks at the Centre for Statistics in Medicine

**Table 9: Comparison of SGA and AGA pregnancies at the first and last visits for jet PI and RI[18]**

| | **AGA** | **SGA** | **P value** |
|---|---|---|---|
| **PI** | *Mean (std dev)* | *Mean (std dev)* | |
| *Visit 1* | 0.49 (0.13) | 0.47 (0.15) | 0.7 |
| *Visit 7* | 0.17 (0.11) | 0.22 (0.14) | 0.1 |
| **RI** | | | |
| *Visit 1* | 0.37 (0.07) | 0.36 (0.09) | 0.6 |
| *Visit 7* | 0.15 (0.09) | 0.19 (0.11) | 0.1 |

[18] Statistical analysis carried out by Jacqueline Birks at the Centre for Statistics in Medicine, Oxford.

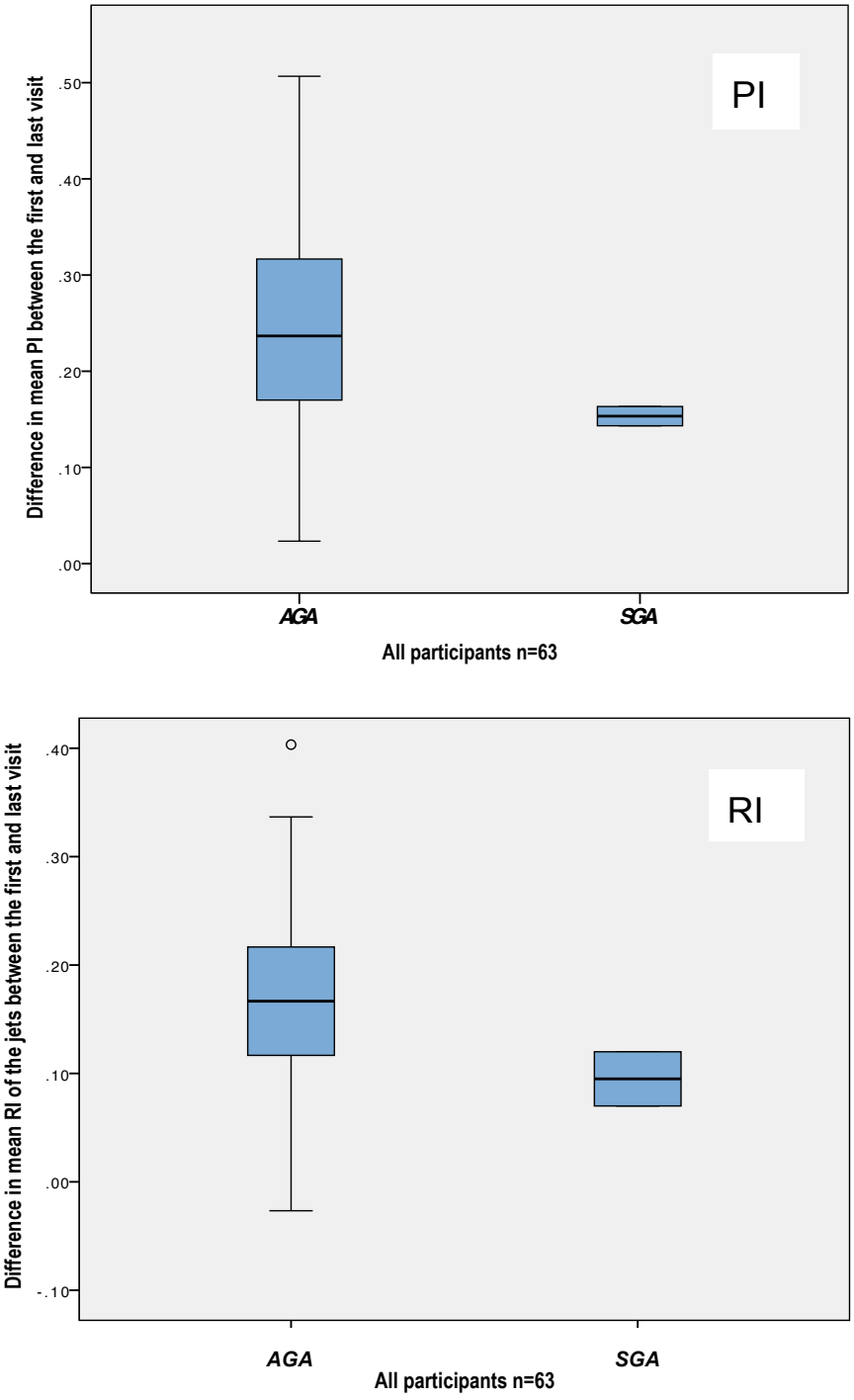



**Figure 19: Difference in the mean PI and RI of the jets between the first and last visit.**

### 4.4.1 Changes in size and velocity of the jets

Both the width (Figure 20, page 87) and length (Figure 21, page 87) of the jets appear to increase with advancing gestation. At <14 weeks' gestation the mean width of the mouth is 2.1mm (range 1.5-5.8mm) whilst at the last visit at >32 weeks this has increased to 3.8mm (1.8-5.8mm). The mean length at <14 weeks is 2.9mm (1.5–5.8mm) rising to 5.5mm (3.0–8.6mm) at the last visit around 33 weeks.

The peak systolic velocity decreases with advancing gestation from a mean of 54 cm/s (19 – 129 cm/s) at <14 weeks to a mean of 20 cm/s (10-34cm/s) at the last measurement (32-34weeks; Figure 22, page 88). Figure 24 (page 90) appears to show that the jet velocity throughout pregnancy is higher in SGA pregnancies compared with AGA. Unsurprisingly given the appearance of the graph, there was no significant difference in the rate of change of the two groups (p=1) when analysed using the linear mixed model.

When the percentage difference in length, and PSV between the first and last visit was compared no significant difference was seen between SGA and AGA pregnancies (p= 0.18 and 0.21 respectively). The percentage difference in mouth width gave a p value of exactly 0.05 and the boxplots show that there may be a trend towards the SGA pregnancies having less relative increase in the size of the mouths of the jets (Figure 23, page 89).

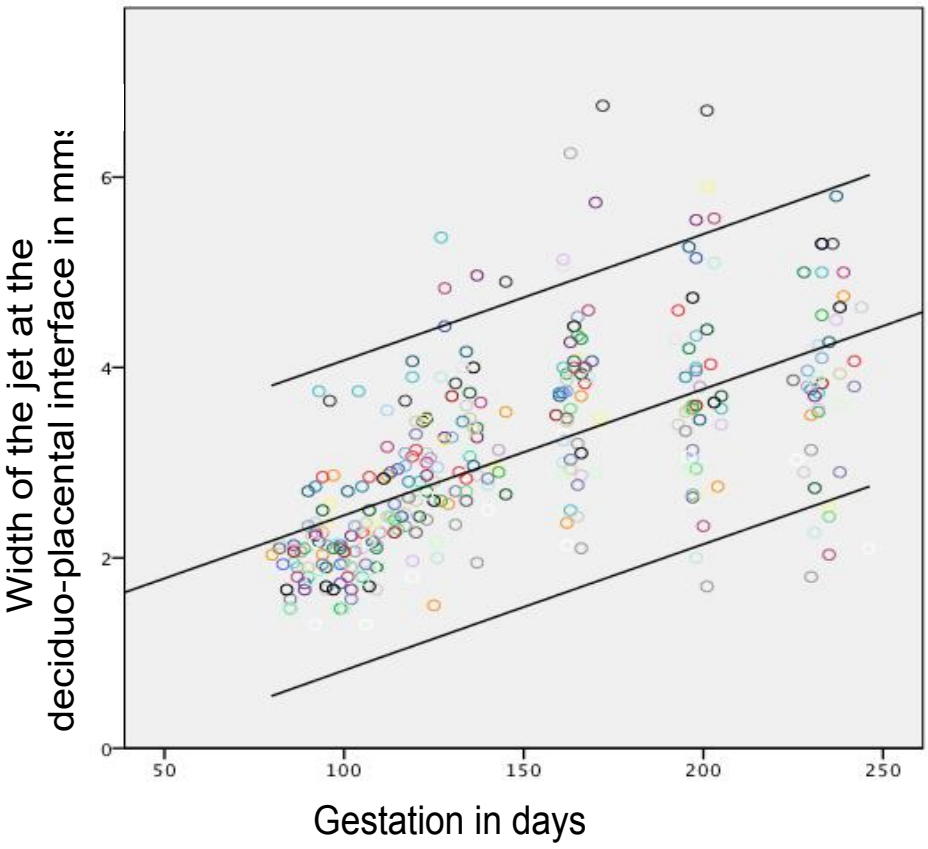



**Figure 20: Jet mouth width for women with normal pregnancy outcomes.**
(Each individual patient has their values plotted a different colour, n=52)

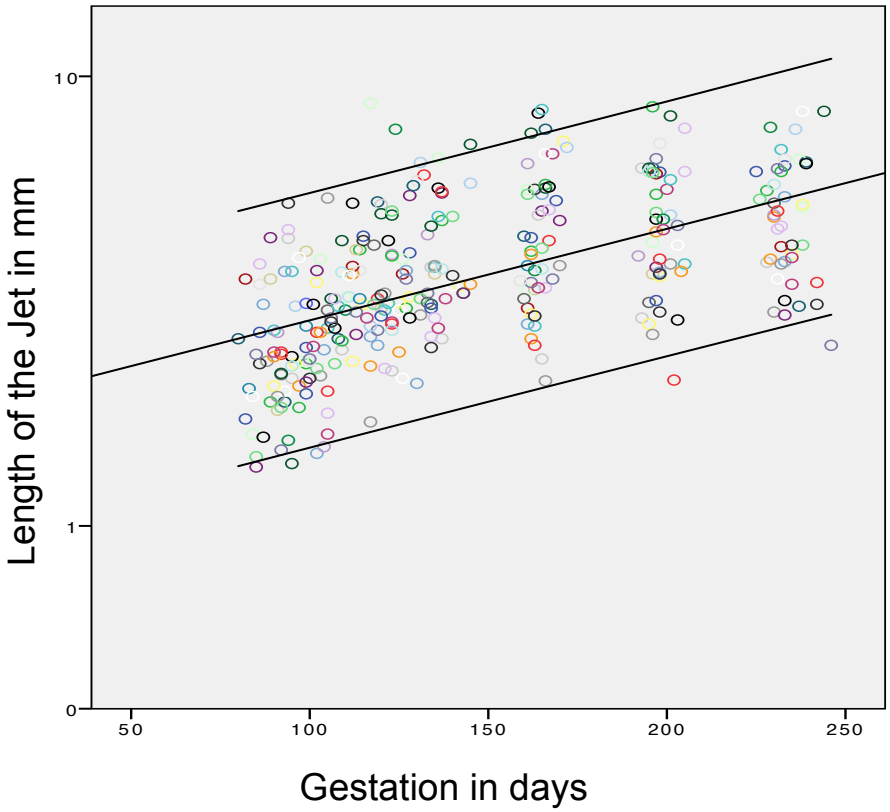



**Figure 21: Jet length in mm, for women with normal pregnancy outcomes.**
(Each individual patient has their values plotted a different colour, n=52)

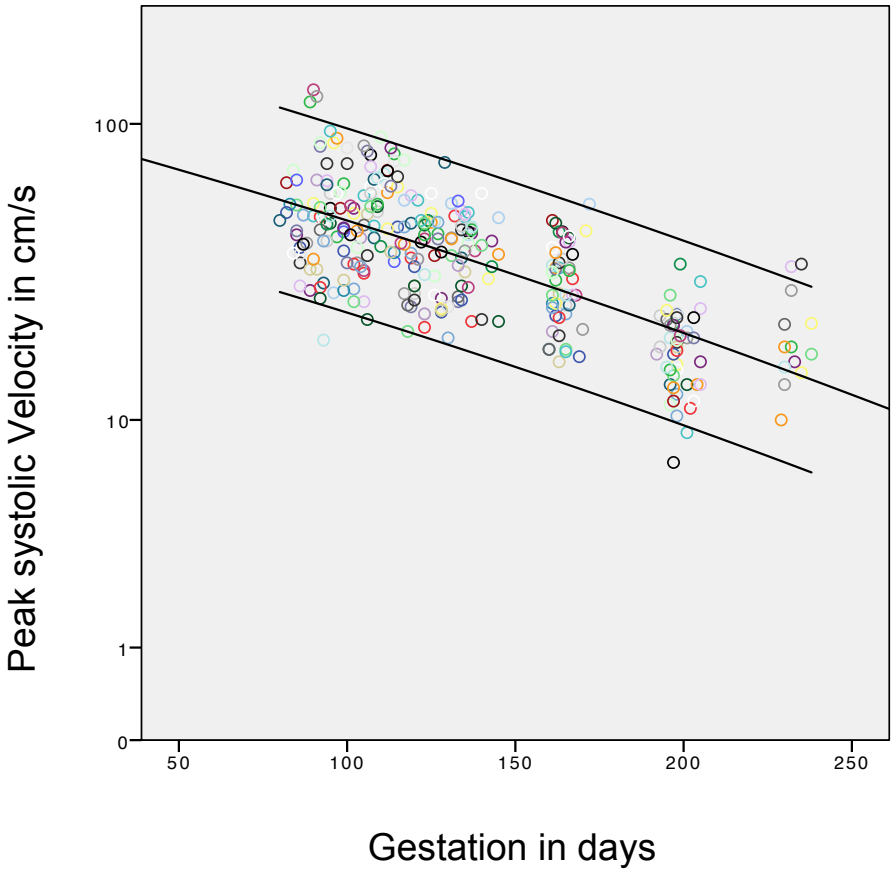



**Figure 22: Jet peak systolic velocity in cm/s, for women with normal pregnancy outcomes.**

(Each individual patient has their values plotted a different colour, n=52)

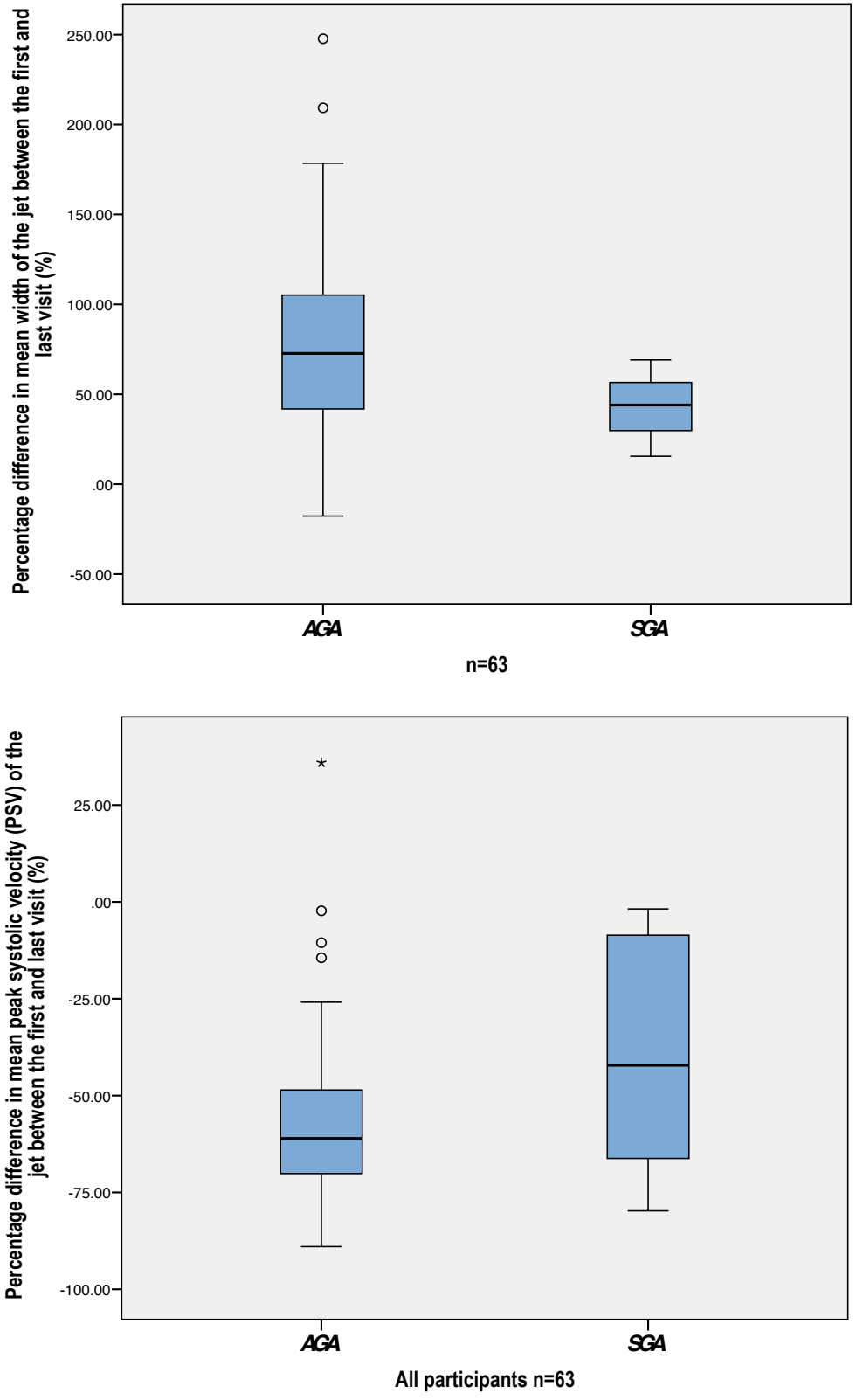



**Figure 23: Percentage difference in the mean mouth width and peak systolic velocity of the jets between the first and last visit.**

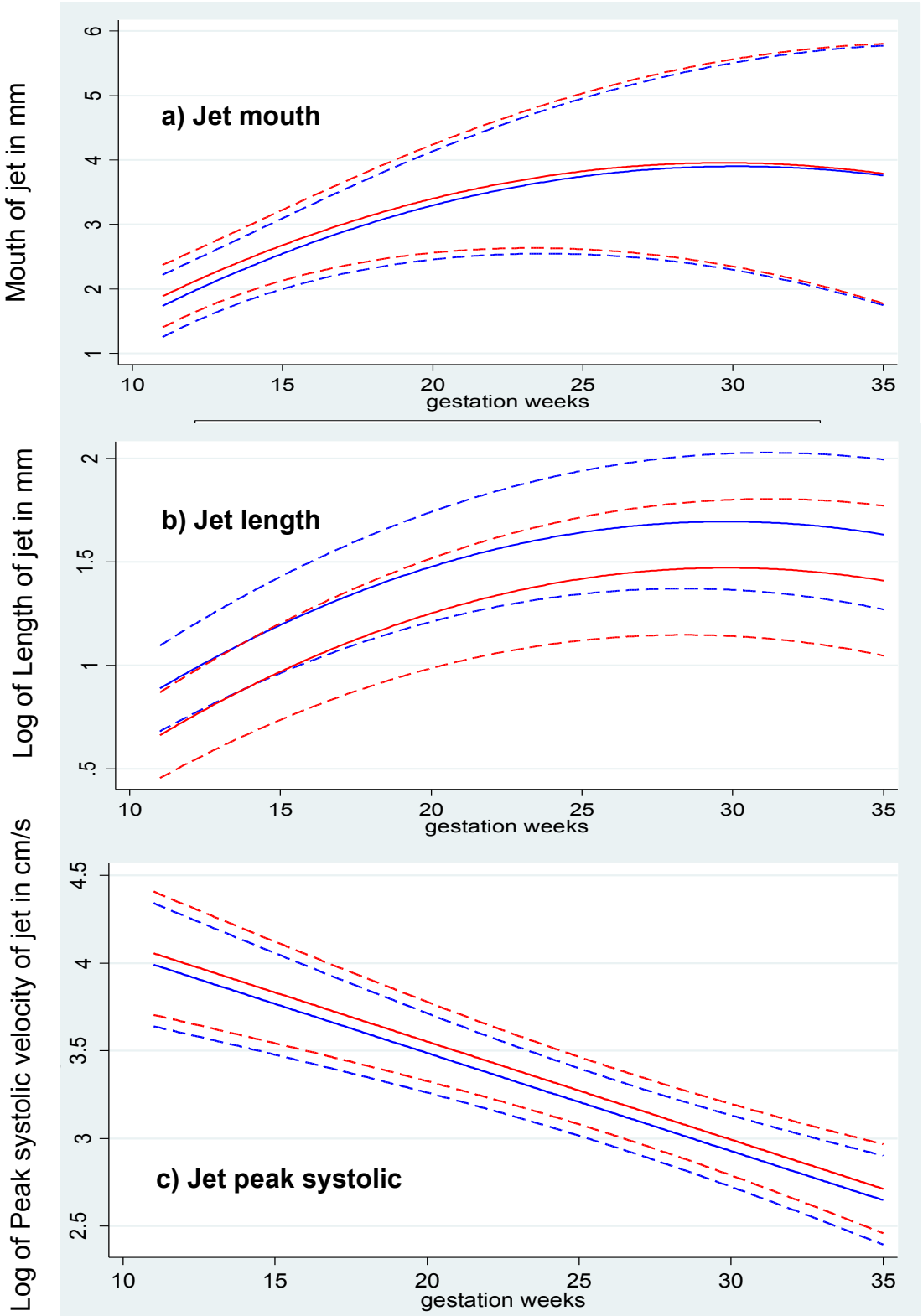



**Figure 24: The change in size of the jet mouths, lengths and velocity of SGA compared with AGA pregnancies.[19]**

The solid blue line indicates the mean of the AGA babies (dotted lines are the 95% bands in which 95% of the measurements lie). The solid red line indicates the mean for the SGA babies.

[19] Graphs supplied by Jacqueline Birks at the Centre for Statistics in Medicine, Oxford.

### 4.4.2 Mega-Jets

Eight women with posterior placentas had the fetus overlying at least some of the placenta at the last one or two scans. This resulted in significant Doppler signal 'drop-out' and therefore the absence of mega-jets could not be completely confirmed. The results from these women were therefore excluded. Consequently, full results on the confirmed presence or absence of mega-jets were available for 52 women delivering at term Figure 25 (page 91)

The frequency distribution of the length of the most prominent jets is not normally distributed (Kolmogarov-Smirnov; $p<0.001$). On examining the histogram it appears to be bimodal (Figure 26, page 92) which would confirm the subjective impression that mega-jets are different to the jets.

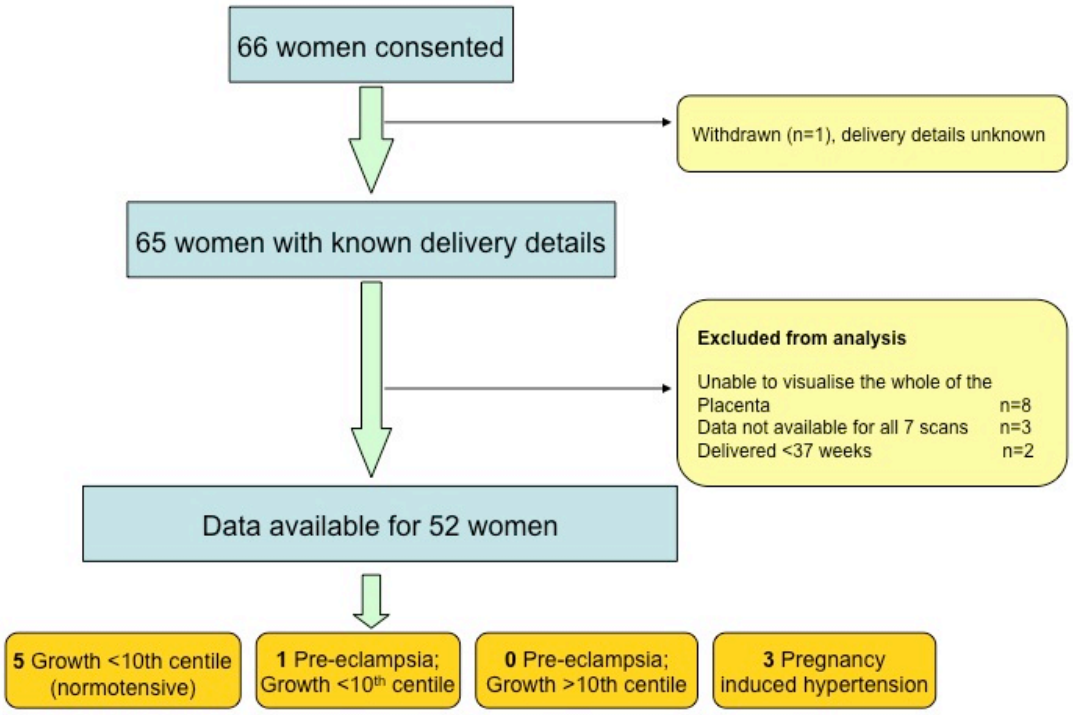



**Figure 25: Breakdown of phase I patients for analysis of mega-jets.**

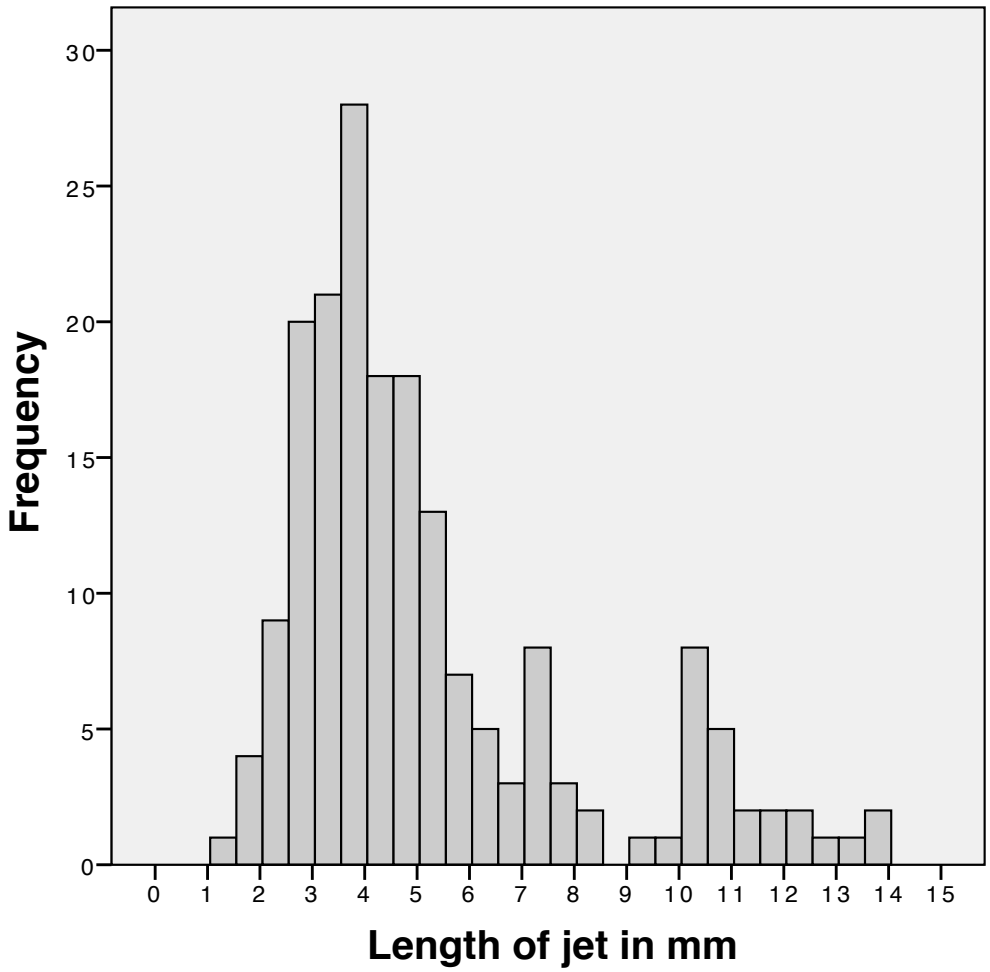



**Figure 26: Frequency distribution of the length measured of the most prominent jets measured at 23 to 24 weeks' gestation**

Mega-jets were seen in 13% (7/52) of women at the first visit (≤13+6 weeks' gestation) and developed in a total of 87% (45/52) by the final visit at <34 weeks (Figure 27, page 93). Log rank testing demonstrated that the mega-jets appeared significantly later in the placentas of the six participants whose pregnancies resulted in SGA babies (including the one woman with pre-eclampsia) compared with the 46 AGA pregnancies (including the women with PIH) (p=0.04) (Figure 28, page 94). This did not quite reach significance when the five normotensive SGA babies were compared with the 43 normotensive AGA babies (p=0.058).

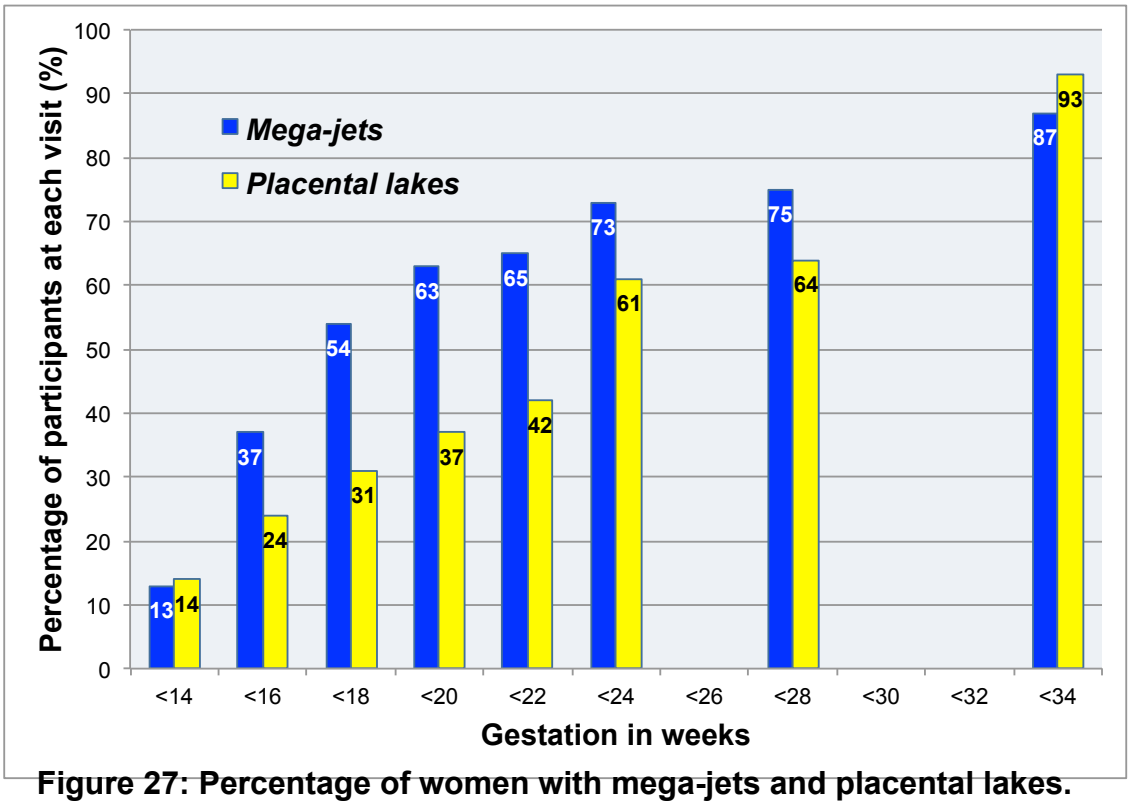



**Figure 27: Percentage of women with mega-jets and placental lakes.**

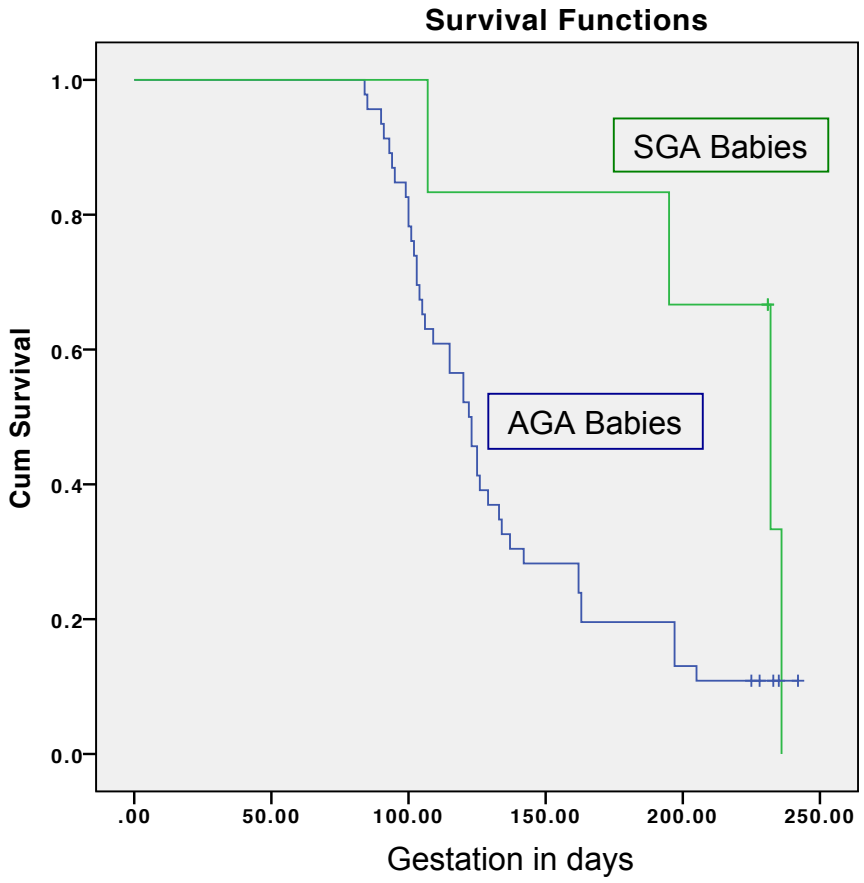



**Figure 28: Kaplan-Meir survival function for the appearance of mega-jets in SGA and AGA babies.**

### 4.4.3 Placental lakes

The presence of placental lakes was noted in both phases of the study therefore information was available on their appearance up to 34 weeks in 59 women (Phase I, Figure 29, page 95) and up to 23 weeks in 138 women (Phases I and II, Figure 30, page 95).

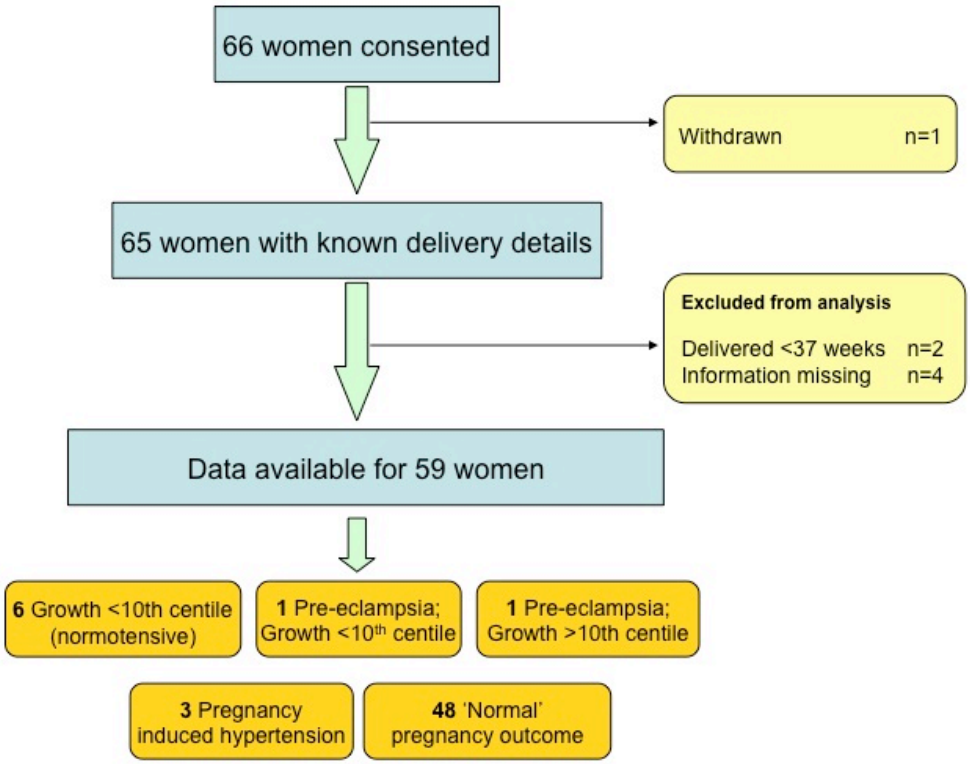



**Figure 29: Breakdown of phase I patients included in analysis placental lakes.**

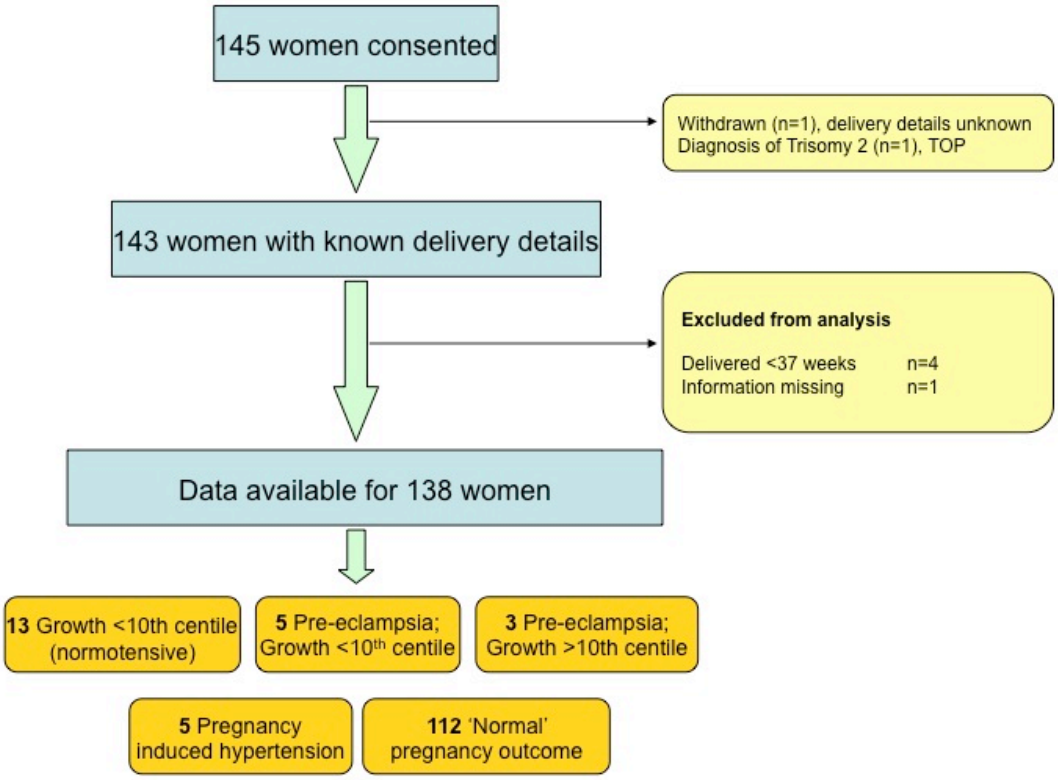



**Figure 30: Breakdown of phase I and II participants included in analysis of placental lakes.**

#### 4.4.3.1 Phase I

Lakes were seen in 14% (8/58) of women at the first visit (<14 weeks) and developed in a total of 93% (55/58) by the final visit at <34 weeks (Figure 27, page 93). Log rank testing showed no significant difference in the timing of appearance of lakes between the seven participants whose pregnancies resulted in SGA babies compared with the 52 AGA pregnancies (p=0.08) or the six normotensive SGA babies when compared with the 48 normotensive AGA babies (p=0.24). However, the lakes were shown to appear significantly later in the SGA and pre-eclamptic pregnancies (n=8) compared with the 51 normal pregnancies (including the women with PIH) (p=0.02).

#### 4.4.3.1 Phases I and II

When the phase II data was combined with the phase I data to give a sample of 138 women scanned five times (up to 25 weeks), it showed a similar trend for the appearance of placental lakes to that seen in phase I. Lakes were seen in 6% (8/138) of women at the first visit (<14 weeks) and developed in a total of 53% (73/138) by the final visit at <26 weeks (Figure 31, page 97).

Log rank testing demonstrated that the lakes did not appear significantly later in the 18 SGA pregnancies babies compared with the 120 AGA (p=0.07) or the 13 normotensive SGA babies when compared with the 112 normotensive AGA babies (p=0.34). However, when the SGA and pre-eclamptic pregnancies (n=21) were compared with the 117 normal pregnancies (including the women with PIH) again the result became statistically significant (p=0.03), Table 10 (page 97).

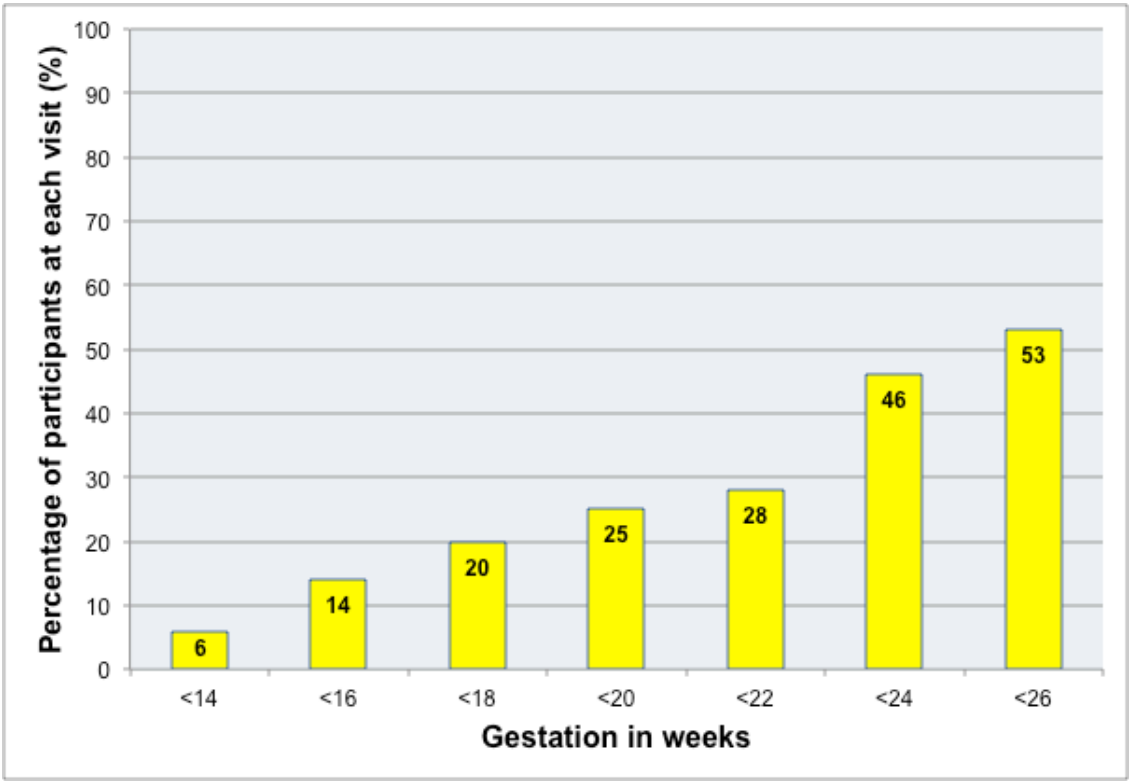



**Figure 31: Percentage of women seen to have placental lakes in phase I and II.**

**Table 10: Log rank testing results for the appearance of lakes before 26 weeks in both Phases I and II**

| **Comparators** | | **Log rank result** |
|---|---|---|
| All term SGA<br>(inc.all hypertensive disorders)<br>n=18 | All term AGA<br>(Inc. all hypertensive disorders)<br>n= 120 | P=0.069 |
| All term SGA & pre-eclampsia<br>n=21 | All term AGA & pregnancy-induced hypertension<br>n=117 | P=0.028 |
| Normotensive SGA<br>n=13 | Normotensive AGA<br>n=112 | P=0.343 |
| AGA PET<br>n=3 | AGA normotensive<br>n= 112 | P=0.203 |

#### 4.4.3.2 Mega-jets and placental lakes

The information on the presence or absence of both mega-jets and placental lakes was available for all seven visits in phase I for 47 women, Figure 32 (page 98). This demonstrates that initially there are more women with only mega-jets than both. However, the number of women with both mega-jets and lakes present gradually increases until at around 20 to 24 weeks there are more women with both. After this point the number of women with only mega-jets seen decreases. The number of women with only placental lakes appears fairly constant throughout.

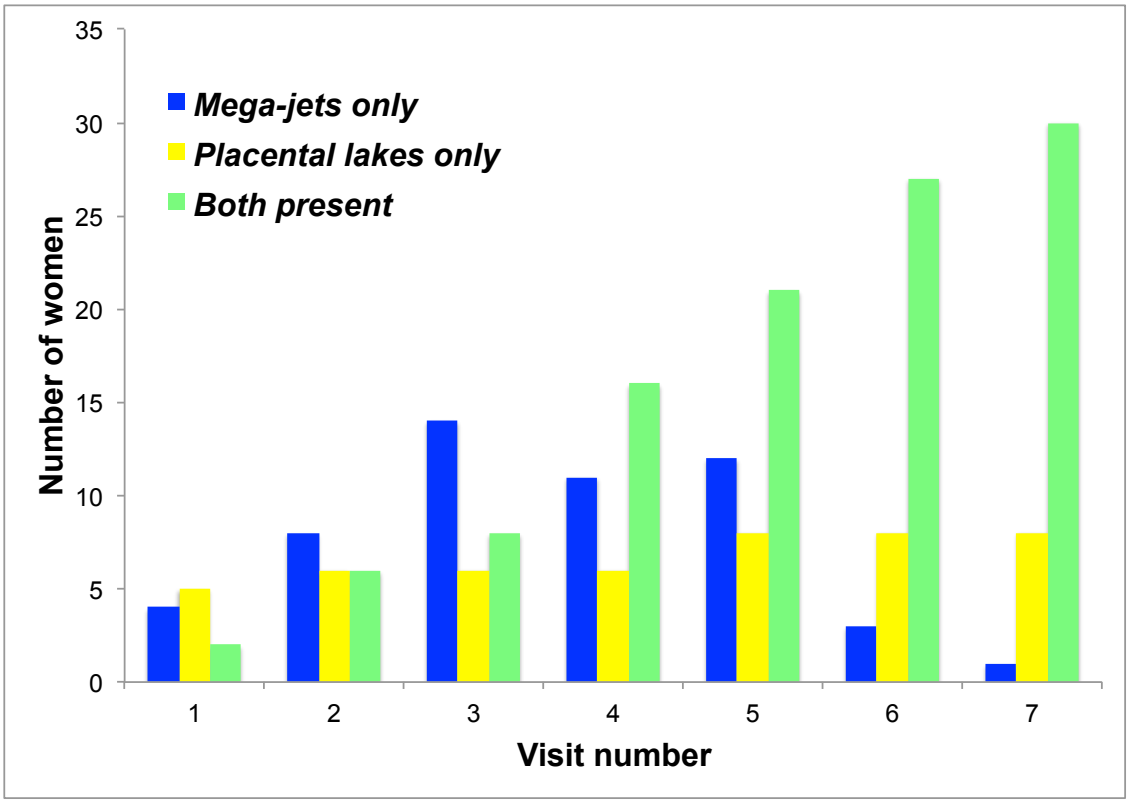



**Figure 32: The number of women with mega-jets and lakes (n=47).**

## *4.5 Discussion*

This is the first time that a technique for measuring the blood flow at the mouth of the spiral artery has been formally described and validated. A related method has been reported for measuring the blood flow in the intervillous space in the cynomolgus monkey (Macaca fascicularis) (Simpson et al. 1997). However, their exact sampling site was not described and it does not appear to have been repeated in human studies.

The value for the RI in the jets at 13 weeks is similar to that measured in a previous study using transvaginal ultrasound and identification of the spiral artery by waveform at the same gestation (van Zalen-Sprock et al. 1994). Both studies showed that the RI of the uterine arteries was higher than the RI measured for the spiral arteries. Despite the difference in methods, the vasculature being assessed is the same, so it is reassuring that the results are similar.

The decision to measure the three most prominent vessels was arbitrary and followed our pre-study findings. The three most prominent vessels were selected so that the best jets were measured in each woman to ensure a good inter-participant comparison. Attempts were made to measure jets as close as possible to the central part of the placenta, as the vessels there have undergone the greatest conversion (Brosens 1988).

The jets were measured in all but one woman for the first three visits. For that participant, the jets were observed and appeared to be pulsatile but could not be accurately recorded in the allocated time. This most likely represents operator inexperience at this time, as the jets were measureable at subsequent visits. In the third trimester the jets could not be reliably observed in a small number of women with posterior placentas. This was usually when the overlying fetus was

very active which disrupted the colour Doppler signal preventing the measurements from being acquired in the allowed time.

It is difficult, from histology, to predict when the jets should become non-pulsatile as the tissue is fixed. It has been suggested that less trophoblast is found in the vessels after 16 to 18 weeks' (Brosens 1988). However, that does not mean that the conversion process stops at this point. The first non-pulsatile jets were seen at 20 weeks' gestation in a woman who went on to deliver an AGA baby. Figure 14 (page 78) demonstrates a steady increase in the proportion of women with non-pulsatile vessels with advancing gestation. By 34 weeks 37% of women had no pulsatile jets. As no further measurements were made after this point we cannot comment on what the percentage might be at term. However, this does suggest that the process of vessel conversion is continuous after 18 weeks and throughout the third trimester. This further suggests that whilst trophoblast invasion may start the process its presence is not required to continue it.

### 4.5.1 Intra-observer and inter-observer variability

The subject numbers used to assess both intra-observer and inter-observer variability were small but were sufficient to demonstrate that the method is both precise and reproducible. The decreasing within-patient variance over time for observer 2 showed a possible 'learning effect'. Therefore, with time, the limits of agreement between the two observers may have reduced further. However, using the 'as low as reasonably achievable' (ALARA) principal it was felt that this was enough to confirm that there was appropriate reproducibility with no systematic bias.

### 4.5.2 Spiral artery jet and uterine artery waveforms

The decreasing PI and RI of the jets (Figure 15, page 79) appear to confirm that there is a gestation dependent change occurring in the vascular tree at the utero-placental interface. Histology studies have demonstrated trophoblast-invasion mediated loss of the musculo-elasticity of the spiral artery wall (De Wolf et al. 1980; Khong et al. 1986; Brosens et al. 2002). If it is assumed that, as Gosling suggested (Gosling et al. 1991), the normal IVS has a low resistance to flow, then the change seen in the waveform of the jet is likely to be reflecting the change in the properties of the spiral artery wall. As the vessel widens, and the elasticity and subsequent wall rebound is lost, the pulsatile nature of the flow would be expected to diminish ultimately leading to continuous forward flow. This is the pattern seen in our data. As the last ultrasound scan was at 34 weeks, we cannot comment on the number of jets that remained pulsatile at term. However, the overall pattern closely resembles that predicted by the histology and models of placental haemodynamics (Burton et al. 2009a). The mean and minimum uterine artery indices showed a similar pattern of correlation between the jets. This lack of difference between the two measures is unsurprising given two recent large studies which indicated that minimum, mean and higher uterine artery PI values are all comparable for predicting pre eclampsia in both the first (Napolitano et al. 2011) and second trimester (Napolitano et al. 2010)

The waveform change with gestation in the spiral artery jets is similar to that of the uterine arteries. This highlights that both are subject to a common mechanism. However, it is not clear if there is a series circuit (i.e. the uterines simply reflect the sum of the spiral arteries), or whether the relationship is more complex.

### 4.5.3 Spiral artery jet waveform differences in SGA babies

This study suggests that the jet waveform of blood entering the intervillous space from the spiral artery is different in pregnancies destined to become SGA. This is in spite of little difference being observed in the uterine arteries.

This study sought to investigate if our new technique could be used to explore the underlying pathology. Subsequently it only had a small number of events. There is a 6% chance of the null hypothesis being true, but as this was a pilot study, this level of significance indicates it is worthy of further investigation. The recruitment strategy also involved actively seeking women at high risk of growth restriction. The resulting customised birth weights distribution was skewed to the left (Figure **9**, page 56). In a random sample of the population the distribution should be normal which may have affected the result.

Although not reaching statistical significance, the difference in the mean PI and RI between the first and last visits suggest that there is less change occurring in the jets of SGA pregnancies. This is also demonstrated by the difference in the rate of change of the PI and RI between SGA and AGA pregnancies. If the underlying pathology of this term growth restriction is due to residual musculo-elasticity in the terminal end of the vessel, it is biologically plausible that both the PI and RI are increased in SGA pregnancies as a result of the retained muscular rebound and increased vascular resistance. As the difference in these indices becomes increasingly prominent in the third trimester it is possible that this could be the underlying mechanism resulting in this type of late onset growth restriction The alternative possibility, that the cause of the difference is a change in the nature of the intervillous space leading to

increased resistance to forward flow, is not supported by the histological data (De Wolf et al. 1980; Khong et al. 1986; Brosens et al. 2002).

Any correlation between early pregnancy waveforms and SGA appears greater in the jets than in the uterine arteries. This is surprising if the changes in the uterine arteries are directly caused by the changes in the downstream spiral arteries, as the 'sum' of all the vessels in the placental bed should be more sensitive than just three individual ones. However, it is known that the uterine arteries have a relatively poor predictive value for growth restriction at term (Cnossen et al. 2008).

If confirmed, this difference in sensitivity for SGA has many potential causes. It is possible that three affected vessels were measured and the uterine artery result is reflecting that there are more normally adapted vessels than abnormal ones and is therefore overall normal. However, what is more likely is that the blood supply from the uterine to the spiral arteries is not a simple series circuit. Evidence for myometrial arterio-venous anastomoses was elegantly presented in a paper by Schaaps (Schaaps et al. 2005). This included the finding of low resistance in the uterine arteries after delivery, suggesting that the vascular network remains functional after placental expulsion. If these anastomoses are able to adequately 'buffer' some of the back pressure from the decidua-placental interface then the pathology would need to be considerable before changes were seen in the uterine artery waveform. This would explain why uterine arteries have better sensitivity and specificity for the severe end of the spectrum.

Recent findings of normal uterine artery waveforms in a third trimester abdominal pregnancy (Collins et al. 2011) adds further evidence for the

complexity of the relationship between trophoblast invasion and Ut A. Changes in Ut A impedance have already been documented in the absence of a placenta. The Ut A waveform in the non-gravid uterus can show decreased impedance in response to cyclical changes (Steer et al. 1990), intrauterine contraceptive devices (Jarvela et al. 1998a; Jimenez et al. 2008) and pharmacological agents including diclofenac (Jarvela et al. 1998b) and sildenafil (Hale et al. 2010). If the intervillous space is not crucial, the change in the mechanical properties must originate elsewhere in the circuit. The vascular anastomotic network in the myometrium (Schaaps et al. 2005) may develop in response to pregnancy-related vaso-active signals producing the decreased resistance in the circuit. Alternatively, the change in the waveform could be the result of the observed dilatation (Makikallio et al. 2004) of the larger vessels in the circuit, possibly in response to endocrine or nitric oxide-mediated signals (Burton et al. 2009a). This signaling may also control the depth of the trophoblast invasion: an immunohistochemical study demonstrated that, in guinea pigs, dilatation of the vessels began before trophoblast cells were found inside the vessels (Nanaev et al. 1995). This appeared to be mediated by the expression of nitric oxide synthase, with invasion and subsequent wall destruction occurring as only a secondary effect.

The correlation seen between the Ut A waveform and the spiral artery changes may not be a causative one but the result of a common mechanism (Burton et al. 2009a). The unifying mechanism may prove to be a form of vascular priming or preconditioning (Brosens et al. 2009), which subsequently determines both the dilatation of the vessels and the depth of the trophoblast invasion. If this is endocrine mediated, oestrogen could be important. Its action on the

endometrium is well established (Ozturk et al. 2010); it also has vasodilatory effects on the uterine arteries (de Ziegler et al. 1991; Jauniaux et al. 1992; Xiao et al. 2009), possibly mediated via adrenomedullin (Ross et al. 2010), extracellular signal-regulated kinase (ERK)1/2 (Xiao et al. 2009) or endothelial nitric oxide synthase (eNOS) expression (Rupnow et al. 2001). Ensuing pathology could be caused by deficiencies in the production of the endocrine mediated signaling molecules or a lack of responsiveness in the maternal vasculature.

### 4.5.4 Changes in size and velocity of the jets

Attempts to measure the size of the mouth of the terminal spiral arteries with increasing gestation is fraught with difficulties, mostly relating to the inherent limitations of Doppler ultrasound. Our estimates of the size of the openings at the deciduo-placental interface are larger than those taken from histological specimens (Harris et al. 1966). Harris and Ramsey's serial slice reconstruction of the terminal portion of the spiral arteries suggested a diameter starting at around 0.5mm and increasing to 2-3mm near term. As our measurements started at 11 to 13 weeks we cannot comment on the non-pregnant size but by 32 to 34 weeks the diameter appeared to be larger than predicted at term, 4 mm (1.8-5.8mm). There may be many explanations for this discrepancy. Although colour Doppler can underestimate the size of a lumen in a phantom model due to signal attenuation (Potter et al. 2008), it may also produce a bloom artefact. This describes a phenomenon where the colour signal appears to smear out beyond the vessel walls making them appear larger than they are (Rubens et al. 2006). Although care was taken to try to avoid including this artefact, represented by the 'faded' colour at the edges of the vessel, the

potential effect of this artefact cannot be dismissed. Also, *in vivo,* the effects of the maternal circulation must be considered (Burton et al. 2009a). The difference in diameters may be a consequence of haemodynamic distention of the vessel walls. However, the discrepancy may also have arisen due to underestimation of the histological specimens. The fixation process may result in vessel wall disruption and shrinkage (Benirschke et al. 2000).

This difference between histomorphometric and imaging measurements has recently been demonstrated in a study of coronary arteries (Gonzalo et al. 2009). This showed an increase of 40% in the estimated vessel size using an intravascular ultrasound technique (which is not thought to be affected by bloom artefact) compared with histomorphometric measurements.

Irrespective of the difficulties determining absolute size, examining the jets in the same women over time has provided a crude *in vivo* insight into the changes occurring in these vessels in pregnancy. We have demonstrated the histologically predicted increase in the size of the spiral artery mouth, *in vivo,* for the first time.

Estimates of the velocity of blood flow using Doppler ultrasound are influenced by the angle of insonation (Johnston et al. 1977; Lunt 1980; Brown et al. 1985; Rasmussen 1987b, a). The accuracy of the measurement is improved by minimizing the insonation angle ($<30^{o}$) and using appropriate angle correction (Deane et al. 1991; Hoskins 1996; Fish et al. 1997; Hoskins et al. 1997). To minimize errors in the estimates of velocity we ensured that the jets were measured with an angle of insonation of $<30^{o}$ and used the angle correction software supplied on the Voluson E8™ (GE Healthcare, Milwaukee, WI, USA). Again our measurements started at the beginning of the second trimester so

we cannot comment on the velocity of blood into the IVS before this point. However, we did record a drop in velocity from a mean of 54cm/s to that of 20cm/s at 34 weeks. If the graph is extrapolated to 40 weeks this would give a velocity of 10cm/s. This is the same as was predicted by a recent mathematical model (Burton et al. 2009a).

### 4.5.5 Mega-jets

Our finding of the gradual appearance of unusually large jets does not appear to have been reported before in the literature. The bi-modal frequency distribution of jet lengths supports the hypothesis that these are a separate entity to jets and not just at the upper end of a 'normal' distribution. We showed that 84% of women had at least one mega-jet by 34 weeks. This seems to indicate that, rather than being unusual, their development may be a normal part of the maturation of the utero-placental unit. In SGA pregnancies they developed significantly later than in pregnancies resulting in AGA babies. The serial slice reconstructions of Harris and Ramsey (Harris et al. 1966) may offer an explanation for this phenomenon. They demonstrated that the invading trophoblast had eroded through the walls of some spiral arteries to connect them not only to other spiral arteries but also to basal arteries. This resulted in the blood from two or more vessels being diverted into the IVS through a single large opening. This could potentially result in the observed mega-jets. If the trophoblast invasion is impaired the inter-vessel communications may develop more slowly, if at all; explaining why the early appearance of mega-jets might be a surrogate marker for the adequacy of placentation.

As these mega-jets had not been described before, we had to select a definition which seemed to best describe them. This attempted to separate

them from the jets whilst also taking into account the increasing size of the jets with advancing gestation. Hence the definition of flow seen to travel ≥10mm or ≥50% of the distance across the placental parenchyma (if the placenta was <20mm thick). Further work is required to characterize mega-jets in order to establish their significance.

### 4.5.6 Placental lakes

We sought to investigate the relevance of placental lakes following the observation that they appeared to be related to mega-jets. Figure 27 (page 93) demonstrates that lakes develop after the mega-jets but are present in 93% of women by 34 weeks. The precise relationship between mega-jets and lakes remains unclear. Although, as many mega-jets were observed to terminate in lakes it is not unreasonable to suggest that their formation may be interrelated. The mega-jets appear to develop earlier but there are ultimately more lakes present (Figure 27, page 93). When the pattern was examined in more detail (Figure 32, page 98) it appears that as more women have both mega-jets and lakes, fewer are seen to have only mega-jets. One possible explanation for this is that the haemodynamics of the mega-jets directly cause the formation of these lakes. This may occur when the extra flow, which results from more than one vessel discharging through a single opening, overwhelms the delicate circulatory system of the IVS. The blood then passes deeper into the placental tissue. Eventually, as the momentum is lost, forceful forward flow stops and a placental lake is formed (hence the ultrasonic appearance of slowly circulating fluid). The blood then slowly disperses back through the placental parenchyma eventually draining via the venous sinus system which would potentially explain the normal appearance of the tissue around them as it is appropriately

perfused, unlike the hypoechogenic tissue around ECLs which are thought to arise from an infarction (Proctor et al. 2010).

This is probably not the only way in which placental lakes form. This is supported by the observation that some women have only placental lakes throughout. The number changes very little from five at the first visit (10%) to 8 at the last (17%). If there are several mechanisms which result in the formation of placental lakes this may explain the contradiction in their prognostic significance seen in the literature (Jauniaux et al. 1996; Thompson et al. 2002; Reis et al. 2005; Cooley et al. 2011). Further work is needed to clarify whether our suggested mechanism does indeed form placental lakes and if there are any easily identifiable differences between these and other observed lakes.

# 5 Placental shape and volume

## *5.1 Introduction, background and aims*

The relationship between the ultimate weight of the placenta and the fetal birth weight has long been recognized (Sinclair 1948; Eskild et al. 2010), as has the pathological significance of a small placenta at delivery (Little 1960). However, it was only with the advent of ultrasound that it became possible to investigate if placental size early in pregnancy could predict growth restriction. This was first attempted in 2-D (Bleker et al. 1977; Hoogland et al. 1980; Wolf et al. 1989) but accurately identifying the required planes limited the usefulness of this technique. The research expanded again with the introduction of 3-D ultrasound in the mid-1990s (Riccabona et al. 1995; Riccabona et al. 1996; Hafner et al. 2001). This has so far proved very promising.

### 5.1.1 Placental volume

A low placental volume (PlaV) between 11 and 13 weeks is associated with fetal growth restriction (Schuchter et al. 2001; Hafner et al. 2006), chromosomal abnormalities (Metzenbauer et al. 2002) and preeclampsia (Hafner et al. 2006). A recent study of over 600 women looking at βhCG, PAPP-A, Ut A PI and other biometric markers demonstrated that, in the first trimester, the PlaV was the only independent predictor of SGA (Law et al. 2009). The mechanism for this remains uncertain. It has been postulated that it is a reflection of the level of trophoblast invasion, which peaks by 10 to 12 weeks (Caniggia et al. 2000). It is highly contentious whether the growth of the fetus is also affected at this stage but it does appear to be to a lesser degree. The Placental Quotient (PQ), which is calculated by dividing the CRL by PlaV,

has been suggested as a simple index to indicate if the placenta is comparatively too small (or large) in relation to the size of the fetus (Metzenbauer et al. 2001). This has the advantage of offering a crude correction for gestation allowing the comparison of placental volume across the 27-day window between 11 and 13+6 weeks. The PQ has been shown to be associated with adverse pregnancy outcomes including pre-eclampsia and pre-term delivery (Schuchter et al. 2001; Hafner et al. 2006) but appears to show the best predictive value for growth restriction (Schwartz et al. 2010). A criticism of this index is that it compares two measurements with different dimensions; length (mm) and volume (ml or $mm^3$). The index generated therefore has a unit i.e. CRL(mm) / PlaV ($mm^3$) = PQ ($mm^{-2}$). This will generate a value that is affected by the units selected. Therefore, whilst it is telling us something about the nature of the underlying situation it is also, to some extent, a human artifact. To make the index mathematically robust it should be dimensionless. A dimensionless quantity is one without an associated physical dimension and as such it is a "pure" number. Some examples are purely mathematical constants such as pi or the golden ratio. However, many can only be determined by experimentation, for example the Reynolds Number (Re) in fluid mechanics (Reynolds 1883; Rott 1990). This is a measure of the ratio of inertial to viscous forces, which quantifies the importance of each for a given set of flow conditions. This produces a universal constant that can be experimentally proved but not explained. Looking at the formulae it is a classic example of a dimensionless quantity and therefore expresses facts about nature, which are wholly independent of any choice of units. Generating a dimensionless index reduces the degrees of freedom within a problem to the

absolute minimum and therefore suggests the most economical scaling laws. It has been shown to be particularly useful in exploratory investigations of novel phenomena for which the equations and boundary conditions are not yet fully understood (Sonin 2004) and consequently is widely used in engineering, physics and economics. They can be defined as products or ratios of quantities that are not themselves dimensionless (such as length and volume), but whose dimensions cancel out when their powers are multiplied.

A dimensionless quantity can be calculated to explore the relationship between CRL and PlaV by dividing $PlaVol^{1/3}$ ($mm^3$) by the CRL (mm). This yields the new index, standardized placental volume (*s*PlaV).

### 5.1.2 Morphometric measurements

Many factors are thought to influence the shape of the placenta including the site of implantation (Benirschke et al. 2000). However, it is unclear if the pathology of utero-placental insufficiency also affects the shape of the resulting placenta. Attempts to compare the morphology of the *ex vivo* placenta with both histological findings and clinical outcome have yielded conflicting results (Yampolsky et al. 2009; Pathak et al. 2010; Salafia et al. 2010; Pathak et al. 2011). Yampolsky reported that a placenta with an umbilical cord displaced from the central position showed a reduced transport efficiency, and hence a smaller birth weight for a given placental weight (Yampolsky et al. 2009). A similar size study indicated that the cord is commonly ‘off centre’ and that there was no difference in any of their derived ‘cord centrality’ indices between normal pregnancies and those with adverse outcomes (Pathak et al. 2010). It also appears that the macroscopic appearance of the placenta may not always correlate with histological findings (Pathak et al. 2011). One of the difficulties

interpreting these findings is that each research group uses their own different indices to define 'normal' and 'abnormal'. Also, as the placenta is being examined flattened *ex vivo,* assumptions must be made that it is appropriately representing the curved shape it would have when perfused *in utero.*

A more clinically useful assessment would be of the placental shape *in vivo.* This has been attempted with simple 2-D ultrasound measurements of length and thickness, mostly at 18 to 23 weeks' gestation, with promising results for predicting adverse pregnancy outcomes (Fisteag-Kiprono et al. 2006; Huppertz et al. 2006; Toal et al. 2007; Costa et al. 2008; Toal et al. 2008). However, the relationship between the pathology and placental shape is probably more complex. It is plausible that the larger the proportionate area of the basal plate, the better the placenta will function as an organ of nutrition and gaseous exchange. It has also been suggested that inadequate spiral artery transformation may lead to the force of blood entering the IVS at higher than normal pressure, literally 'pushing' the placenta from the basal plate and changing its shape (Jauniaux et al. 1994; Burton et al. 2009a). This would result in changes in the basal plate area to placental volume ratio. The 'globular' appearing placenta has been linked with adverse pregnancy outcome (Fisteag-Kiprono et al. 2006), although the difficulty still remains with the subjective definition of 'globular'. An objective measure of placental shape or compactness may prove important when attempting to predict SGA (Hypothesis 2.1.3, page 31).

### 5.1.3 Previously employed methods for placental volume estimation

Previously PlaV, or any index derived from it, could not be used as a screening test due to the time-consuming methods required to generate it. The PlaV can be calculated using a multiplanar method (Hafner et al. 2001; Metzenbauer et al. 2001; Schuchter et al. 2001). This involved manually tracing around the outlines of parallel slices of the 3-D image of the placenta, then summing the area of these slices and calculating the distance between them to generate a volume. A recent advance was introduced in the Virtual Organ Computer-aided AnaLysis imaging tool (VOCAL™ - GE Healthcare, Milwaukee, WI, USA) as a part of 4D View™ (version 9.1, GE Kretz, Zipf, Austria). This performs volume estimation by interpolating a number of contours based around a set point of interest in arbitrary rotational steps (typically $6^{o}$, $9^{o}$, $15^{o}$ or $30^{o}$ steps) Figure 33, page 114.

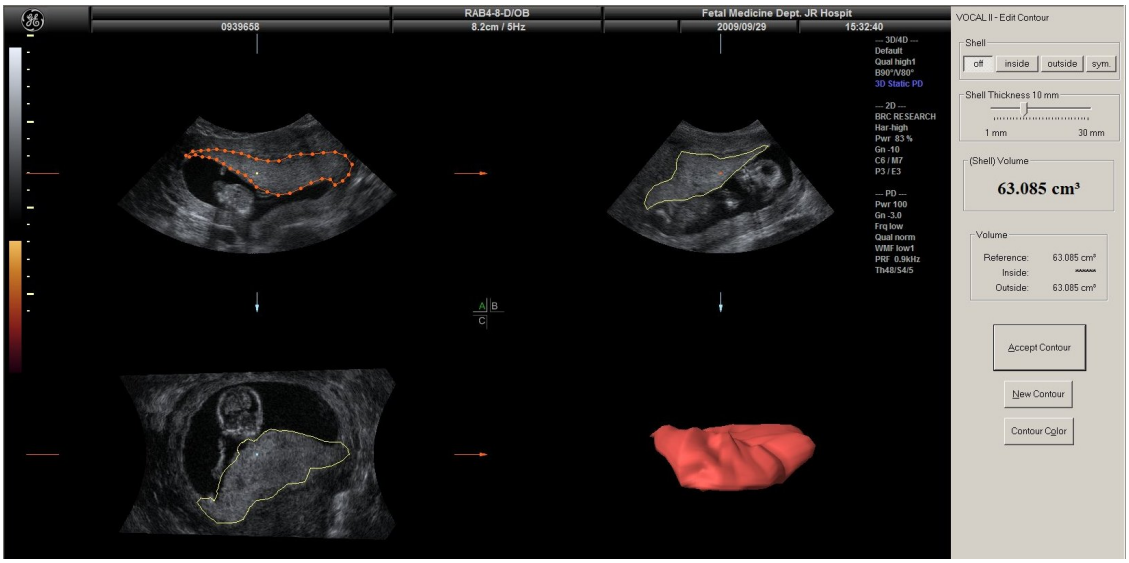



**Figure 33: Example of generating a placental volume in VOCAL™.**

Many concerns have been raised about the reproducibility of VOCAL™ measurement of PlaV, with studies giving conflicting results (Deurloo et al. 2007a; Burstein et al. 2009; Cheong et al. 2010; Huster et al. 2010). However, a simple phantom model found it to be reliable and valid (Barreto et al. 2010) and results for multiplanar and $15^{o}$ VOCAL™ segmentation methods have been demonstrated to be concordant (Nowak et al. 2008). VOCAL™ has been used by a number of groups for research on PlaV (Hafner et al. 2001; Metzenbauer et al. 2001; Schuchter et al. 2001; Hafner et al. 2006; Jones et al. 2010). Although typically faster than manual segmentation, problems still remain with the VOCAL™ method. It is time consuming, the exact rotational method used is unknown and appears to be considerably smoothed, it produces only a numerical volume and the generated surface contour images cannot be saved or their morphology compared.

### 5.1.4 A new semi-automated placental segmentation technique

A rapid segmentation technique producing a 3-D volume which can be saved and further manipulated to generate total surface area (TSA), the area of the basal plate (BPA) and hence an estimate of shape, would be highly desirable. Such a method has been developed for use in our research by Gordon Stevenson (GS) in the Institute of Biomedical Engineering (IBME), University of Oxford (Stevenson et al. 2010). This uses a random walker segmentation algorithm to generate an estimate of the placental volume (Figure 34, page 118). The operator labels the voxels representing the placenta within the 3D volume and the other voxels as being background (maternal tissue or amniotic fluid) (Figure 34b, page 118). This is 'seeding' the image (See formal protocol 8.3, page 192). The random walker then generates a volume by taking successive 3-D random steps and calculating the probability that each unlabeled voxel encountered is either placenta or background tissue. Based on these probabilities, a threshold and weighting can be applied which generates an image segmentation. This can then be used to provide an estimate of the placental volume and total surface area. By then re-seeding the segmentation to indicate the placental-amniotic interface the area of the basal plate can then be calculated (Stevenson 2011).

#### 5.1.4.1 Validation of the new technique[20]

A placental segmentation protocol was devised in collaboration with GS, details of which are given in the appendices (8.3, page 192). This was then validated against manual segmentation and VOCAL™ using 3D US scans captured between 12 and 14 weeks' gestation, in 10 women with anterior placentas and a BMI<25. Two observers (GS and SC) performed measurement of placenta volume manually, using VOCAL™ and using the new semi automatic volumetric method on the same image. Measurement was repeated three times per volume for each technique.

Statistical analyses were performed on the volume results. Measurement difference was illustrated by Bland-Altman plots between the novel method and manual segmentation (the gold-standard). (Figure 35, page 119).

These results demonstrated that the new method was concordant with the accepted gold standard of manual segmentation based on ICC values for intra/inter-observer variation and mean difference. However, it outperformed VOCAL™ in aspects of observer repeatability and agreement. This accurate, time-efficient method to calculate placental volume has the potential to be used as a screening technique.

[20] This research forms part of Gordon Stevenson's D. Phil thesis and is predominantly his work

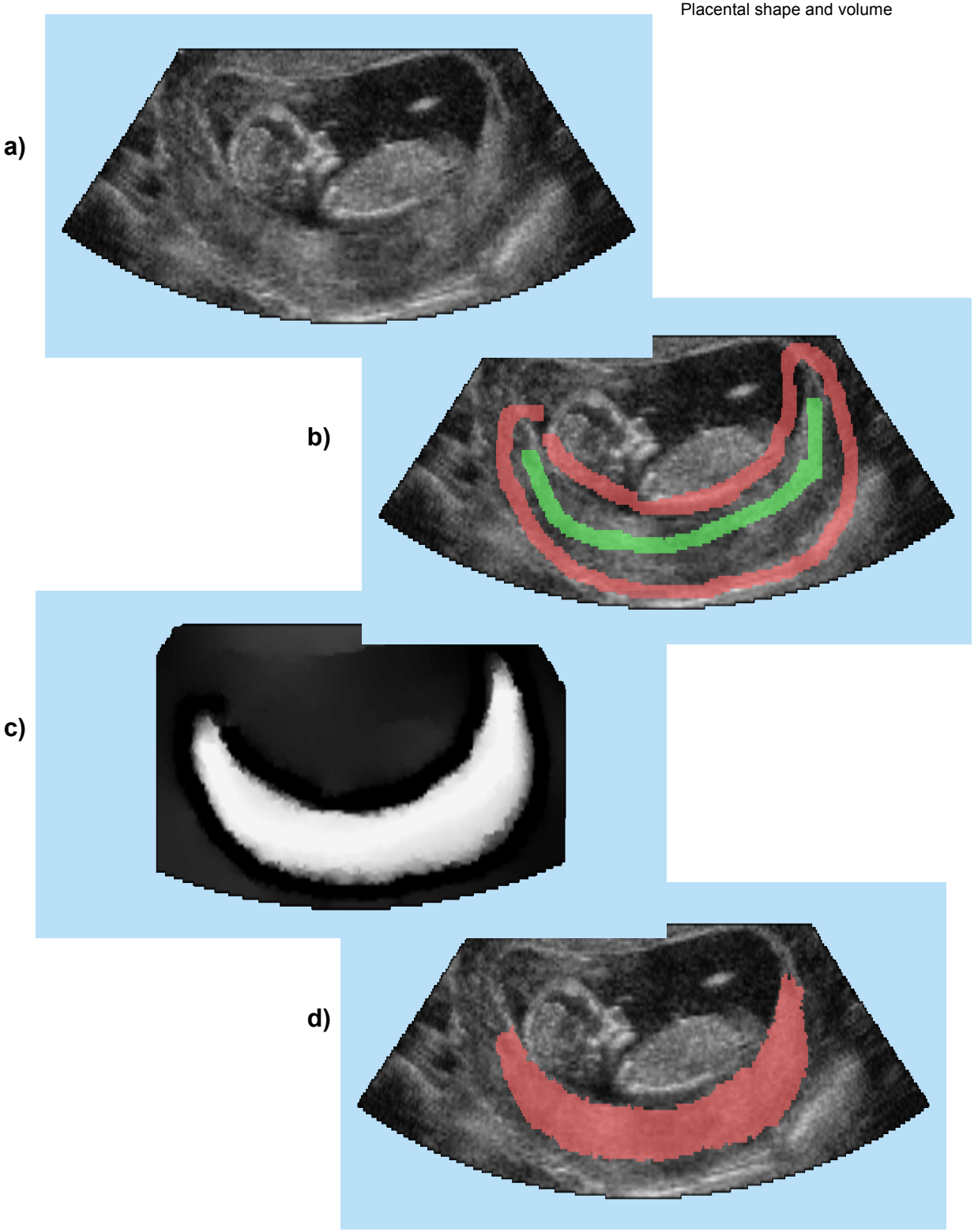



**Figure 34: Illustration of Random Walker segmentation of a placenta.**[21]

a) B-mode ultrasound slice; b) operator seeding where red = background (not placenta) and green = foreground (placenta); c) The probabilities mapped from black = 0 to white = 1; d) Placental segmentation produced by taking those pixels with a probability of ≥ 0.5.

[21] Images supplied by Gordon Stephenson, IBME, University of Oxford, UK.

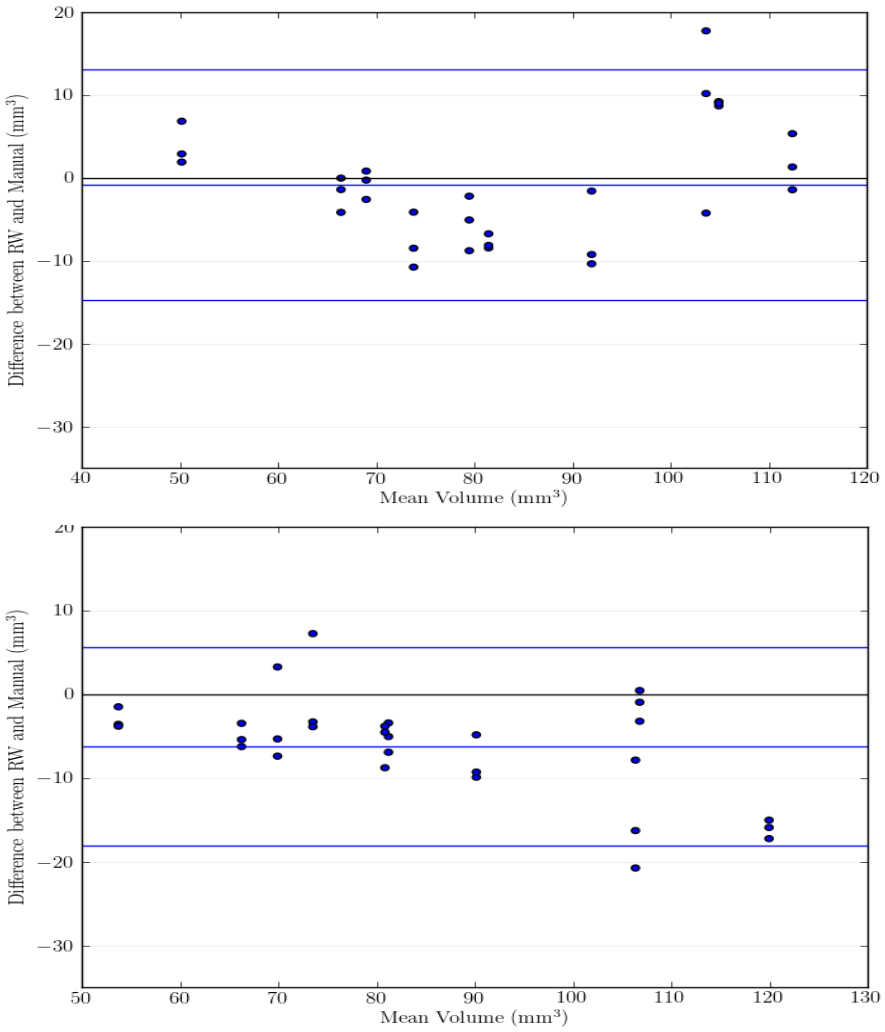



**Figure 35: Bland Altman plots – (a) new method vs. manual for Observer 1 (b) – new method vs. Manual for Observer 2.[22]**

**Table 11: Intra-observer & inter-observer variability by measurement type[21]**

| | Intra-Observer Variability | | Inter-Observer Variability |
|---|---|---|---|
| Measurement Type | ICC (95% CI) Observer 1 | ICC (95% CI ) Observer 2 | ICC (95% CI) |
| Manual Segmentation | 0.98 (0.94,0.99 | 0.90 (0.76,0.97) | 0.943 (0.88,0.97) |
| New Method | 0.97 (0.91,0.99) | 0.96 (0.88,0.99) | 0.906 (0.81,0.95) |
| VOCAL™ | 0.91 (0.77,0.98) | 0.93 (0.81,0.98) | 0.79 (0.61,0.90) |

[22] Reproduced with permission from Stevenson, GN, Collins, SL, Impey, L, and Noble, JA (2010)

### 5.1.5 Aims of this chapter

This chapter explores **Hypothesis 2.1.2, page 31** by investigating:

1. At what gestation between 11 and 24 weeks the whole placental volume could be reliably captured using 3-D ultrasound in our population.
2. If the new semi-automated placental volume technique was able to detect any differences in the PlaV at 11-13+6 weeks between SGA and AGA pregnancies.
3. The performance of the novel, dimensionless index, standardized placental volume (*s*PlaV) in the prediction of SGA.

This chapter also explores **Hypothesis 2.1.3, page 31** by investigating:

1. If placental surface area, area of the basal plate, placental volume and CRL could be combined to develop an objective morphometric index which correlates with birth weight.
2. Whether placental sphericity, (an established, objective measure of compactness of shape of an object) correlates with birth weight.
3. If any of the morphometric measurements at 11 to 13+6 weeks can predict SGA pregnancies.

## *5.2 Methods*

The data for this part of the study was collected from both phase I and II of the study. Full details are given in 3.3.4, page 47 and 3.4.3, page 50.

### 5.2.1 Placental volume with advancing gestation

All the volumes were examined off-line on a personal computer using Virtual Organ Computer-aided AnaLysis II (VOCAL II™) on 4-D View™ (GE Healthcare, Milwaukee, WI, USA) to check whether the captured volume included the whole placenta for each visit up to 24 weeks. The point at which the placenta became too large to be included in a single volume was recorded and analysed using the Kaplan-Meier estimator. The difference in trends of appearance between normal pregnancies and those with adverse outcomes were analysed using a Log rank (Mantel-Cox) test.

### 5.2.2 Placental volume in SGA pregnancies

The images for all the placentas between 11 and 13+6 weeks were segmented using the previously described novel, semi-automated technique (5.1.4, page 116) and an estimate of the PlaV generated.

The Placental Quotient was calculated by dividing the CRL by the PlaV (Metzenbauer et al. 2001). A dimensionless index, the standardized placental volume (*s*PlaV) was also calculated by dividing ($PlaV^{1/3}$) by CRL. The normality of each of the distributions was tested using Kolmogorov-Smirnov test, histograms and Q-Q plots. The relationships between PlaV, gestation and birth weight were explored using regression analysis. The Mann-Whitney test was used to compare the PQ and *s*PlaV for SGA and AGA babies. The ability to predict SGA was examined by performing receiver–operating characteristics

(ROC) curve analysis including calculating the area under the curve (AUC) for PQ and *s*PlaV. To compare these novel markers to a marker well known in obstetrics, the sum of the Ut A PI at 23 weeks for our population was included in the ROC curve analysis.

### 5.2.3 Morphometric measurements in SGA pregnancies

The segmentations were then re-seeded to identify the feto-placental surface (the fetal side of the placenta which provides an interface between the placenta and the amniotic fluid) Figure 36, page 122. The algorithm then subtracted the feto-placental surface area from the total surface area ($A_t$) enabling calculation of the area of the basal plate, which can be regarded as the 'functional area' of the placenta ($A_f$).

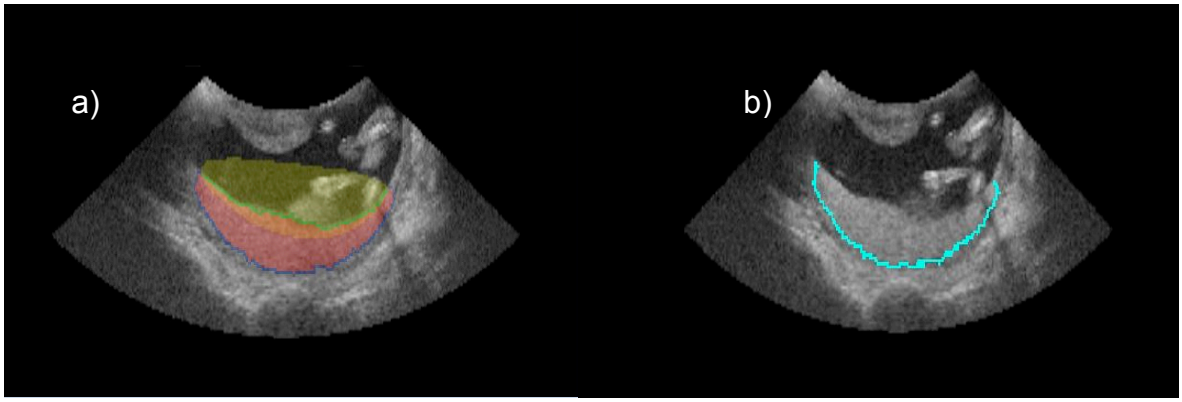



**Figure 36: Demonstrating a) the masking process to generate b) the area of the basal plate.[23]**

[23] Images supplied by Gordon Stephenson, IBME, University of Oxford, UK.

#### 5.2.3.1 Novel, morphometric dimensionless index

The dimensionless index was calculated according to Buckingham π theorem. This provides a method for computing sets of dimensionless parameters from given variables, even if the form of the equation is unknown (Buckingham 1914). This states that to generate a meaningful equation involving a set number of physical variables (n), which can be expressed in terms of independent fundamental physical quantities (k), then the original expression is equivalent to an equation involving a set of dimensionless parameters (p) constructed from the original variables (p= n−k). Therefore, for the combination of the CRL and morphometric data generated, the best equation for modeling the relationship should be derived from combination of four dimensionless parameters. Buckingham's theorem only provides a way of generating the set of dimensionless parameters that can then be tested to produce the best index. It will not choose the most 'physically meaningful' parameters, hence the Placental Functional Quotient (PFQ) Table 12 (page 124) which has to be included in the mathematical process but does not appear to make sense biologically.

The four dimensionless parameters were calculated for all participants using the variables (PlaV, CRL, $A_f$, $A_t$) measured at the first visit (between 11 and 13+6 weeks). Logarithmic regression of the generated parameters against the normally distributed variable of ‘gestation corrected birth weight’ was then used to calculate the best equation to model the relationship[24] with birth weight.

[24] Mathematical advice and assistance from Dr Robert J. Whittaker, School of Mathematics, UEA.

**Table 12: The four dimensionless parameters generated by Buckingham π theorem for the available physical variables**

| **Index Name** | **Index Abbreviation** | **Formula** |
|---|---|---|
| Standardised Placental Volume | ***s*PlaV** | $\frac{(PlaV)^{1/3}}{CRL}$ |
| Functional Area Quotient | **fAQ** | $\frac{\text{Area of basal plate } (A_f)}{\text{Total surface area } (A_t)}$ |
| Standardised Functional Area | ***s*FA** | $\frac{\text{Area of basal plate } (A_f)}{(CRL)^2}$ |
| Placental Functional Quotient | **PFQ** | $\frac{\text{CRL x basal plate area } (A_f)}{PlaV}$ |

5.2.3.2 Sphericity

Sphericity (Ψ) is a well-established dimensionless index, which is used to provide an estimate of the 'roundness' of an object. As such, it is an example of a compactness measure of shape (Wadell 1935). The closer the value is to 1 the more spherical the object is. Therefore, a thin 'pancake-like' placenta should have a lower value than a more rounded 'globular' placenta. It is the ratio of the surface area of a sphere (with the same volume as the given object) to the surface area of that object (Equation 1, page 124).

$$\Psi = \frac{\pi^{1/3}(6V_p)^{2/3}}{A_p}$$

(Vp is the volume of the particle and Ap the surface area)

**Equation 1: Sphericity.**

### 5.2.4 Combined screening model for SGA

The relationships between birth weight, and; the dimensionless parameters; the generated indices; sphericity and the available known predictors of SGA (including PAPP-A, and Ut A PI) were explored using univariate analysis. The normality of the distribution of each variable was tested using Kolmogorov-Smirnov test, histograms and Q-Q plots. Non-normally distributed variables were log-normalised before further regression analysis was performed.

Multiple regression analysis was then used on the variables significantly correlated with birth weight, to determine which were independent risk factors and generate predictive models for SGA. The regression model used requires that the residuals be normally distributed, this was examined using Kolmogorov-Smirnov test, histograms and Q-Q plots. The performance of each marker for predicting all SGA in the total population, was then further examined using ROC curve analysis. This was repeated to assess prediction of SGA in the term normotensive population and prediction of SGA in the population assessed to be low-risk at booking using routine antenatal care standards.

## *5.3 Results*

Data from 143 women were available to be analysed (Figure 10, page 57).

### 5.3.1 Placental volume with advancing gestation

Figure 37 (page 127) demonstrates that the proportion of placentas which could be captured in a single 3-D volume, decreases with advancing gestation. Only at the first visit (<14 weeks) were the placental volumes captured for all participants. By 18 weeks over a quarter were too large to be completely included in a single volume sweep. Figure 38 (page 127) demonstrates the survival curve for the number of placentas that could be captured in a single static 3-D volume with advancing gestation. No significant difference in the rate at which the whole placenta became too large to capture was demonstrated for any sub-group analysis (Table 13, page 128).

The placental volume was seen to correlate with the gestation over the 27-day recruitment period between 11+0 and 13+6 weeks'. The placental volume of pregnancies destined to result in SGA babies was significantly smaller when the effect of gestation was controlled for (p=0.001), Figure 39 (page 128).

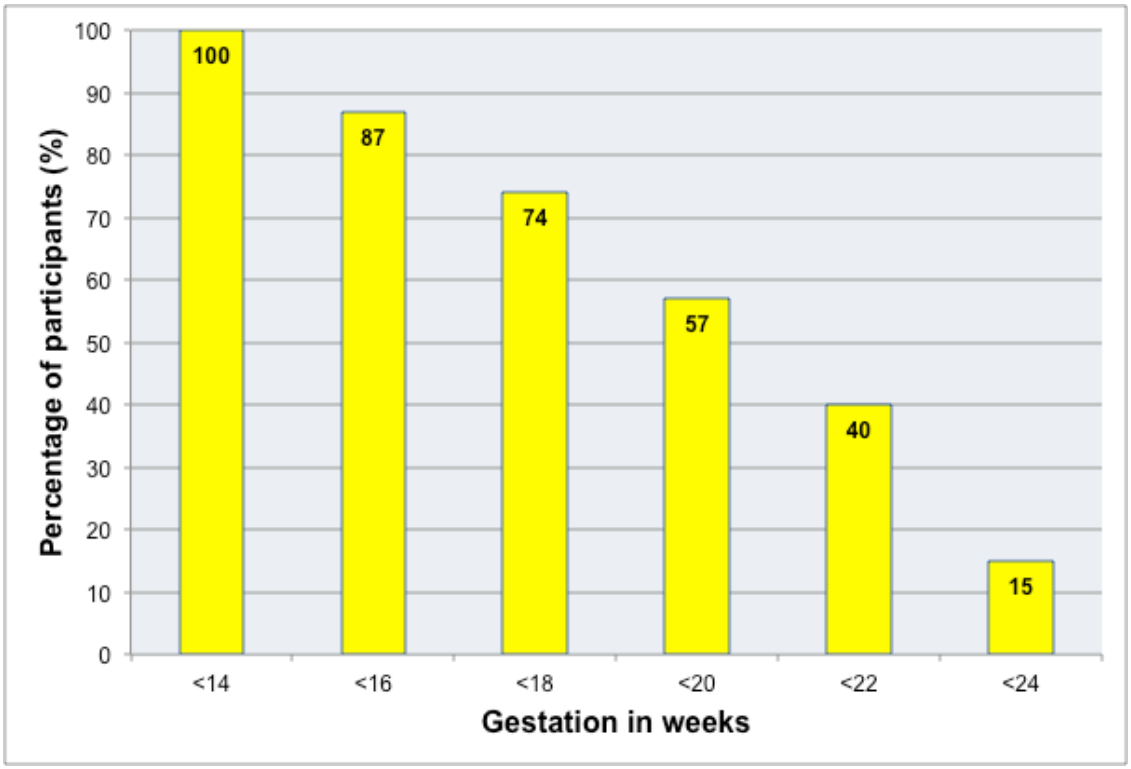



**Figure 37: Percentage of participants in whom the whole placenta could be captured in a single volume.**

(n=143)

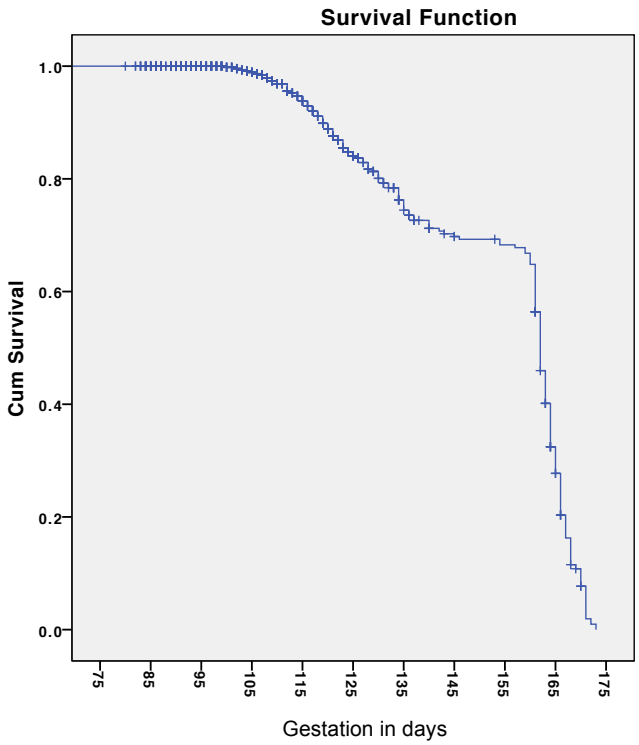



**Figure 38: Kaplan-Meier for capture of the whole placenta.**

Demonstrating the decreasing number of placentas small enough to be captured in a single volume with advancing gestation.

**Table 13: Log rank testing for the survival functions of the placentas becoming too large to be included in a single volume**

| Comparators | | Log rank result |
|---|---|---|
| All SGA<br>(inc.all hypertensive disorders)<br>n=20 | All AGA<br>(inc.all hypertensive disorders)<br>n= 123 | P=0.11 |
| Term SGA<br>(inc.all hypertensive disorders)<br>n=18 | Term AGA<br>(inc.all hypertensive disorders)<br>n=121 | P=0.36 |
| Term normotensive SGA<br>n=13 | Term normotensive AGA<br>n=113 | P=0.62 |

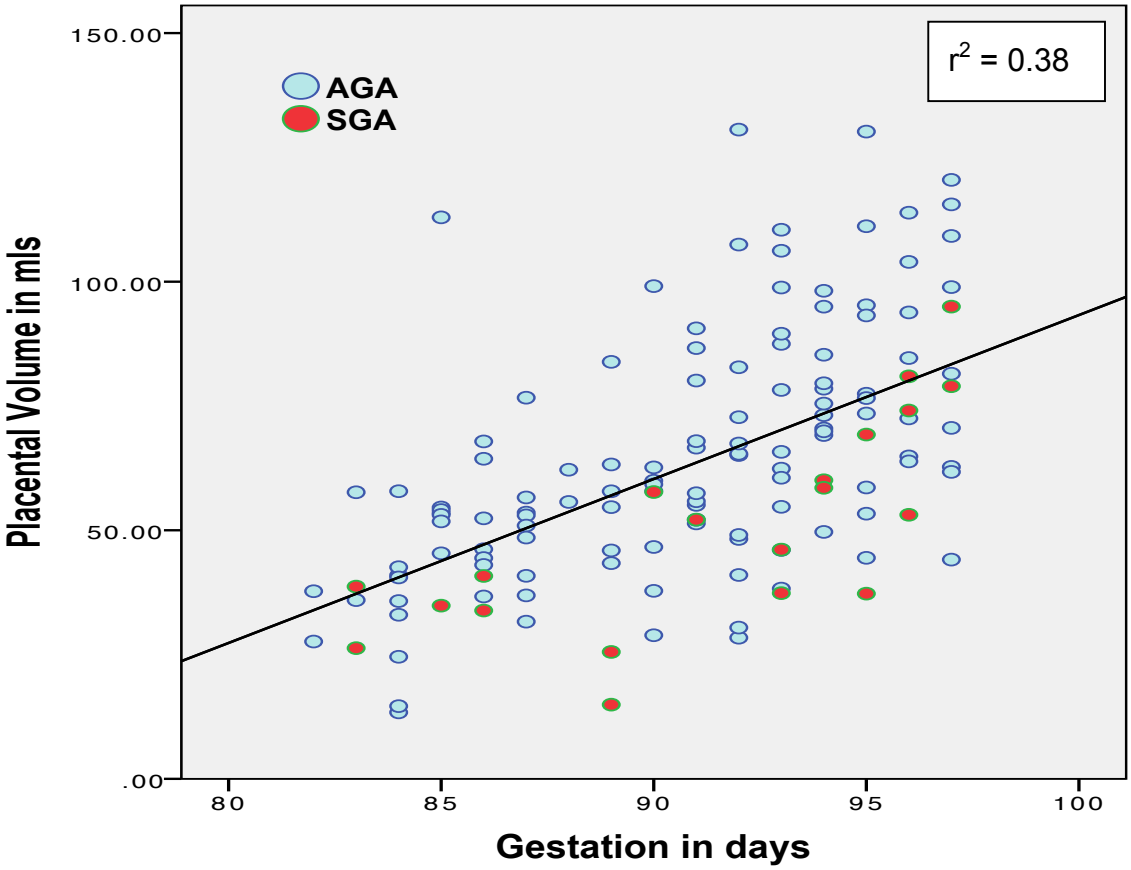



**Figure 39: Placental volume for each participant between 11 and 13+6 weeks.**

### 5.3.2 Placental volume in SGA pregnancies

The PlaV, PQ and *s*PlaV of the pregnancies resulting in SGA babies were significantly different at 11 to 13+6 weeks to those pregnancies resulting in AGA babies (p=0.002, 0.026 and 0.001 respectively; Table 14). A significant difference was seen between SGA and AGA for *s*PlaV and PlaV for all term pregnancies and term, normotensive pregnancies but not for PQ. The AUCs in the prediction of SGA across the whole population by the PQ, *s*PlaV and the Ut Doppler PI are shown in Table 15 (page 130) and Figure 38 (page 127).

**Table 14: Differences in placental volume and its derived indices between SGA and AGA pregnancies**

| **Groups compared** | | | **P value** |
|---|---|---|---|
| All SGA<br>(inc.all hypertensive disorders)<br>n=20 | All AGA<br>(inc.all hypertensive disorders)<br>n= 123 | **PQ**<br>***s*PlaV**<br>**PlaV** | 0.003*<br><0.001*<br>0.002** |
| Term SGA<br>(inc.all hypertensive disorders)<br>n=18 | Term AGA<br>(inc.all hypertensive disorders)<br>n=121 | **PQ**<br>***s*PlaV**<br>**PlaV** | 0.008*<br>0.001*<br>0.006** |
| Term normotensive SGA<br>n=13 | Term normotensive AGA<br>n=113 | **PQ**<br>***s*PlaV**<br>**PlaV** | 0.056*<br>0.002*<br>0.026** |

* Mann-Whitney test ** Regression analysis (controlling for gestation)

**Table 15: Screening performance of PQ, *s*PlaV and Ut A PI**

| | | Area under the ROC curve (95% CI) | | |
|---|---|---|---|---|
| | n (%) | **PQ** | ***s*PlaV** | **Ut A PI** |
| All SGA | 20 (14%) | 0.72 (0.61-0.83) | 0.77 (0.66-0.87) | 0.67 (0.52-0.82) |
| Term SGA | 18 (13%) | 0.70 (0.58-0.82) | 0.75 (0.63-0.86) | 0.65 (0.50-0.81) |
| Term, normotensive SGA | 13 (10%) | 0.67 (0.52-0.81) | 0.77 (0.65-0.88) | 0.55 (0.37-0.73) |

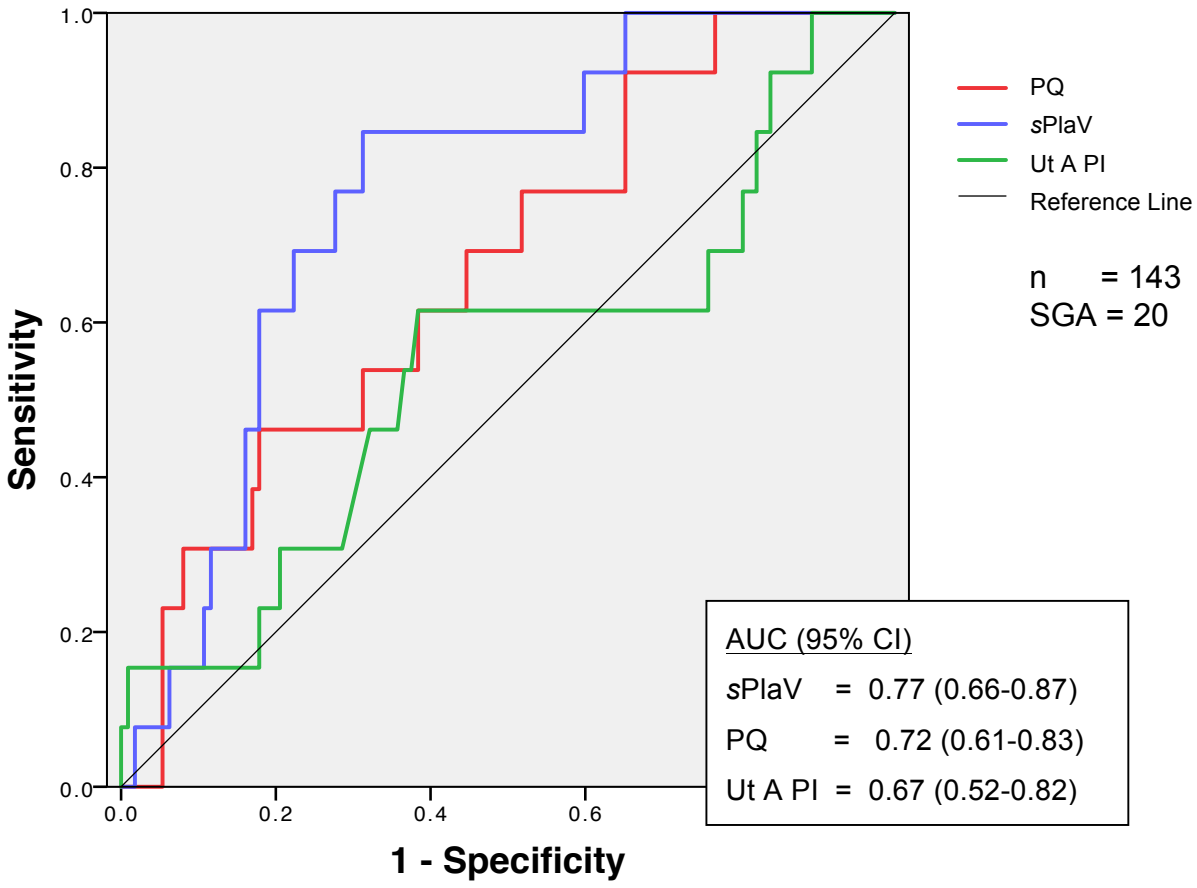



**Figure 40: Screening receiver-operating characteristics curves for prediction of all cases of SGA in the whole population.**

(including pre-term and gestational hypertensive disorders).

### 5.3.3 Morphometric measurements in SGA pregnancies

#### 5.3.3.1 Novel, morphometric dimensionless index

The formulae for the four dimensionless parameters generated by Buckingham π theorem are shown in Table 12, page 124. The results for the analysis of their normality of distribution are given in 8.4, page 195. Univariate linear regression analysis demonstrated that only *s*PlaV and *s*FA were significantly correlated to birth weight (Table 16, page 133). Multivariate logistic regression against birth weight demonstrated that all of the dimensionless indices were inter-dependent co-factors. Therefore they could not be combined in any way to improve the performance of the model for the prediction of birth weight.

The two parameters significantly correlated with birth weight (*s*PlaV and *s*FA) were analysed using ROC curves. This demonstrated there was no predictive advantage in using *s*FA, over the simpler *s*PlaV, Figure 41 (page 132).

#### 5.3.3.2 Sphericity

There was no significant correlation between the placental sphericity and birth weight ($p=0.1$).

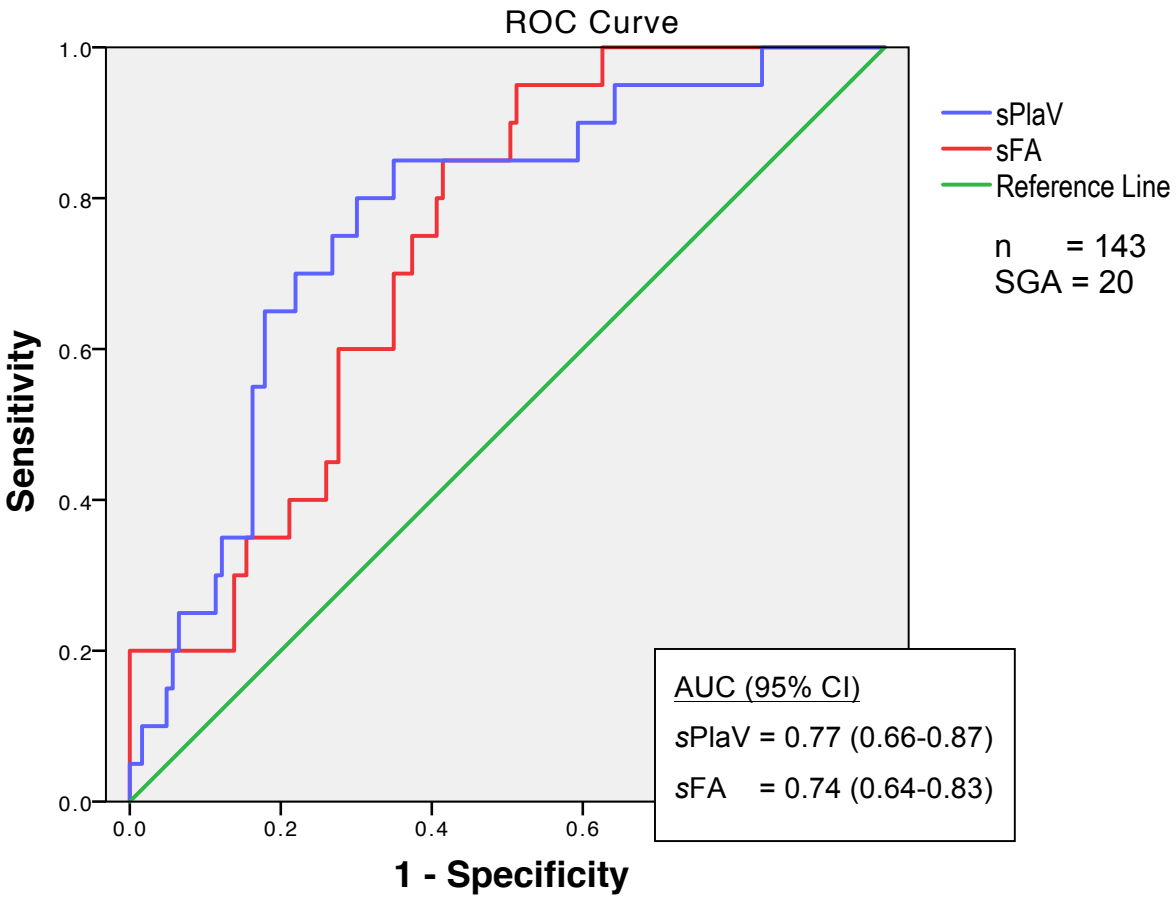



**Figure 41: Screening receiver-operating characteristics curves for prediction of all cases of SGA in the whole population.**

(including pre-term and gestational hypertensive disorders).

**Table 16: The results for univariate analysis against birth weight for the four dimensionless parameters**

| Index Name | Index Abbreviation | Formula | ANOVA p-Value |
|---|---|---|---|
| Standardised Placental Volume | ***s*PlaV** | $\frac{(PlaV)^{1/3}}{CRL}$ | <0.0001 |
| Functional Area Quotient | **fAQ** | $\frac{\text{Area of basal plate } (A_f)}{\text{Total surface area } (A_t)}$ | 0.44 |
| Standardised Functional Area | ***s*FA** | $\frac{\text{Area of basal plate } (A_f)}{(CRL)^2}$ | <0.0001 |
| Placental Functional Quotient | **PFQ** | $\frac{CRL \times \text{basal plate area } (A_f)}{PlaV}$ | 0.24 |

### 5.3.4 Combined screening model for SGA

The results for the normality of distribution analysis for each variable included are given in the Appendices (8.4, page 195). Univariate analysis demonstrated that, in our sample, customised birth weight significantly correlated with PAPP-A (MoMs), NT (MoMs), and 2nd trimester Ut A PI (Table 17, page 134). When multiple regression analysis was performed only *s*PlaV, *s*FA, PAPP-A (MoMs) and NT (MoMs), were shown to be independent predictors of customised birth weight. However, *s*FA and *s*PlaV were not independent of each other. Therefore two models can be generated for the prediction of birth weight. These are shown in Equation 2 (page 134).

**(Model 1 - *s*PlaV)**

Estimated Birth weight = 0.97 + (56.00 x *s*PlaV) + (0.42 x PAPP-A) + (0.70 x NT)

**(Model 2 - *s*FA)**

Estimated Birth weight = 12.40 + (1.40 x *s*FA) + (0.51 x PAPP-A) + (0.71 x NT)

**Equation 2: Models generated to predict SGA babies**

**Table 17: Results of univariate linear regression against customised birth weight**

| ***Parameter*** | ***R squared value*** | ***ANOVA p value*** |
|---|---|---|
| Maternal age | <0.01 | 0.54 |
| Maternal BMI | 0.03 | 0.53 |
| PAPP-A (MoMs) | 0.09 | <0.01 |
| NT (MoMs) | 0.04 | 0.03 |
| βhCG (MoMs) | 0.01 | 0.28 |
| 1$^{st}$ trimester Ut A PI | 0.02 | 0.12 |
| 2nd trimester Ut A PI | 0.63 | 0.03 |
| Booking mean arterial pressure (MAP) | <0.01 | 0.95 |

The ROC curves for prediction of all cases of SGA (including pre-term deliveries and women who developed hypertensive disorders) show AUCs of 0.80 (0.69–0.92) for model 1 (*s*PlaV) and 0.78 (0.67—0.89) for model 2 (*s*FA). This is an improvement on *s*PlaV and *s*FA alone, achieving a sensitivity for predicting all SGA of 67% and 56% respectively for a false positive rate of 20% (Figure 42, page 136).

When the models were used to predict normotensive, term SGA the ROC curves improved slightly (Figure 43, page 137) and continue to perform better than *s*PlaV and *s*FA alone with sensitivities of 83% and 59% for a 20% false positive rate.

The models were used to predict SGA in just the population considered to be low risk at 11 to 13 weeks (midwifery-led care with no known risk factors for pregnancy complications and low risk combined screening test results; n=106). For this population the AUCs remain very good (0.82 (0.69-0.94) and 0.84 (0.72-0.95) respectively) with sensitivity of 70% for 20% false positive rate (Figure 44, page 137).

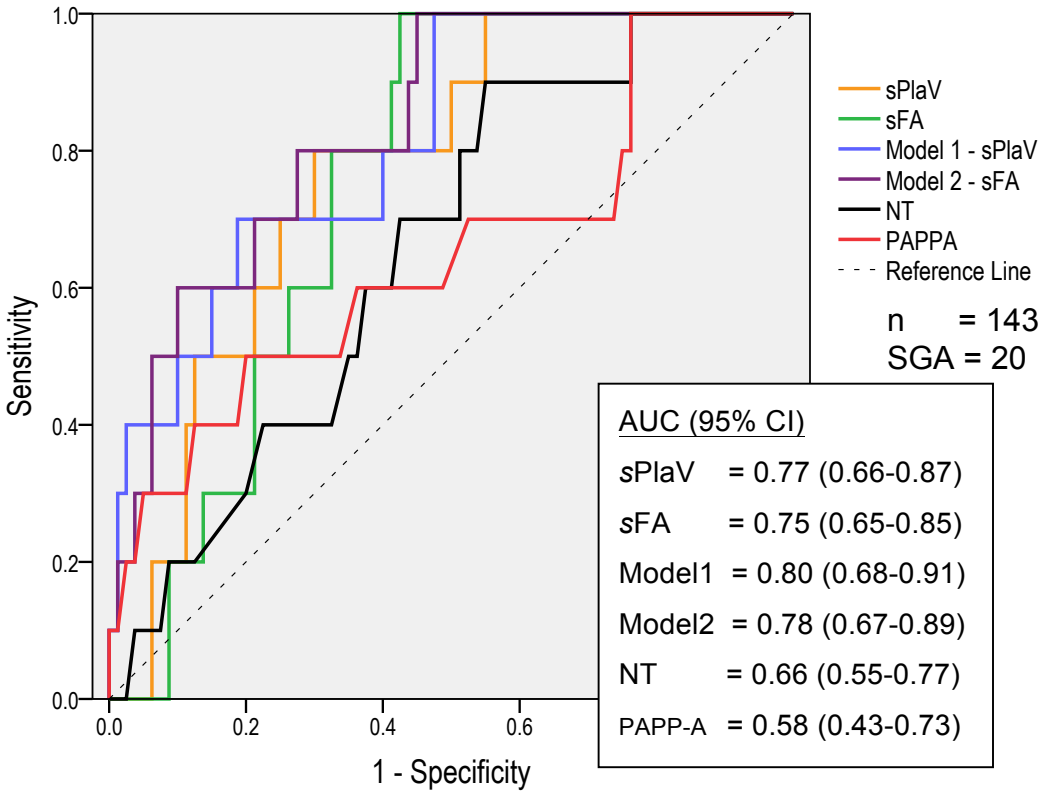



**Figure 42: Screening receiver-operating characteristics curves to predict all SGA in the whole population.**

(including pre-term and gestational hypertensive disorders).

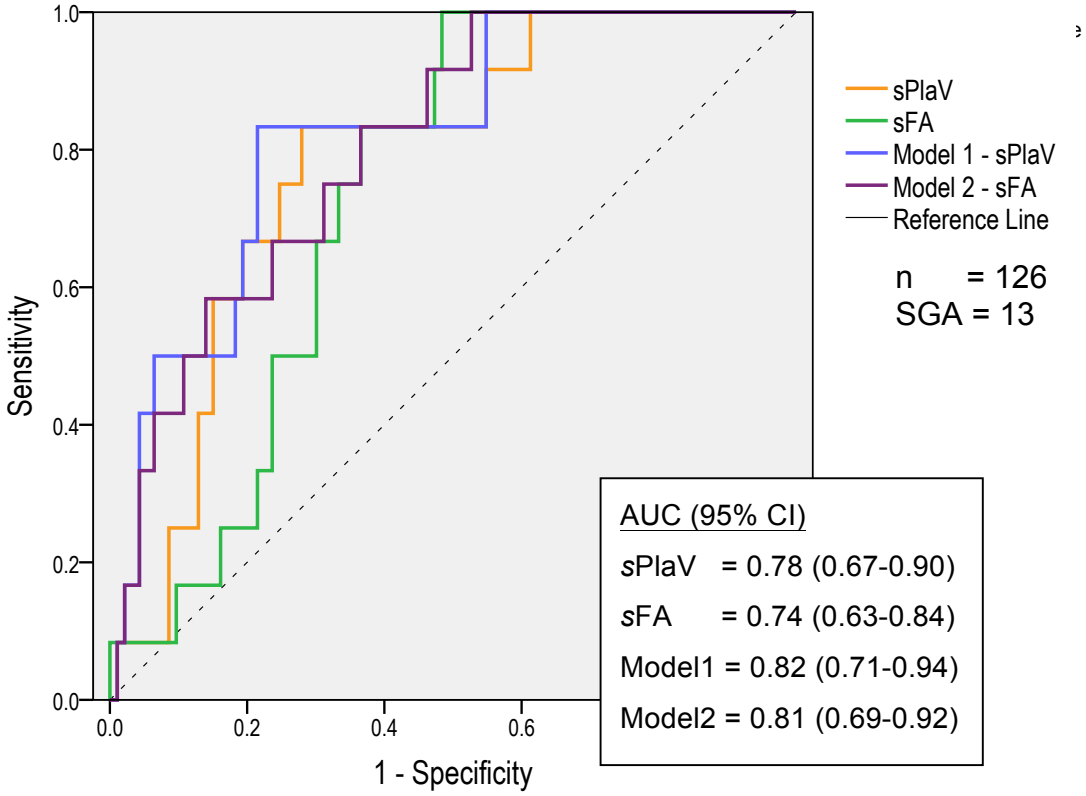



**Figure 43: Screening receiver-operating characteristics curves to predict term, normotensive SGA babies.**

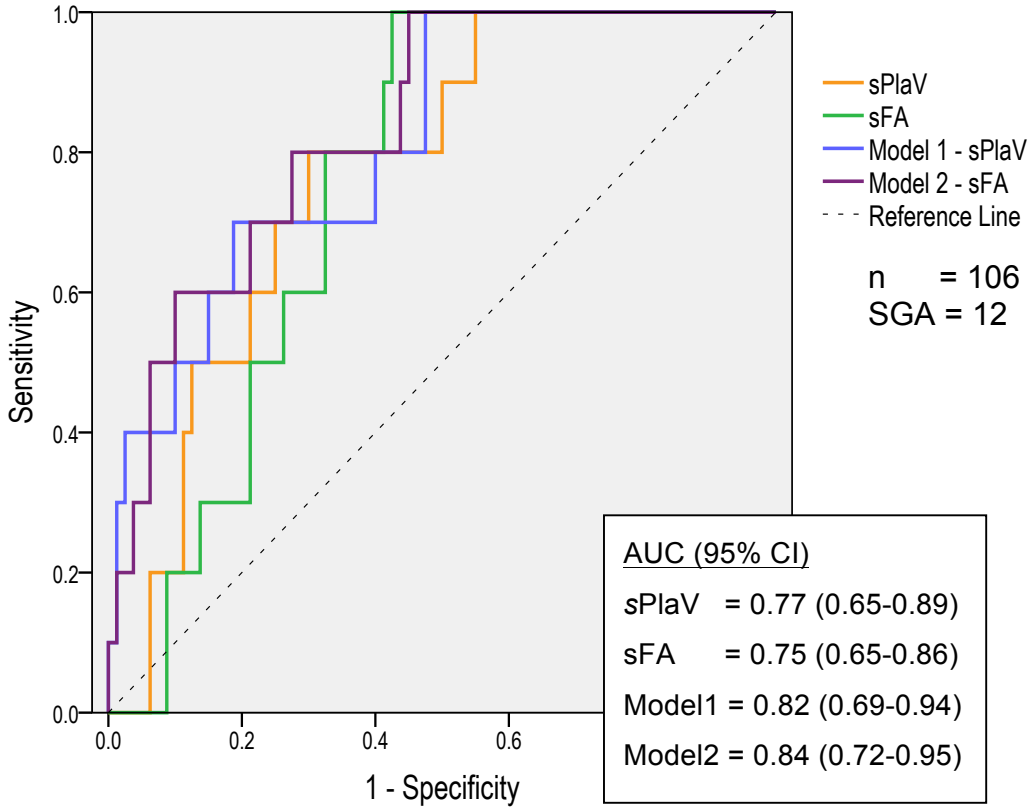



**Figure 44: Screening receiver-operating characteristics curves to predict SGA in a population deemed to be 'low risk' at booking.**

## *5.4 Discussion*

### 5.4.1 Novel, semi-automated process

This is the first clinical study to use the semi-automated method for generating placental volume developed by the IBME, Oxford University (Stevenson et al. 2010; Stevenson 2011). This has been shown to produce comparable results to those generated by manual segmentation (the gold standard) and to outperform VOCAL™ in terms of both the inter and intra-observer variance (Stevenson et al. 2010). The estimates of volume generated were similar to those reported by previous studies (Hafner et al. 2001; Schuchter et al. 2001; Metzenbauer et al. 2002; Hafner et al. 2006; Law et al. 2009; Schwartz et al. 2010). Furthermore, the estimates produced were robust enough to predict SGA, even in a low risk population. Until now, using placental volume as part of a screening test has been an impractical suggestion due to the time consuming, operator dependent process required to generate it. The development of this semi-automated process allied with these promising study results are an important step towards making early placental volume a realistic ultrasound marker for SGA.

### 5.4.2 Optimal gestation for a placental volume screening test

Only before 14 weeks' gestation could the whole placental volume be reliably captured in all the study population. Studies undertaken in the developing world have reported that placental volume can be measured in a single volume sweep up to 40 weeks' gestation (Thame et al. 2001; de Paula et al. 2008). This is most likely to be a reflection of the differences between the populations sampled. Other, European, studies have suggested that up to 97% of

placentas can be acquired before 18 weeks (Deurloo et al. 2007a) but that the observer bias increases with advancing gestation (Jones et al. 2010). This study had a lower acquisition rate at 18 weeks' gestation (74%). There may be several reasons for this. The sample size in this study was considerably larger than the others, which only had 34 (Deurloo et al. 2007b) and 20 (Jones et al. 2010) participants. Neither of the other studies states the BMI of their participants. Spiral 3-D only excluded women with a BMI >35, which is relatively generous for research involving a transabdominal ultrasonography technique. The other studies do not report how it was decided that the whole placental volume had been included. It is most likely that, as in this study, it was an assessment by the operator. It is possible that the subjective exclusion standards were different between the studies. Pragmatically, it would be more cost-effective to incorporate any new screening test into the already existing screening programme (i.e. 11-13+6 weeks or 20 weeks). The consensus from these and other studies appears to be that by 20 weeks not all placentas can be captured and the volumes are less reliable at this point (Pomorski et al. 2011). Therefore, the volume and morphometric research focused on ultrasound data obtained at the first visit.

### 5.4.3 Controlling for gestation in the potential screening test

The data confirmed that there is a considerable difference in the volume of a placenta between 11 weeks and 13+6 weeks (Metzenbauer et al. 2002; Hafner et al. 2006; Law et al. 2009; Plasencia et al. 2011). For any screening test developed to be used at the same time as the combined test, the normal change in volume over the 27-day testing period needs to be controlled for. This can be performed by, either sampling a very large population and

calculating gestation specific MoMs, or by relating it to another measurement believed to be relatively consistent across the majority of pregnancies. The second solution was the basis for the development of the PQ which can be used as a surrogate marker for appropriateness of placental size (Hafner et al. 2001). However, despite the NICE recommendation (NICE 2008b), and widespread use of CRL to date pregnancy, the assumption that embryonic growth is uniform in the first trimester remains contentious. Studies have demonstrated that early fetal growth is affected by fetal gender (Bukowski et al. 2007), maternal ethnicity (Bottomley et al. 2009) and chromosomal abnormalities (Schemmer et al. 1997). Placental pathology has also been reported to affect early gestational sac volume (Falcon et al. 2005). Consequently, using the CRL as an exact surrogate marker of gestation may be flawed. However, as the PQ is a ratio it corrects for the effect of gestation without needing to assign dates to the pregnancy. If the underlying pathology does affect both the placenta and fetus the remaining issue will be the sensitivity of the test. However, if as suspected, the placental volume is disproportionately affected compared with the CRL, a ratio between the two measurements should correct for gestation whilst retaining adequate sensitivity.

### 5.4.4 The use of a dimensionless index - *s*PlaV

To the best of our knowledge, this is the first time that the standardized placental volume (*s*PlaV) has been suggested and investigated as a predictor of SGA. The importance of using dimensionless quantities has long been recognized in mathematics and engineering. This index is not only mathematically more robust but is also normally distributed, unlike the PQ (8.4,

page 195). This explains why it may be prove to be a better clinical indicator for prediction of SGA, even though it is a ratio of the same measurements use to generate the PQ.

### 5.4.5 Early placental morphology

The compactness of shape of the placenta expressed as sphericity, did not correlate with ultimate birth weight. There is a correlation between various measures of placental surface area and birth weight, but the effect is not independent of the placental volume. Therefore, combining the dimensionless parameters generated by the Buckingham π theorem (Buckingham 1914), did not produce a better model than using *s*PlaV alone. As the calculation of the *s*FA requires a second seeding this increases the risk of process errors as well as making it more time consuming to estimate. Therefore, the *s*PlaV appears to be more useful in the prediction of SGA

The lack of difference in objective morphology measures was disappointing. It is possible that the novel processes used were not robust enough to detect differences in the morphology. However, it is more likely that the differences reported in placental morphology from 20 weeks onwards (Fisteag-Kiprono et al. 2006; Huppertz et al. 2006; Toal et al. 2007; Costa et al. 2008; Toal et al. 2008) are not apparent at this early stage in placental development.

### 5.4.6 Calculating a model to predict SGA

The precise relationship between the 3-D placental volume estimate and the maternal serum concentration of PAPP-A remains unclear. A previous study suggested that PAPP-A was not independent of placental volume (PlaV) (Law et al. 2009). However, the results of this study, and another recently published

one (Plasencia et al. 2011), indicate that both PlaV and PAPP-A are independent risk factors for SGA and therefore can be combined to produce a better predictive model. For a fixed false positive rate of 10%, the sensitivity of placental volume for the detection of growth restriction has been reported as 27% (Hafner et al. 2006), 23% (Law et al. 2009) and 29 % (Plasencia et al. 2011). When combined with PAPP-A and maternal characteristics this increased to 34% (Plasencia et al. 2011). This study demonstrates that the combination of *s*PlaV, PAPP-A and NT measurements increased the sensitivity to 40% for 10% false positive. The NT measurement is not commonly associated with prediction of growth restriction however other studies have also demonstrated a significant correlation between NT measurement and birth weight (Karagiannis et al. 2011; Papastefanou et al. 2011).

There may be many reasons for the differences in these findings. 1) The definition of growth restriction used, 2) the way in which the effect of placental volume has been assessed and 3) the inclusion of other risk factors such as maternal characteristics or NT in the model.

The other study which produced a combined predictive model (Plasencia et al. 2011) defined SGA as $<5^{th}$ centile using a reference range of birth weight for gestation at delivery defined from their population. When the *s*PlaV model developed by this study is used to predict severe SGA ($<5^{th}$ centile on customised birth weight centiles) the sensitivity for detection of SGA increases to 50% for 10% false positive rate (Figure 45, page 145). Care must be taken when interpreting this though as there are only a small number of cases of severe SGA (n=8).

The Law study reports that placental volume “was transformed into gestation dependent z-scores” (Law et al. 2009). Whilst their sample size was 601 women, this is probably not large enough to demonstrate the true nature of the underlying distribution. The other recent paper, with an impressive sample size of 3,104 (Plasencia et al. 2011), used placental volumes, which were made Gaussian after log transformation, to calculate the MoMs for the growth restricted group from the underlying distribution of the AGA sample. The use of *s*PlaV greatly simplifies the gestation correction process and so less statistical manipulation is required. This is important as whilst transformations are an important statistical technique they can potentially mask subtleties within a dataset. This study did not demonstrate that any underlying maternal characteristics were significantly correlated with birth weight. This is unsurprising for age, BMI and ethnicity as this has already been taken into account when generating the customised birth weight centiles. Unfortunately, the sample size was too small to accurately assess other known risk factors such as past obstetric history. However, this would be an important consideration in future larger trials.

### 5.4.7 Limitations

The limitations include the size of the study and the method of recruitment. This is especially relevant when interpreting the ROC curve analyses. These were included purely for comparison and must be interpreted with caution in a selected population. The underlying prevalence of the outcome being considered has the potential to distort the results for example, there were few pre-term severe SGA cases hence the observed very poor predictive value of the second trimester Ut A PI. The most reliable ROC curve calculated is for the

unselected low risk pregnancies (Figure 44, page 137) where, the values for the AUC for sPlaV and the two generated models are very encouraging. Also the small numbers give rise to large step changes in the values generated by these analyses making a clear indication of sensitivity to false positive rate difficult.

Five women with known low PAPP-A on combined screening were referred to the fetal medicine unit and then recruited as part of the selected high-risk population. One of these women was found to have a fetus with trisomy 21 and chose to terminate the pregnancy, the remaining four were included in the analysis. Even though this only a small number of women it will introduce a level of selection bias which must be considered when interpreting the results of the models. However, as none of these women had a pregnancy that resulted in an SGA baby this should have skewed the data away from demonstrating a correlation between low PAPP-A and low birth weight, yet a significant relationship was still demonstrated. This may be part of the reason for the improved performance of the model in the population assigned to be low risk.

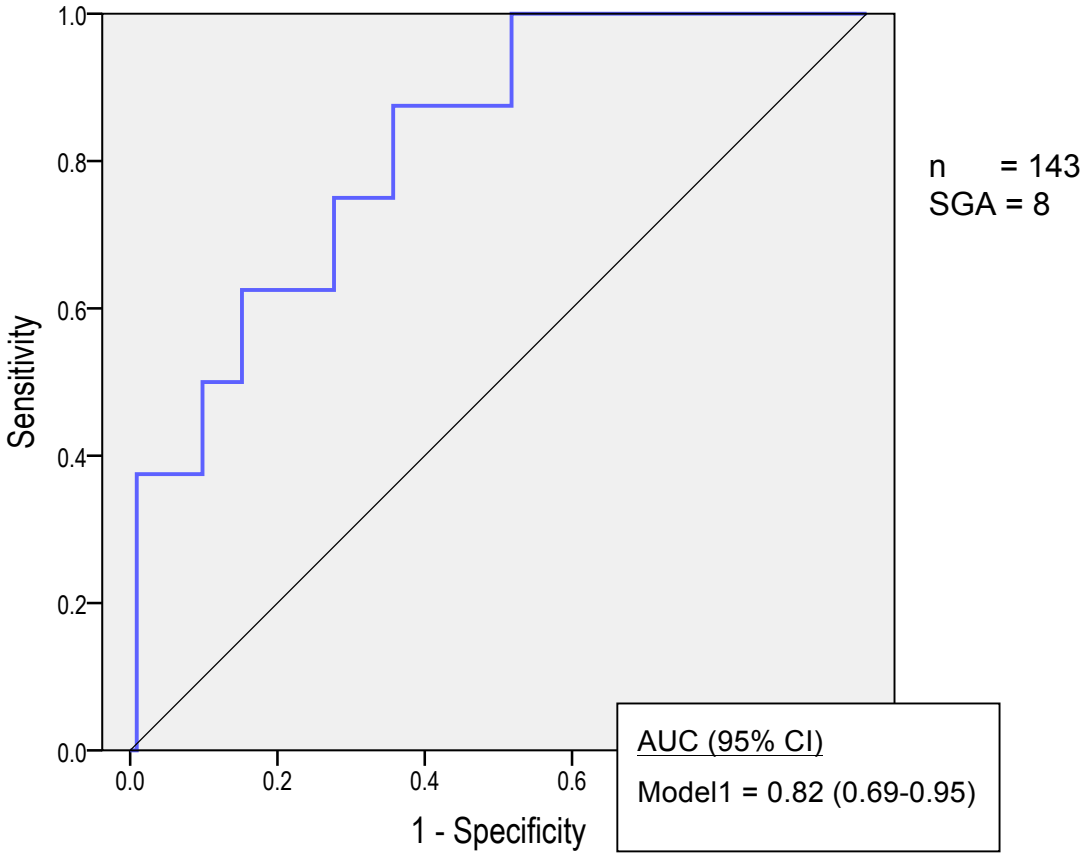



**Figure 45: Screening receiver-operating characteristics curves to predict all severe SGA (<5th centile) in the whole population.**

(including pre-term and gestational hypertensive disorders).

# 6 3-D Power Doppler studies

## *6.1 Introduction and background*

For the last two decades researchers have been tantalized by the prospect of using non-invasive techniques to evaluate tissue perfusion (Dymling et al. 1991; Carson et al. 1993). Power Doppler ultrasound imaging was initially suggested as a possible answer (Dymling et al. 1991; Carson et al. 1993). Unlike colour Doppler it is based on the analysis of amplitude (or power) of the Doppler shift (Doppler 1843) rather than estimating the mean frequency shift (Rubin et al. 1994). As the direction of flow (negative or positive frequency shift) and velocity (high or low frequency shift) are disregarded in this analysis, the power (energy) of the many different frequency shifts are added to form the 'power Doppler' signal (Rubin et al. 1994). The power mode is therefore very sensitive to any movement at all in the target scatterers (erythrocytes) and as such is able to record blood flow at much lower velocities than colour Doppler ultrasound. The power Doppler signal is therefore virtually independent of the angle of insonation, has no aliasing and has an increased dynamic range for display (MacSweeney et al. 1996; Adler 2001; Welsh 2004). This makes it a promising tool for studying the low resistance, low flow vasculature of the placental bed. With the advent of 3-D ultrasound imaging techniques came 3-D Power Doppler. This offered the promise that, in addition to 2-D assessment of flow in a single vessel, a quantitative measure of blood flow through an entire organ might be obtained (Yu et al. 2003).

The subsequent development of 3-D PD software packages such as VOCAL™, then introduced ease and automation to the process of PD imaging giving clinicians a tool to generate numerical indices (VI, FI and VFI). These commonly used indices are often quoted as approximating to 'flow' or 'perfusion' in the volume sampled (Moran et al. 2011). Whilst they are very unlikely to be representing flow, their exact meaning in relationship to the underlying tissue vascularity remains hotly debated, as does the validity of results generated using them (Martins 2010; Welsh 2010).

### 6.1.1 Factors affecting power Doppler results

The power Doppler signal displayed is known to be influenced by a large number of factors (including machine settings, and tissue attenuation) (Rubin et al. 1994; Derchi et al. 1997; Martinoli et al. 1997; Martins 2010). This has also been shown to affect the calculated VOCAL™ indices in phantom models (Raine-Fenning et al 2008 a,b,c). To enable appropriate comparison of PD results between patients, these factors need to be controlled for. The most commonly used approach to this problem is to ensure that all the ultrasound machine settings are kept constant (Raine-Fenning et al. 2008a; Martins 2010; Martins et al. 2010a). This should allow for most of the factors demonstrated to affect PD results. However, this cannot control for inherent differences in the beam path between patients (related to the depth and type of tissues being insonated). In transabdominal obstetric studies this is very important as the position of the placenta, and the amount of tissue being insonated may vary considerably between patients.

### 6.1.2 Power Doppler gain setting

The power Doppler gain can be thought of as analogous to a 'volume controller' of the sound waves which allows for the degree of signal attenuation encountered by passing through the tissue. Where there is a lot of tissue or the tissue is very dense, the gain (volume) will need to be set to a high level to ensure sufficient sounds waves reach the target and are reflected back. If the gain (volume) level selected is too high for the amount of tissue encountered, 'noise' artefact is seen. Therefore, as the beam path will be different in every patient, it is counter-intuitive to suggest keeping the PD gain setting constant for all participants in a study. Early research in PD appreciated the need to attempt to individualise the gain setting in order to maximise meaningful signal recorded. This was done by increasing the gain to the level at which obvious artefactual noise became present at the insonation target, then slowly reducing it to a level just below this threshold (i.e. to where the 'noise' artefact just disappears) (Bude et al. 1994; Rubin et al. 1994; Martinoli et al. 1997; Carson et al. 1998). This, thereby indicates the maximum gain (volume) setting to allow for the tissue attenuation between probe and target for that individual. This can be set each time the participant is scanned, thereby controlling for any movement in the target organ (the passage of the gravid uterus from the pelvis into the abdomen) or other increase in tissue depth (maternal weight gain in pregnancy).

Whilst the phantom models have also demonstrated that PD gain has an effect upon the commonly used VOCAL™ 3D indices (Martins et al. 2010b), the exact nature of this influence *in vivo* remains unknown, as does the impact of keeping the gain setting constant across all participants in a study. It is possible to

investigate this *in utero* by using the patient as her own control. Keeping all other factors constant and only altering the gain level will allow the influence of the gain setting on the calculated VOCAL™ indices to be studied for that participant.

### 6.1.3 Fetal and maternal circulations

Another unknown factor is the effect of the differences in the fetal and maternal circulations on power Doppler signal. Not only is fetal haemoglobin structurally different and the haematocrit higher (Chang et al. 1972) but the red cells may also behave differently due to their rheological properties. Fibrinogen is one of the most rheologically active plasma proteins (Lowe 1987). This causes red cell aggregation forming rouleaux at low velocity flow, which has the effect of increasing the size of some of the scatters thereby changing the behaviour of the scattered PD signal in the maternal circulation (Rubin et al. 1995). Fetal blood is relatively low in fibrinogen making it less likely to develop rouleaux (Linderkamp et al. 1984a; Linderkamp et al. 1984b; Rampling et al. 1989). Previous studies have demonstrated that this produces a homogeneity of scatterers not seen in adult blood flow (Welsh et al. 2005). Therefore, the effects of change in PD gain may be different in the fetal and maternal circulations.

### 6.1.4 Aims of this chapter

This chapter explores **Hypothesis 2.1.4 page 32** by investigating:

1. The *in vivo* influence of gain on the PD signal using the calculated VOCAL™ 3D indices as a surrogate marker of output and the participant as her own control.

2. Whether the gain setting can be individualised to allow appropriate comparison of the results between patients.

3. Whether changing the PD gain setting produced different effects in fetal and maternal circulations.

## *6.2 Methods*

### 6.2.1 Data collection

The data for this part of the study were collected during Phase I. After confirmation of viability and identification of placental position, the optimal position for 3-D acquisition of the whole placenta was identified. Five anatomically identical static 3-D power Doppler volumes of the placenta were acquired in rapid succession using a previously saved machine configuration, only changing the PD gain setting (Full details: 3.3.4, page 145). The value of the individualised 'sub-noise' gain (SNG) setting SN was decided by increasing the gain until artefactual noise was present (seen as a PD signal scattered throughout the whole image), then slowly reducing it to a level just below this threshold (i.e. to where the 'noise' artefact just disappears).

The data were then stored using Sonoview and analysed off-line on a personal computer using Virtual Organ Computer-aided AnaLysis II (VOCAL II™) on 4-D View™ (GE Healthcare, Milwaukee, WI, USA).

To avoid the introduction of any potential confounding factors due to pathology only the data from pregnancies resulting in a 'normal' outcome were included. A 'normal' pregnancy outcome was defined as: uncomplicated live birth after 37 completed weeks' gestation; customised birth weight ≥10th centile; no admission to the NICU; no evidence of maternal hypertensive disorders, gestational diabetes or other significant pregnancy related maternal morbidity.

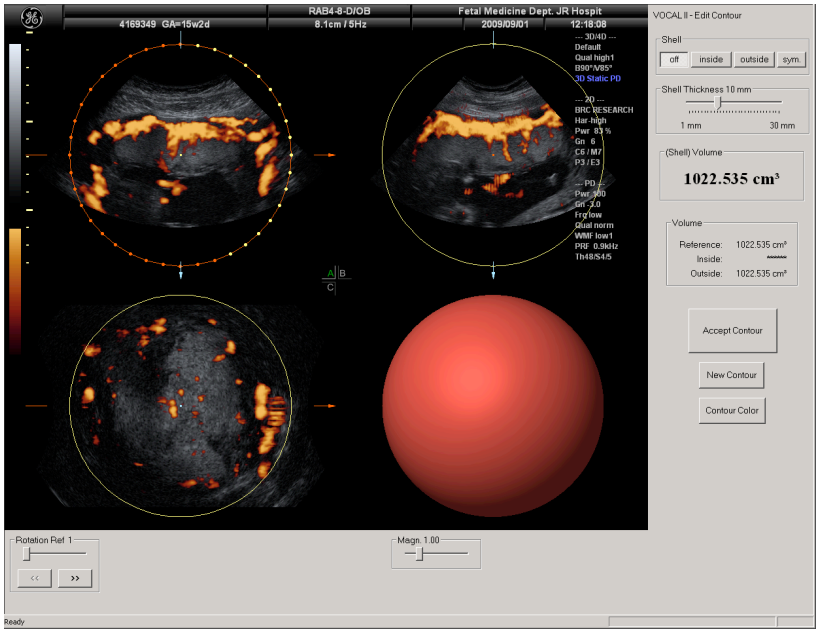
### 6.2.2 Data analysis - the whole placenta

Each static volume was opened in 4-D view and analysed without any initial image manipulation. The maximum sized sphere allowed by VOCAL™ was selected, using 6-degree rotational steps centered on the reference image (Figure 46, page 153). The sphere included the whole captured placenta. The sample volume was checked to see if it was in the same anatomical position and identical in size for each of the five volumes. This ensured that all the same vasculature was included in each sample thereby minimising any potential errors that could be introduced by sampling different sized vessels. This meant that for each participant the only difference in the five samples analysed was the setting of the power Doppler gain. The VOCAL™ histogram was then viewed and the values of the vascularisation index (VI), flow index (FI) and vascularisation flow index (VFI) were recorded.

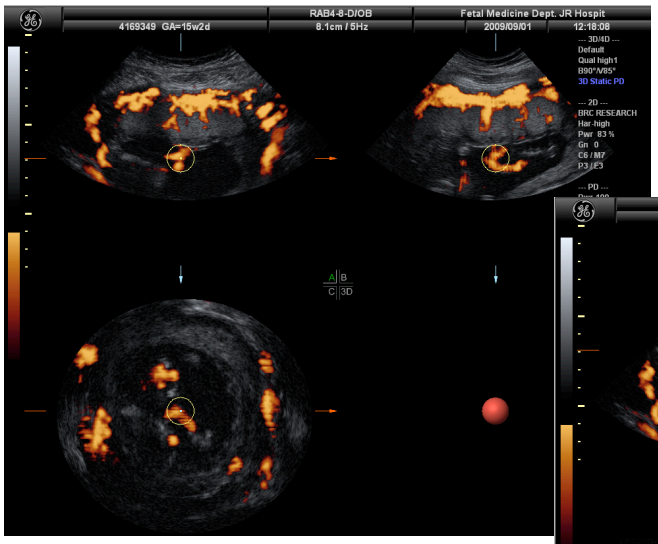
### 6.2.3 Data analysis – separate fetal and maternal samples

The VOCAL™ sphere was reduced to the smallest size allowed by the software at a magnification of 1.0 of the original image (to ensure size consistency) and placed with its border at the point of the cord insertion into the placenta (Figure 46, page 153), ensuring that only the PD signal scattered by fetal cells was recorded. The size of the ROI was noted and the value for VI, FI, and VFI was recorded. The region of interest was then moved vertically and placed over the maternal tissues directly opposite the cord insertion with the border of the sphere abutting the deciduo-placental interface (Figure 46, page 153), ensuring that only the PD signal scattered by maternal circulation was recorded. The size of the ROI was noted and the values for VI, FI and VFI were recorded.

a)




b)




c)

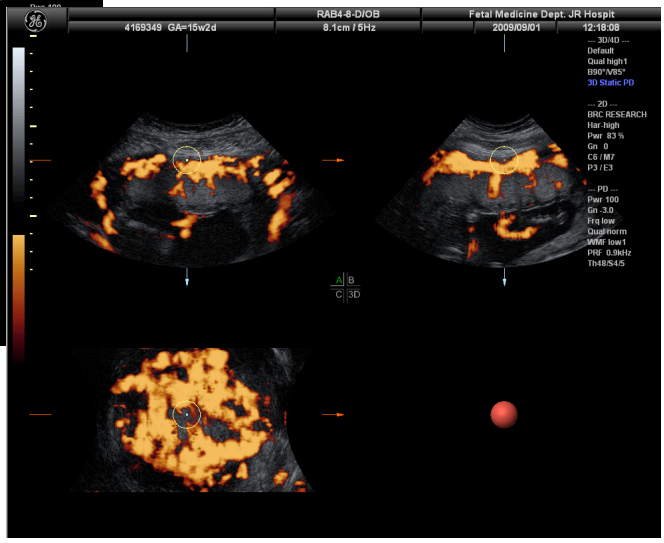



**Figure 46: The sphere used to ensure identical regions of interest (ROI) are sampled for each volume at different gain settings.**

a) includes the whole placenta; b) the fetal sample at the cord insertion; c) the maternal sample taken from the basal plate of the placenta in the vertical plane from the cord insertion.

### 6.2.4 Data analysis – calculations and statistics

The absolute value of the VOCAL™ indices should be different for each participant. This is because the 'true' vascularity of each placenta is different reflecting such things as the adequacy of placentation and maturity of the placental vasculature. Therefore, the values of the VI, FI, & VFI captured at the individualised SNG were chosen as each individual's internal gold standard. The percentage difference from this absolute value was calculated for all the other gain settings and then plotted against the absolute difference in gain value (e.g. if SNG setting was -2 and the VI at the SNG=100 and VI at a gain of -5=75, the percentage difference is -25% and the absolute difference in gain value was -3).

The relationship between the percentage value and the absolute difference in the gain value from the SNG value was explored using linear regression analysis. To test the difference in the gradients between the lines above and below the SNG we proposed a null hypothesis that the gradient of the line above was equal to the gradient of the line below. It can be shown that this hypothesis takes a t-distribution and therefore it was appropriate to test with the Student t-test. The Gauss-Markov theorem states that linear regression is the best unbiased estimator among the class of linear estimators and this is therefore an appropriate test regardless of whether the underlying distribution is normal or not (Dudewicz et al. 1988). Statistical analyses were performed using SPSS (version 16.0, IBM Corporation, NY, USA) & Excel 2004 (Microsoft Corp., Washington, USA). Results were considered to be statistically significant when $p<0.05$.

## *6.3 Results*

Sixty-six women with a singleton pregnancy were recruited at between 11+0 weeks and 13+6 weeks' gestation (Full Details: 3.3. page 37). Fifty-two women were defined as having a 'normal' pregnancy outcome. Of these, two were found to have at least one suboptimal image in their set of five and were excluded. Therefore, data from 50 women were included in the final analysis. Their demographics are shown in Table 1 (page 54).

Figure 47 (page 156) demonstrates that as the gain was reduced so the noise artefact disappeared up to the SNG point (-6.4dB). After this point, as the gain was further reduced, there was no obvious loss of vascular detail apparent in the image although the results clearly demonstrate that the values for VI & VFI are steadily falling. This would result in an underestimation of the indices without the operator being aware from the appearance of the image.

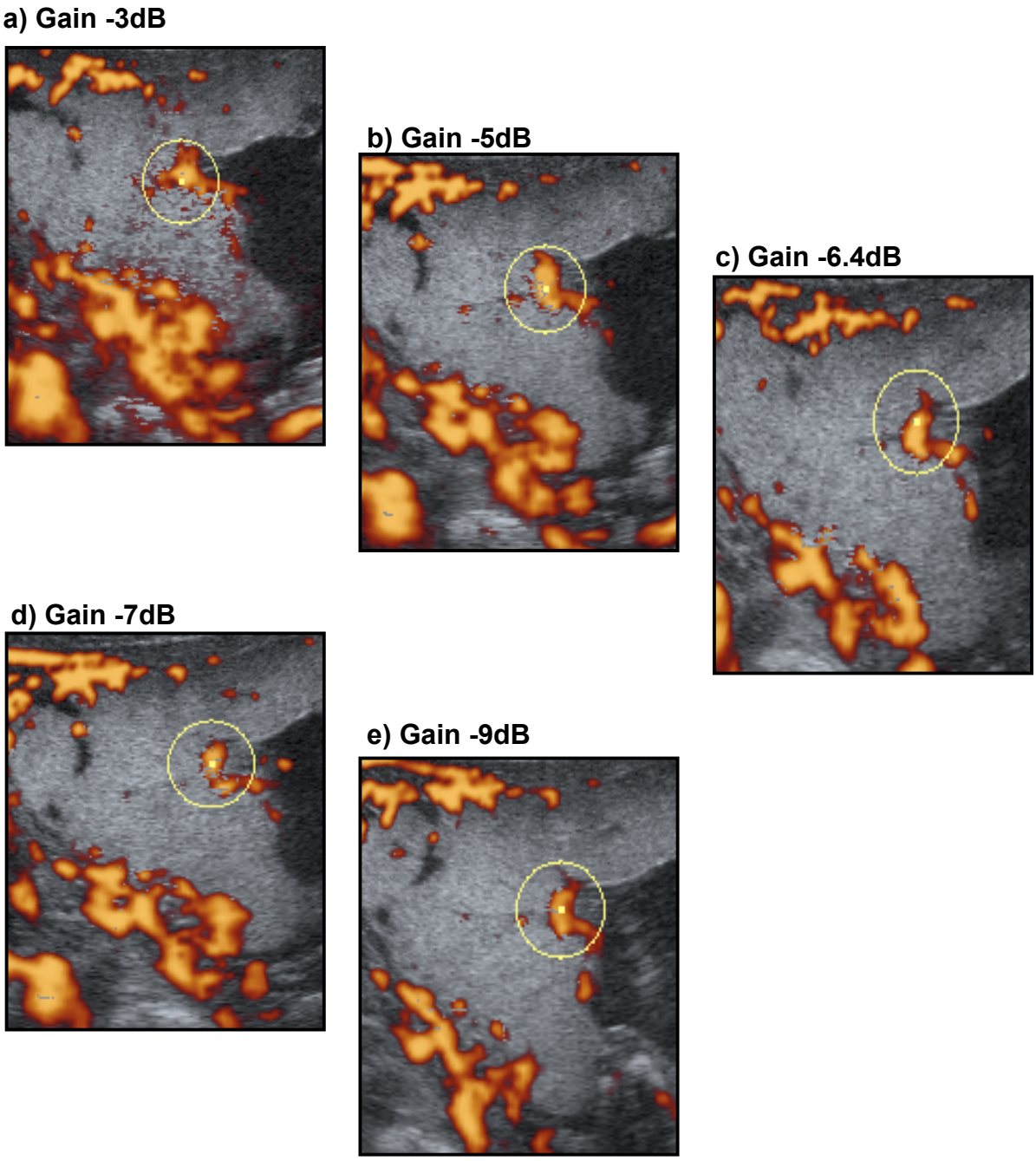



**Figure 47: Influence of gain on the fetal vascular image.**

a) Noise artefact is seen with excess gain; b) some artefact remains; c) the individual sub-noise gain setting for this participant (-6.4 dB); d) & e) below the sub-noise gain level, images are not significantly visually altered but have lower VI & VFI values.

The circle indicates the cord insertion; the point fetal sample

**Table 18: The linear regression analysis comparing the VI, FI & VFI with different gain settings**

| **Gain below the sub-noise value** | **$R^2$ value** | **P value** |
|---|---|---|
| **VI** - Whole Image | 0.68 | p <0.0001 |
| **FI** - Whole Image | 0.01 | p = 0.31 |
| **VFI** - Whole Image | 0.72 | p <0.0001 |
| **Gain above the sub-noise value** | **$R^2$ value** | **P value** |
| **VI** - Whole Image | 0.79 | p <0.0001 |
| **FI** - Whole Image | 0.02 | p = 0.39 |
| **VFI** - Whole Image | 0.79 | p <0.0001 |
| **Gain below the sub-noise value** | **$R^2$ value** | **P value** |
| **VI -** Fetal sample | 0.24 | p <0.0001 |
| **FI -** Fetal sample | 0.03 | p = 0.37 |
| **VFI -** Fetal sample | 0.18 | p <0.0001 |
| **Gain above the sub-noise value** | **$R^2$ value** | **P value** |
| **VI -** Fetal sample | 0.29 | p = 0.023 |
| **FI -** Fetal sample | 0.001 | p = 0.83 |
| **VFI -** Fetal sample | 0.69 | p = 0.05 |
| **Gain below the sub-noise value** | **$R^2$ value** | **P value** |
| **VI -** Maternal sample | 0.27 | p <0.0001 |
| **FI -** Maternal sample | 0.04 | p = 0.16 |
| **VFI -** Maternal sample | 0.1 | p <0.0001 |
| **Gain above the sub-noise value** | **$R^2$ value** | **P value** |
| **VI -** Maternal sample | 0.21 | p = 0.002 |
| **FI -** Maternal sample | 0.004 | p = 0.68 |
| **VFI -** Maternal sample | 0.18 | p = 0.005 |

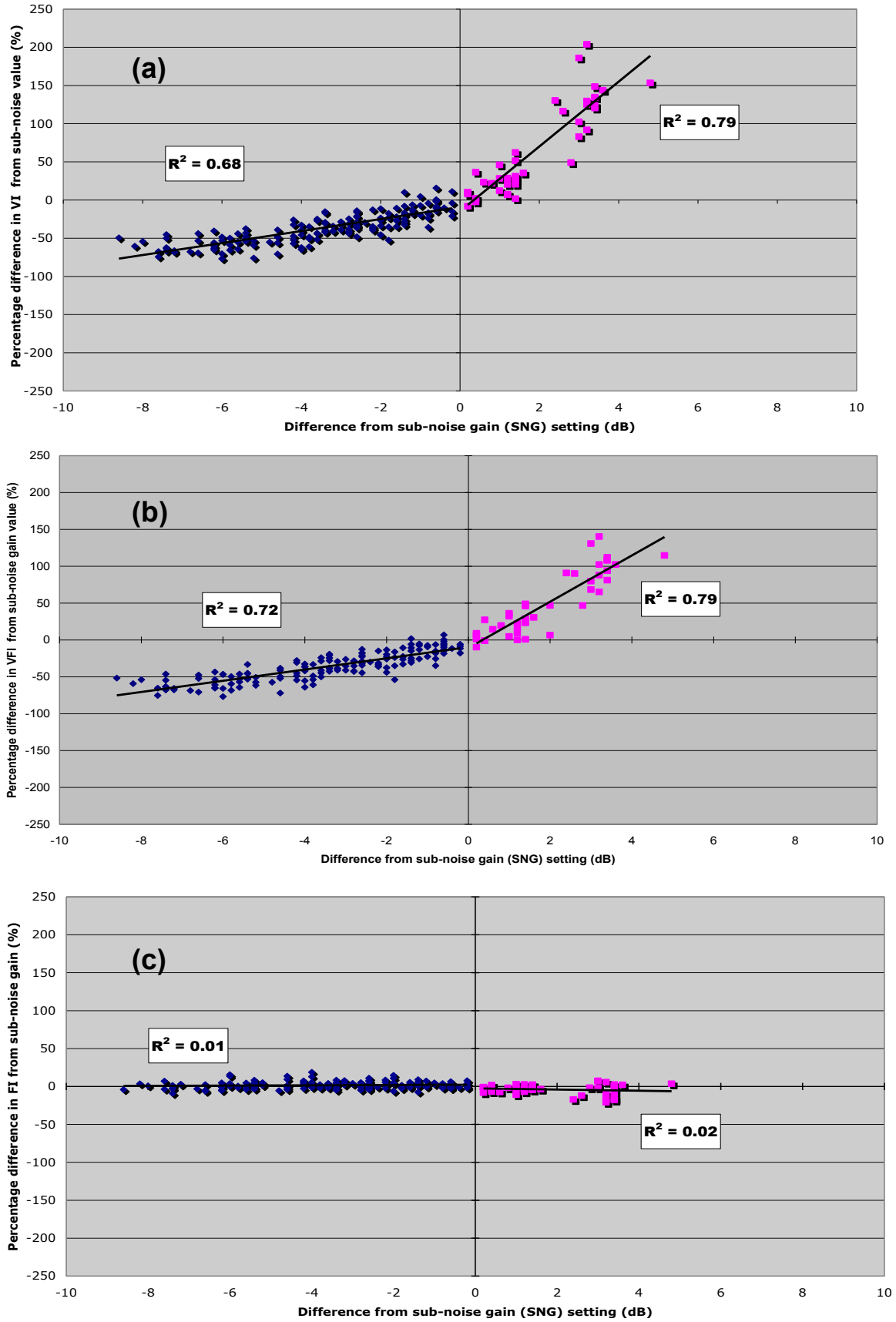



**Figure 48: The effect of changing the PD gain on VOCAL™ indices.**

Zero indicates the individual sub-noise gain setting; a) Vascularisation Index (VI); b) Vascularisation Flow Index (VFI); c) Flow Index (FI).

Linear regression analysis showed that the percentage difference in VI, and consequently VFI, was significantly linearly related to the difference in gain setting from the SNG value (Figure 48, page 158).

Whilst the relationships above and below the SNG point, are both linear their gradients are significantly different ($p<0.001$). Above the SNG point the slope is steeper as the noise artefact appears. No such relationship was demonstrated for FI when the gain was changed (

Figure 48c, page 158). These results are seen for analysis of the whole volume and the fetal and maternal samples.

The values for the SNG setting were weakly related to the participant's BMI at booking ($r^2 = 0.21$, $p = 0.001$) Figure 49.

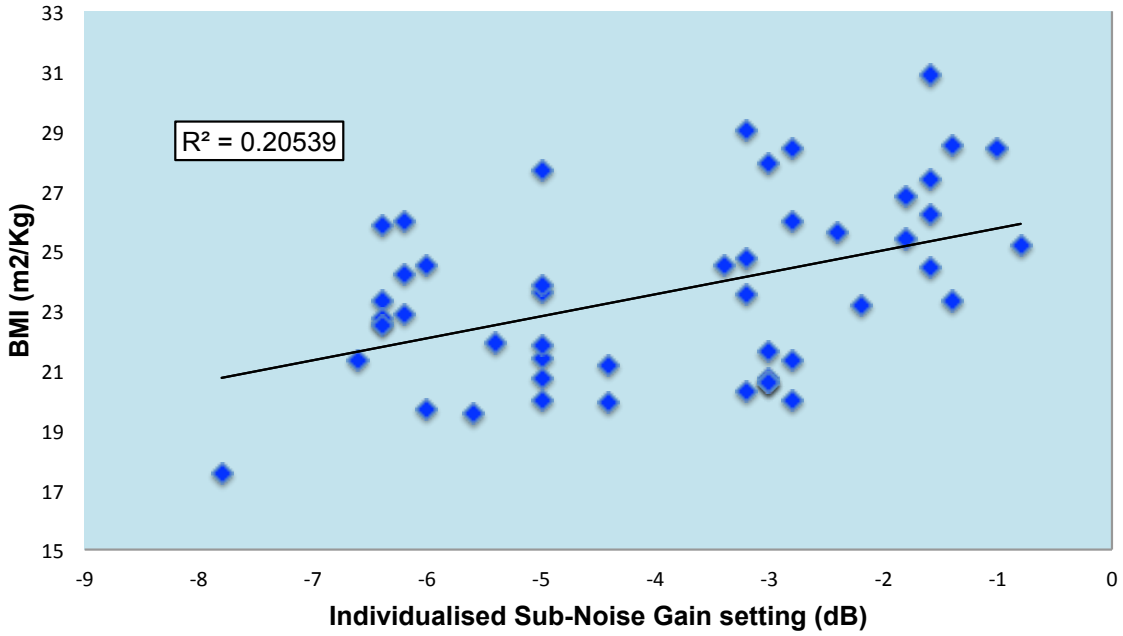



**Figure 49: Demonstrating the correlation between BMI and the individualised SNG setting.**

## 6.4 Discussion

The VOCAL™ indices are derived from the presence and intensity of PD signal at a given voxel, though information on their exact derivation from the raw Doppler signal is currently unavailable (personal communication with GE). Consequently, the relationship between these indices, the number and behaviour of underlying scatterers, and hence tissue vascularity, remains unknown. The published literature is presumptive or experimental regarding the association (Jones et al. 2009). This is the first time that the reported phantom model findings (Raine-Fenning et al. 2008b) have been confirmed, *in vivo*.

However, whilst the phantom experiment (Raine-Fenning et al. 2008b) showed a similar influence of gain, it did not demonstrate a change in the relationship at the point where noise artefact appears. Consequently, this phantom model could not continue to explore the level for optimising meaningful information in the absence of artefact. What is uncertain is whether these experimental models actually produce a similar noise artefact to that seen in the placenta. This may be a phenomenon specific to biological systems where there are not only vessels at different depths, angles and velocities, but extracellular fluid. It is likely that artefacts produced *in vivo* and in experimental phantoms are not the same. Given this uncertainty and the differences in machine type, probe and settings between the phantom studies (Raine-Fenning et al. 2008b; Martins et al.) and this *in vivo* work, it is difficult to draw precise associations between results. In particular, the positive FI trend shown by Raine-Fenning et al. (Raine-Fenning et al. 2008b) appears to occur over a much higher range of gain level (24.8 to -44.0dB) compared to those suitable for the participants in this study (-9.0 to -0.8dB).

The linear relationship of the PD gain to the VI value indicates that, what is essentially the 'volume control' (gain in decibels), directly affects the calculated value of the VI, so this has to raise further questions about the interpretation of these indices. As the gain setting is dropped below the SNG level, the value calculated for VI decreases proportionately as Doppler information is lost. However, the image on the screen does not noticeably change, so the operator would be unaware of the loss of this information (Figure 47, page 156). Above the SNG point a significantly different linear relationship is seen as with a steeper slope as the image rapidly becomes disrupted by noise artefact. The same pattern is seen for both the fetal and maternal samples but with greater scatter resulting in lower $r^2$ values. This is most likely due to the sampling error introduced by having to select the position of the spheres manually, as any small difference between their position may result in a change in the calculated VOCAL™ indices (Lai et al. 2010).

This study suggests that the use of the SNG optimises the information gained for each subject. This will improve between patient comparisons, as it ensures that the maximum information available for one patient is being compared with the maximum for another, thereby minimizing the effect of beam path on between patient comparisons. Whilst selecting the gain setting just below the noise point is inherently subjective it is a simple, easily explained method. However, further studies will be required to confirm reproducibility.

The previously documented suggestion that the gain should be set 'somewhere in the middle of the range' (Martins et al. 2010b) and kept constant for all patients may actually result in information being lost for some patients with

artefact being introduced in others due to differences in signal attenuation from the beam path. This could possibly result in the introduction of errors into the calculated VI & VFI values. This protocol was initially developed to collect 3-D volumes with gain settings between -3 and -9dB. These values were arbitrary and selected as this was anticipated to be the most likely 'range' for the study population. In fact, the SNG value ranged between -0.8 and -7.8dB (mean -3.9, standard deviation 1.9) in the 50 participants. Had -6dB been selected as the mid-point gain, the SNG would have been chosen, and the optimal information calculated, for only two women. The indices for 10 women would have been recorded above the SNG thereby overestimating the value of VI & VFI, and in the remaining 38 participants the values would have been underestimated. This means that 96% of these VOCAL™ 'vascularisation' measurements would have been either sub-optimal or containing noise artefact.

This PD gain evaluation has several limitations. It is relatively small in size but as the effect size was unknown in advance a power calculation could not be performed. However, as all the statistical tests have demonstrated a very high level of significance ($p<0.001$), n=50 was sufficient. The fixed gain levels of -3, -5, -7, and -9dB were arbitrarily selected. It may have been better if more gains had been evaluated (possibly including 0 and +3). However, taking a sequence of five volumes in exactly the same place on the abdomen without the operator or participant moving at all was difficult. Therefore, pragmatically, a series of five was selected.

Several studies have demonstrated that PD is subject to attenuation, rendering it dependent on factors including the depth and type of intervening tissue

(Gudmundsson et al. 1998; Welsh et al. 2005). A weak positive relationship was seen between the SNG level and the participant's BMI at booking. This presumably reflects the need for gain increase to compensate for signal attenuation, as previously demonstrated in phantom models (Jones et al. 2009). The BMI is known to be an imperfect measure of degree and distribution of adiposity and hence intervening attenuating tissue (Bergman et al. 2011) explaining the weak relationship between BMI and SNG. Other factors such as type of tissue (e.g. scar tissue) may also be responsible for signal attenuation. Several participants in the study had previously had abdominal surgery including abdominoplasty and caesarean section.

Once adequately standardised, 3-D PD ultrasound may then be used to sample the placental basal plate, producing the 'vascular volume'. This chapter demonstrates that use of SNG is an important step in optimising 3-D PD imaging.

# 7 General discussion

## *7.1 Summary of principal new findings*

*From Chapter 4*

- A technique for measuring the jet of blood from the mouth of the spiral artery has been formally described and validated.
- The blood flow from the spiral arteries into the intervillous space is pulsatile and this pulsatility decreases with advancing gestation. This correlates with the histologically observed, gestation dependent changes seen in the utero-placental interface.
- The histologically predicted increase in the size of the spiral artery mouth can be demonstrated *in vivo*.
- The jet entering the intervillous space from the spiral artery is different in pregnancies destined to be SGA.
- Mega-jets can be demonstrated in the developing placenta, which appear to develop significantly later than in pregnancies resulting in SGA babies.

*From Chapter 5*

- A semi-automated, time efficient method for generating the placental volume has been used to investigate prediction of SGA babies.
- Morphometric measures derived from the surface area and area of the basal plate has been used to investigate the prediction of SGA.
- The standardized placental volume (*s*PlaV) has been shown to be an early predictor of SGA

- The standardized placental volume (*s*PlaV) is a risk factor independent of the value of PAPP-A and can be combined with this and the NT measurement to improve the prediction of SGA.

*From Chapter 6*

- The use of the SNG optimises the information gained for each subject, which should improve between patient comparisons.
- The relationship demonstrated between the calculated value of VOCAL™ indices and the PD gain setting calls into question the common research practice of using the same 'fixed gain' for all participants in a trans-abdominal studies of the placenta.

## *7.2 Limitations*

There are several issues which may have limited this study.

### 7.2.1 Definition of fetal growth restriction

The most fundamental limitation is the highly contentious issue of defining growth restriction. The choice of <10th centile on customised birth weight was selected as evidence is mounting that using these customised birth weight centiles reduces the rate of constitutionally small babies being classed as growth restricted (false positive rate) whilst helping to increase detection of pathologically small babies (Gardosi 2006; Figueras et al. 2007; Figueras et al. 2009, 2011).

### 7.2.2 Study size

Another issue is the size of the study, especially the Phase I Doppler investigation of the jets. As the size of the effect being studied in the jets was completely unknown a power calculation could not be performed to indicate what size of study was required. Therefore, the study initially aimed to recruit 250 women with on-going statistical analysis to decide when the sample size was sufficient. The measurement of the jets was a 'proof of concept' part of the study aimed at investigating if there was a difference in the blood flow into the intervillous space in 2-D before moving on to looking at it in 3-D. It was initially analysed when the sample size reached 65 at which point it appeared to be well enough powered to detect the difference which had been predicted histologically. The p values produced were all less than 0.06 indicating that there is likely to be an effect underlying the difference which may be worthy of further investigation. The small size of the study must also be considered when interpreting the ROC curve analyses. The small numbers give rise to large step changes in the values generated by these analyses making a clear indication of sensitivity to false positive rate difficult. However, the values for the AUC for sPlaV and the two generated models are very encouraging. Likewise, a Kaplan-Meir estimator was used to examine the survival curves for the placental lakes and mega-jets. This is not ideal, as the fortnightly scanning schedule has forced a discrete pattern onto a continuous process. Following statistical advice it was felt that it was the most appropriate test for this data.

The number of women selected for the inter-observer variability study was also small. Decreasing within patient variance over time for both observers demonstrated a 'learning effect'. Therefore, with time, the limits of agreement

between the two observers may have reduced further. However, using the 'as low as reasonably achievable' (ALARA) principal it was felt that this was enough to confirm that there was appropriate reproducibility with no systematic bias. This would be a major stumbling block if this process were to become more than just a research tool.

### 7.2.3 Vessel selection

The decision to measure the three most prominent vessels was arbitrary but our initial investigations in a small number of women indicated that measuring three is likely to be representative of the jets. This maximized the number of women who could be scanned in the fixed amount of time available, whilst minimizing their colour Doppler exposure. The three most prominent were selected so that the optimal jets were measured in each woman to ensure the best possible inter-participant comparison. The method for measuring the jets was difficult and time consuming.

### 7.2.4 Recruitment strategy

The recruitment strategy also involved actively seeking women at high risk of growth restriction. This included five women with a known low PAPP-A. This introduced some selection bias. The resulting birth weights distribution was demonstrated be skewed to the left (Figure **9**, page 56). In a random sample of the population the distribution should be normal. This may have potentially affected the results. However, given the performance of the combined sPlaV model for the prediction of SGA in the un-selected, low risk population, this effect appears to be minimal.

### 7.2.5 Measurements with Doppler

Attempts to measure the size of the mouth of the terminal spiral arteries and the length and velocity of the jet is fraught with difficulties. These mostly relate to the inherent limitations of trying to interpret measurements obtained using colour Doppler ultrasound. In an attempt to overcome these, the degree and rate of change of these factors were studied longitudinally in the same patient. It is these relative measures which can be commented on, more than the absolute values obtained.

## *7.3 Future work*

### 7.3.1 Confirmation of technique

The results from this small study are very promising. However, the findings need confirming with a larger sample. Work is currently underway to obtain a data set which has already had the volumes calculated by another technique (VOCAL™) (Plasencia et al. 2011) in order to re-analyse it with the new semi-automated technique and calculate *s*PlaV.

### 7.3.2 Vascular volume

The suggestion that the blood flow at the basal plate is indeed different in pregnancies which result in term SGA babies suggests that this anatomical site holds promise for research into both the pathology and early prediction of growth restriction. Once adequately standardised, 3-D PD ultrasound should be able to be used to sample the placental basal plate, producing the 'vascular volume' (Hypothesis 2.1.4, page 32). This was originally planned to be part of this thesis and the development of the SNG was the first step in this

standardisation process. However, this is proving much more technically difficult than it first appeared and will therefore require a considerable amount of research before a valid technique is fully developed. Work is currently underway to develop an appropriate method for calculating a 3-D value for fractional moving blood volume (FMBV). Any predictive value of this vascular volume will then need to be thoroughly tested.

### 7.3.3 Development of a screening test

Implementation of any new screening test would be considerably more cost-effective if it can be incorporated into an antenatal service already widely offered. Given the results of this study it does not seem unreasonable to propose that a test for SGA could share data with the aneuploidy testing in the future. The acquisition of a simple 3-D placental volume is relatively quick and can be obtained by an ultrasonographer with minimal extra training. Its simplicity and objectivity makes it arguably less prone to operator error than the measurement of the uterine artery, which can be technically difficult and requires subjective judgment regarding presence of the end-diastolic notch. The rapid advances in image processing technology make fully automated placental volume calculation from a single greyscale 3-D image a distinct possibility. The fact that the two of the markers, PAPP-A and NT, have been demonstrated to be independent and improve prediction in such small numbers appears to increase its potential.

Fetal growth restriction is currently often missed during routine antenatal care, especially in the low risk population (Hepburn et al. 1986; Backe et al. 1993). Developing an early screening test for SGA should help to direct the limited NHS scanning services towards monitoring those babies actually at risk. This

should remove the perceived need for a routine third trimester ultrasound scan whilst ensuring that vulnerable babies are appropriately monitored and delivered in a timely fashion. This should also help to facilitate the NICE recommendation to treat healthy, low risk pregnancies as a normal physiological process.

# References


Adler, R. S. (2001). "On the relationship between power mode and pressure amplitude decorrelation." Ultrasound Med Biol **27**(9): 1291-1296.

Backe, B., et al. (1993). "Effectiveness of antenatal care: a population based study." Brit J Obstet Gynaecol **100**(8): 727-732.

Barker, D. J. (2006). "Adult consequences of fetal growth restriction." Clin Obstet Gynecol **49**(2): 270-283.

Barker, D. J., et al. (2009). "Growth and chronic disease: findings in the Helsinki Birth Cohort." Ann Hum Biol **36**(5): 445-458.

Barreto, E. Q., et al. (2010). "Reliability and validity of in vitro volume calculations by 3-dimensional ultrasonography using the multiplanar, virtual organ computer-aided analysis (VOCAL), and extended imaging VOCAL methods." J Ultrasound Med **29**(5): 767-774.

Bartelmez, G. W. (1957). The form and function of the uterine vessels in the rhesus monkey. Washington, Carnegie Inst.

Bayliss, H., et al. (2002). "Anti-hypertensive drugs in pregnancy and fetal growth: evidence for "pharmacological programming" in the first trimester?" Hypertens Pregnancy **21**(2): 161-174.

Belkacemi, L., et al. (2010). "Maternal undernutrition influences placental-fetal development." Biol Reprod **83**(3): 325-331.

Benirschke, K., et al. (2000). Pathology of the human placenta; 4th Edition. New York, Springer-Verlag.

Bergman, R. N., et al. (2011). "A Better Index of Body Adiposity." Obesity **19**(5): 1083-1089.

Bernstein, I. M., et al. (1996). "Case for hybrid "fetal growth curves": a population-based estimation of normal fetal size across gestational age." J Matern Fetal Med **5**(3): 124-127.

Bleker, O. P., et al. (1977). "The volumetric growth of the human placenta: a longitudinal ultrasonic study." Am J Obstet Gynecol **127**(6): 657-661.

Bobrow, C. S., et al. (1999). "Fetal growth velocity: a cautionary tale." Lancet **353**(9163): 1460.

Borell, U., et al. (1952). "The diagnostic value of arteriography of the iliac artery in gynaecology and obstetrics." Acta radiol **38**(4): 247-263.

Bottomley, C., et al. (2009). "Assessing first trimester growth: the influence of ethnic background and maternal age." Hum Reprod Update **24**(2): 284-290.

Bower, S., et al. (1993). "Improved prediction of preeclampsia by two-stage screening of uterine arteries using the early diastolic notch and color Doppler imaging." Obstet Gynecol **82**(1): 78-83.

Boyd, J. D., et al. (1970). The Human Placenta. Cambridge, W Heffner & sons.

Breeze, A. C., et al. (2007). "Prediction and perinatal outcomes of fetal growth restriction." Semin Fetal Neonatal Med **12**(5): 383-397.

Brenner, W. E., et al. (1976). "A standard of fetal growth for the United States of America." Am J Obstet Gynecol **126**(5): 555-564.

Brosens, I. (1988). "The utero-placental vessels at term - the distribution and extent of physiological changes." Trophoblast Res **3**: 61-67.

Brosens, I., et al. (1977). "Fetal growth retardation and the arteries of the placental bed." Br J Obstet Gynaecol **84**(9): 656-663.

Brosens, I., et al. (1967). "The physiological response of the vessels of the placental bed to normal pregnancy." J Pathol Bacteriol **93**(2): 569-579.

Brosens, J. J., et al. (2009). "A role for menstruation in preconditioning the uterus for successful pregnancy." Am J Obstet Gynecol **200**(6): 615.e611-616.

Brosens, J. J., et al. (2002). "The myometrial junctional zone spiral arteries in normal and abnormal pregnancies: a review of the literature." Am J Obstet Gynecol **187**(5): 1416-1423.

Brown, M. A., et al. (2001). "The classification and diagnosis of the hypertensive disorders of pregnancy: statement from the International Society for the Study of Hypertension in Pregnancy (ISSHP)." Hypertens Pregnancy **20**(1): IX-XIV.

Brown, T. D., et al. (1985). "A three-dimensional computational simulation of some sources of measurement artifact in microvascular pulsed ultrasound Doppler velocimetry." J Biomech Eng **107**(3): 274-280.

Buckingham, E. (1914). "On physically similar systems: Illustrations of the use of dimensional equations." Phys Rev **4**: 345-376.

Bude, R. O., et al. (1994). "Power versus conventional color Doppler sonography: comparison in the depiction of normal intrarenal vasculature." Radiology **192**(3): 777-780.

Bukowski, R., et al. (2001). "Impairment of growth in fetuses destined to deliver preterm." Am J Obstet Gynecol **185**(2): 463-467.

Bukowski, R., et al. (2007). "Human sexual size dimorphism in early pregnancy." Am J Epidemiol **165**(10): 1216-1218.

Bukowski, R., et al. (2008). "Individualized norms of optimal fetal growth: fetal growth potential." Obstet Gynecol **111**(5): 1065-1076.

Burstein, E., et al. (2009). "Three-dimensional placental volume measurements between 11 and 13 weeks' gestation." Am J Perinatol **26**(2): 169-171.

Burton, G. J., et al. (2009a). "Rheological and physiological consequences of conversion of the maternal spiral arteries for uteroplacental blood flow during human pregnancy." Placenta **30**(6): 473-482.

Burton, G. J., et al. (2009b). "Placental endoplasmic reticulum stress and oxidative stress in the pathophysiology of unexplained intrauterine growth restriction and early onset preeclampsia." Placenta **30 Suppl A**: S43-48.

CARE-Study-Group (2008). "Maternal caffeine intake during pregnancy and risk of fetal growth restriction: a large

prospective observational study." Br Med J **337**: a2332.
Carson, P. L., et al. (1998). "3-D color Doppler image quantification of breast masses." Ultrasound Med Biol **24**(7): 945-952.
Carson, P. L., et al. (1993). Approximate quantification of detected fractional blood volume in the breast by 3D color flow and Doppler signal amplitude imaging. Piscataway, NJ., IEEE.
Chafetz, I., et al. (2007). "First-trimester placental protein 13 screening for preeclampsia and intrauterine growth restriction." Am J Obstet Gynecol **197**(1): 35 e31-37.
Chan, P. Y., et al. (2010). "The long-term effects of prematurity and intrauterine growth restriction on cardiovascular, renal, and metabolic function." Int J Peds **2010**: 280402.
Chang, L. L., et al. (1972). "Some hematological differences between the blood of mothers and their newborn infants." Singapore Med J **13**(6): 280-283.
Cheong, K. B., et al. (2010). "Comparison of inter- and intraobserver agreement and reliability between three different types of placental volume measurement technique (XI VOCAL, VOCAL and multiplanar) and validity in the in-vitro setting." Ultrasound Obstet Gynecol **36**(2): 210-217.
Clausson, B., et al. (1999). "Outcomes of post-term births: the role of fetal growth restriction and malformations." Obstet Gynecol **94**(5 Pt 1): 758-762.
Clausson, B., et al. (2001). "Perinatal outcome in SGA births defined by customised versus population-based birthweight standards." Br J Obstet Gynaecol **108**(8): 830-834.
Cnattingius, S., et al. (1998). "Prepregnancy weight and the risk of adverse pregnancy outcomes." New Eng J Med **338**(3): 147-152.
Cnossen, J. S., et al. (2008). "Use of uterine artery Doppler ultrasonography to predict pre-eclampsia and intrauterine growth restriction: a systematic review and bivariable meta-analysis." CMAJ **178**(6): 701-711.
Collins, S. L., et al. (2011). "Abdominal pregnancy: A perfusion confusion?" Placenta **32**(10): 793-795.
Cooley, S. M., et al. (2011). "The impact of ultrasonographic placental architecture on antenatal course, labor and delivery in a low-risk primigravid population." J Matern Fetal Neonatal Med **24**(3): 493-497.
Cooperberg, P. L., et al. (1979). "Ultrasonographic demonstration of a placental maternal lake." J Clin Ultrasound **7**(1): 62-64.
Costa, S. L., et al. (2008). "Screening for Placental Insufficiency in High-risk Pregnancies: Is Earlier Better?" Placenta **29**(12): 1034-1040.
Cowans, N. J., et al. (2008). "First-trimester maternal placental protein 13 levels in pregnancies resulting in adverse outcomes." Prenat Diagn **28**(2): 121-125.
Cox, P., et al. (2009). "Pathological assessment of intrauterine growth restriction." Best Pract Res Clin Obstet Gynaecol **23**(6): 751-764.
Cruz-Martinez, R., et al. (2009). "The role of Doppler and placental screening."

Best Pract Res Clin Obstet Gynaecol **23**(6): 845-855.
Dadhwal, V., et al. (2011). "The obstetric outcome following treatment in a cohort of patients with antiphospholipid antibody syndrome in a tertiary care center." J Postgrad Med **57**(1): 16-19.
Daron, G. H. (1936). "The arterial pattern of the tunica mucosa of the uterus in the Macaus rhesus." Am J Anat **58**: 349-419.
de Paula, C. F., et al. (2008). "Placental volumes measured by 3-dimensional ultrasonography in normal pregnancies from 12 to 40 weeks' gestation." J Ultrasound Med **27**(11): 1583-1590.
De Wolf, F., et al. (1980). "Fetal growth retardation and the maternal arterial supply of the human placenta in the absence of sustained hypertension." Br J Obstet Gynaecol **87**(8): 678-685.
de Ziegler, D., et al. (1991). "Vascular resistance of uterine arteries: physiological effects of estradiol and progesterone." Fertil Steril **55**(4): 775-779.
Deane, C. R., et al. (1991). "Accuracy of colour Doppler ultrasound velocity measurements in small vessels." J Biomech Eng **13**(3): 249-254.
Derchi, L. E., et al. (1997). "[Power Doppler: physical and constructive principles and comparison with Doppler color]." La Radiologia medica **93**(4): 329-335.
Deurloo, K., et al. (2007a). "Reproducibility of 3-dimensional sonographic measurements of fetal and placental volume at gestational ages of 11-18 weeks." J Clin Ultrasound **35**(3): 125-132.
Deurloo, K. L., et al. (2007b). "Color Doppler ultrasound of spiral artery blood flow for prediction of hypertensive disorders and intra uterine growth restriction: a longitudinal study." Prenat Diagn **27**(11): 1011-1016.
Doctor, B. A., et al. (2001). "Perinatal correlates and neonatal outcomes of small for gestational age infants born at term gestation." Am J Obstet Gynecol **185**(3): 652-659.
Dombrowski, M. P., et al. (2010). "Asthma in pregnancy." Clin Obstet Gynecol **53**(2): 301-310.
Doppler, C. (1843). "Über das farbige Licht der Doppelsterne end einiger anderer Gerstirne des Himmels. ." Abh Konigl-Böhm Ges **2**: 465-482.
Drake, R., et al. (2007). Gray's Atlas of Anatomy. Edinburgh, Churchill Livingston.
Dudewicz, E. J., et al. (1988). Modern Mathematical Statistics. New York, John Wiley & sons.
Dymling, S. O., et al. (1991). "Measurement of blood perfusion in tissue using Doppler ultrasound." Ultrasound Med Biol **17**(5): 433-444.
Ego, A., et al. (2006). "Customized versus population-based birth weight standards for identifying growth restricted infants: a French multicenter study." Am J Obstet Gynecol **194**(4): 1042-1049.
Eskild, A., et al. (2010). "Do pregnancies with pre-eclampsia have smaller placentas? A population study of 317 688 pregnancies with and without growth restriction in the offspring." Br J Obstet Gynaecol **117**(12): 1521-1526.

Falcon, O., et al. (2005). "Gestational sac volume measured by three-dimensional ultrasound at 11 to 13 + 6 weeks of gestation: relation to chromosomal defects." Ultrasound Obstet Gynecol **25**(6): 546-550.

Farrell, T., et al. (2002). "The effect of body mass index on three methods of fetal weight estimation." Br J Obstet Gynaecol **109**(6): 651-657.

Figueras, F., et al. (2008). "Predictiveness of antenatal umbilical artery Doppler for adverse pregnancy outcome in small-for-gestational-age babies according to customised birthweight centiles: population-based study." Br J Obstet Gynaecol **115**(5): 590-594.

Figueras, F., et al. (2007). "Customised birthweight standards accurately predict perinatal morbidity." Arch Dis Child Fetal Neonatal Ed **92**(4): F277-280.

Figueras, F., et al. (2009). "Should we customize fetal growth standards?" Fetal Diagn Ther **25**(3): 297-303.

Figueras, F., et al. (2011). "Intrauterine growth restriction: new concepts in antenatal surveillance, diagnosis, and management." Am J Obstet Gynecol **204**(4): 288-300.

Fish, P. J., et al. (1997). "Developments in cardiovascular ultrasound: Part 1: Signal processing and instrumentation." Med Biolog Eng Comput **35**(6): 561-569.

Fisher, C. C., et al. (1976). "Placental aging monitored by gray scale echography." Am J Obstet Gynecol **124**(5): 483-488.

Fisteag-Kiprono, L., et al. (2006). "Perinatal outcome associated with sonographically detected globular placenta." J Reprod Med **51**(7): 563-566.

Froen, J. F., et al. (2004). "Restricted fetal growth in sudden intrauterine unexplained death." Acta Obstet Gynecol Scand **83**(9): 801-807.

Gagnon, A., et al. (2008). "Obstetrical complications associated with abnormal maternal serum markers analytes." J Obstet Gynaecol Can **30**(10): 918-949.

Gardosi, J. (2006). "New definition of small for gestational age based on fetal growth potential." Horm Res **65 Suppl 3**: 15-18.

Gardosi, J., et al. (1992). "Customised antenatal growth charts." Lancet **339**(8788): 283-287.

Gardosi, J., et al. (2009a). "The value of customised centiles in assessing perinatal mortality risk associated with parity and maternal size." Br J Obstet Gynaecol **116**(10): 1356-1363.

Gardosi, J., et al. (2011). "The customised growth potential: an international research tool to study the epidemiology of fetal growth." Paediatr Perinat Epidemiol **25**(1): 2-10.

Gardosi, J., et al. (2009b). "Adverse pregnancy outcome and association with small for gestational age birthweight by customized and population-based percentiles." Am J Obstet Gynecol **201**(1): 28 e21-28.

Gardosi, J., et al. (2009c). "A customized standard to assess fetal growth in a US population." Am J Obstet Gynecol **201**(1): 25 e21-27.

Gardosi, J., et al. (2005). "Classification of stillbirth by relevant condition at death (ReCoDe): population based cohort

study." Br J Obstet Gynaecol **331**(7525): 1113-1117.
Garite, T. J., et al. (2004). "Intrauterine growth restriction increases morbidity and mortality among premature neonates." Am J Obstet Gynecol **191**(2): 481-487.
Gelson, E., et al. (2011). "Effect of maternal heart disease on fetal growth." Obstet Gynecol **117**(4): 886-891.
Gonzalo, N., et al. (2009). "Quantitative ex vivo and in vivo comparison of lumen dimensions measured by optical coherence tomography and intravascular ultrasound in human coronary arteries." Revista espanola de cardiologia **62**(6): 615-624.
Gosling, R. G., et al. (1991). "Interpretation of pulsatility index in feeder arteries to low-impedance vascular beds." Ultrasound Obstet Gynecol **1**(3): 175-179.
Gudmundsson, S., et al. (1998). "Factors affecting color Doppler energy ultrasound recordings in an in-vitro model." Ultrasound Med Biol **24**(6): 899-902.
Hafner, E., et al. (2001). "Correlation of first trimester placental volume and second trimester uterine artery Doppler flow." Placenta **22**(8-9): 729-734.
Hafner, E., et al. (2006). "Comparison between three-dimensional placental volume at 12 weeks and uterine artery impedance/notching at 22 weeks in screening for pregnancy-induced hypertension, pre-eclampsia and fetal growth restriction in a low-risk population." Ultrasound Obstet Gynecol **27**(6): 652-657.
Hale, S. A., et al. (2010). "Sildenafil increases uterine blood flow in nonpregnant nulliparous women." Reprod Sci **17**(4): 358-365.
Harris, J. W. S., et al. (1966). The morphology of human uteroplacental vasculature. Washington, Carnegie Institute.
Harris, R. D., et al. (1990). "Placental hypoechoic-anechoic areas and infarction: sonographic-pathologic correlation." Radiology **176**(1): 75-80.
Hasner, E. (1946). Endometriets vasculatte Cyklus. Copenhagen, Det Berlingske Bogtrykkeri.
Hecher, K., et al., Eds. (2000). Fetal and Placental Dopplers. London, The Parthenon Publishing Group.
Hepburn, M., et al. (1986). "An audit of the detection and management of small-for-gestational age babies." Br J Obstet Gynaecol **93**(3): 212-216.
Hoogland, H. J., et al. (1980). "Placental size during early pregnancy and fetal outcome: a preliminary report of a sequential ultrasonographic study." Am J Obstet Gynecol **138**(4): 441-443.
Hoskins, P. R. (1996). "Accuracy of maximum velocity estimates made using Doppler ultrasound systems." Br J Radiol **69**(818): 172-177.
Hoskins, P. R., et al. (1997). "Colour ultrasound imaging of blood flow and tissue motion." Br J Radiol **70**(837): 878-890.
Hsieh, Y. Y., et al. (2000). "Longitudinal doppler sonographic measurements of vascular impedance in the central and peripheral spiral arteries throughout

pregnancy." J Clin Ultrasound **28**(2): 78-82.
Hung, T. H., et al. (2001). "In vitro ischemia-reperfusion injury in term human placenta as a model for oxidative stress in pathological pregnancies." Am J Pathol **159**(3): 1031-1043.
Hunter (1774). The anatomy of gravid uterus exhibited in figures. Birmingham, John Baskerville.
Huppertz, B., et al. (2006). "Placental morphology: from molecule to mother -- a dedication to Peter Kaufmann -- a review." Placenta **27 Suppl A**: S3-8.
Huster, K. M., et al. (2010). "Reproducibility of placental volume and vasculature indices obtained by 3-dimensional power Doppler sonography." J Ultrasound Med **29**(6): 911-916.
Jacobsson, B., et al. (2008). "Cerebral palsy and restricted growth status at birth: population-based case-control study." Br J Obstet Gynaecol **115**(10): 1250-1255.
Jarvela, I., et al. (1998a). "The effect of a levonorgestrel-releasing intrauterine system on uterine artery blood flow, hormone concentrations and ovarian cyst formation in fertile women." Hum Reprod **13**(12): 3379-3383.
Jarvela, I., et al. (1998b). "The effect of diclofenac on uterine artery blood flow resistance during menstruation in patients with and without a copper intrauterine device." Hum Reprod **13**(9): 2480-2483.
Jauniaux, E., et al. (1992). "Influence of human chorionic gonadotrophin, oestradiol and progesterone on uteroplacental and corpus luteum blood flow in normal early pregnancy." Hum Reprod **7**(10): 1467-1473.
Jauniaux, E., et al. (1996). "Placental lakes, absent umbilical artery diastolic flow and poor fetal growth in early pregnancy." Ultrasound Obstet Gynecol **7**(2): 141-144.
Jauniaux, E., et al. (1994). "Ultrasonographic investigation of placental morphologic characteristics and size during the second trimester of pregnancy." Am J Obstet Gynecol **170**(1 Pt 1): 130-137.
Jimenez, M. F., et al. (2008). "The effect of the levonorgestrel-releasing intrauterine system and the copper intrauterine device on subendometrial microvascularization and uterine artery blood flow." Fertil Steril **90**(5): 1574-1578.
Johnston, K. W., et al. (1977). "Errors and artifacts of Doppler flowmeters and their solution." Arch Surg **112**(11): 1335-1342.
Jones, N. W., et al. (2009). "In Vitro Dual Perfusion of Human Placental Lobules as a Flow Phantom to Investigate the Relationship between Fetoplacental Flow and Quantitative 3D Power Doppler Angiography." Placenta **30**(2): 130-135.
Jones, N. W., et al. (2010). "Evaluating the intra- and interobserver reliability of three-dimensional ultrasound and power Doppler angiography (3D-PDA) for assessment of placental volume and vascularity in the second trimester of pregnancy." Ultrasound Med Biol **37**(3): 376-385.
Jurkovic, D., et al. (1991). "Transvaginal color Doppler assessment of the

uteroplacental circulation in early pregnancy." Obstet Gynecol **77**(3): 365-369.

Karagiannis, G., et al. (2011). "Prediction of small-for-gestation neonates from biophysical and biochemical markers at 11-13 weeks." Fetal Diagn Ther **29**(2): 148-154.

Khong, T. Y., et al. (1986). "Inadequate maternal vascular response to placentation in pregnancies complicated by pre-eclampsia and by small-for-gestational age infants." Br J Obstet Gynaecol **93**(10): 1049-1059.

Khong, Y., et al. (2011). "Defective deep placentation." Best Pract Res Clin Obstet Gynaecol **25**(3): 301-311.

Kim, Y. M., et al. (2003). "Failure of physiologic transformation of the spiral arteries in patients with preterm labor and intact membranes." Am J Obstet Gynecol **189**(4): 1063-1069.

Kramer, M. S., et al. (2001). "A new and improved population-based Canadian reference for birth weight for gestational age." Pediatrics **108**(2): E35.

Kremkau, F. W. (1992). "Doppler color imaging. Principles and instrumentation." Clin Diag Ultrasound **27**: 7-60.

Kurjak, A., et al. (1997). "Intervillous circulation in all three trimesters of normal pregnancy assessed by color Doppler." J Perinat Med **25**(4): 373-380.

Lai, P. K., et al. (2010). "Reproducibility of regional placental vascularity/perfusion measurement using 3D power Doppler." Ultrasound Obstet Gynecol **36**(2): 202-209.

Law, L. W., et al. (2009). "Which ultrasound or biochemical markers are independent predictors of small-for-gestational age?" Ultrasound Obstet Gynecol **34**(3): 283-287.

Law, T. L., et al. (2011). "Customized Versus Population Based Growth Curves: Prediction of Low Body Fat Percent at Term Corrected Gestational Age Following Preterm Birth." J Matern Fetal Neonatal Med **Sep 22**: Epub ahead of print.

Linderkamp, O., et al. (1984a). "Red blood cell aggregation in preterm and term neonates and adults." Pediatric research **18**(12): 1356-1360.

Linderkamp, O., et al. (1984b). "Contributions of red cells and plasma to blood viscosity in preterm and full-term infants and adults." Pediatrics **74**(1): 45-51.

Lindley, A. A., et al. (2000). "Effect of continuing or stopping smoking during pregnancy on infant birth weight, crown-heel length, head circumference, ponderal index, and brain:body weight ratio." Am J Epidemiol **152**(3): 219-225.

Little, W. A. (1960). "The significance of placental/fetal weight ratios." Am J Obstet Gynecol **79**: 134-137.

Loughna, P., et al. (2009). "Fetal size and dating: charts recommended for clinical obstetric practice." Ultrasound **17**(3): 161-167.

Lowe, G. D. (1987). "Blood rheology in vitro and in vivo." Bailliere's clinical haematology **1**(3): 597-636.

Lubchenco, L. O., et al. (1963). "Intrauterine growth as estimated from Liveborn birth-weight data at 24 to 42 weeks of gestation." Pediatrics **32**: 793-800.

Lunt, M. J. (1980). "The optimum frequency and angle of insonation for a Doppler ultrasonic flow velocity meter." Physic Med Biol **25**(5): 839-848.

Lyall, F. (2002). "The human placental bed revisited." Placenta **23**(8-9): 555-562.

MacSweeney, J. E., et al. (1996). "Colour Doppler energy (power) mode ultrasound." Clin Radiol **51**(6): 387-390.

Makikallio, K., et al. (2004). "Uteroplacental hemodynamics during early human pregnancy: a longitudinal study." Gynecol Obstet Invest **58**(1): 49-54.

Martinoli, C., et al. (1997). "Gain setting in power Doppler US." Radiology **202**(1): 284-285.

Martins, W. P. (2010). "Three-dimensional power Doppler: validity and reliability." Ultrasound Obstet Gynecol **36**(5): 530-533.

Martins, W. P., et al. (2010a). "Analysis and acquisition reproducibility of 3D power Doppler." Ultrasound Obstet Gynecol **36**(3): 392-393.

Martins, W. P., et al. (2010b). "Quantitative three-dimensional power Doppler angiography: a flow-free phantom experiment to evaluate the relationship between color gain, depth and signal artifact." Ultrasound Obstet Gynecol **35**(3): 361-368.

Matijevic, R., et al. (1995). "Spiral artery blood flow in the central and peripheral areas of the placental bed in the second trimester." Obstet Gynecol **86**(2): 289-292.

McCowan, L., et al. (2010). "Risk factors for small-for-gestational-age infants by customised birthweight centiles: data from an international prospective cohort study." Br J Obstet Gynaecol **117**(13): 1599-1607.

McCowan, L. M., et al. (2000). "Umbilical artery Doppler studies in small for gestational age babies reflect disease severity." Br J Obstet Gynaecol **107**(7): 916-925.

McCowan, L. M., et al. (2005). "Customized birthweight centiles predict SGA pregnancies with perinatal morbidity." Br J Obstet Gynaecol **112**(8): 1026-1033.

Melchiorre, K., et al. (2009). "First-trimester uterine artery Doppler indices in the prediction of small-for-gestational age pregnancy and intrauterine growth restriction." Ultrasound Obstet Gynecol **33**(5): 524-529.

Metzenbauer, M., et al. (2001). "Three-dimensional ultrasound measurement of the placental volume in early pregnancy: method and correlation with biochemical placenta parameters." Placenta **22**(6): 602-605.

Metzenbauer, M., et al. (2002). "First-trimester placental volume as a marker for chromosomal anomalies: preliminary results from an unselected population." Ultrasound Obstet Gynecol **19**(3): 240-242.

Miller, J., et al. (2008). "Fetal growth restriction." Semin Perinatol **32**(4): 274-280.

Mills, J. L., et al. (1984). "Maternal alcohol consumption and birth weight. How much drinking during pregnancy is safe?" J Am Med Assoc **252**(14): 1875-1879.

Misenhimer, H. R., et al. (1972). "Effects of vasoconstrictive drugs on the placental circulation of the Rhesus monkey. A preliminary report." Invest Radiol **7**(6): 496-499.

Mongelli, M., et al. (2007). "A customized birthweight centile calculator developed for an Australian population." Aust N Z J Obstet Gynaecol **47**(2): 128-131.

Moran, M., et al. (2011). "Imaging and assessment of placental function." J Clin Ultrasound **39**(7): 390-398.

Morken, N. H., et al. (2006). "Fetal growth and onset of delivery: a nationwide population-based study of preterm infants." Am J Obstet Gynecol **195**(1): 154-161.

Murakoshi, T., et al. (1996). "Uterine and spiral artery flow velocity waveforms in pregnancy-induced hypertension and/or intrauterine growth retardation." Ultrasound Obstet Gynecol **7**(2): 122-128.

Nanaev, A., et al. (1995). "Physiological dilation of uteroplacental arteries in the guinea pig depends on nitric oxide synthase activity of extravillous trophoblast." Cell Tiss Res **282**(3): 407-421.

Napolitano, R., et al. (2011). "Uterine artery Doppler screening for pre-eclampsia: comparison of the lower, mean and higher first-trimester pulsatility indices." Ultrasound Obstet Gynecol **37**(5): 534-537.

Napolitano, R., et al. (2010). "Sensitivity of higher, lower and mean second-trimester uterine artery Doppler resistance indices in screening for pre-eclampsia." Ultrasound Obstet Gynecol **36**(5): 573-576.

NICE (2008a). Antenatal Care - routine care for the healthy pregnant woman - Clinical Guideline (2nd edition), National Collaborating Centre for Women's and Children's Health. RCOG Press.

NICE (2008b). "Antenatal care: Routine care for the healthy pregnant woman." National Institute for Health and Clinical Excellence, Clinical Guideline 62. .

Nohr, E. A., et al. (2008). "Combined associations of prepregnancy body mass index and gestational weight gain with the outcome of pregnancy." Am J Clin Nut **87**(6): 1750-1759.

Nowak, P. M., et al. (2008). "Comparison of placental volume in early pregnancy using multiplanar and VOCAL methods." Placenta **29**(3): 241-245.

Ozkaya, U., et al. (2007). "Doppler examination of uteroplacental circulation in early pregnancy: can it predict adverse outcome?" J Clin Ultrasound **35**(7): 382-386.

Ozturk, S., et al. (2010). "Particular functions of estrogen and progesterone in establishment of uterine receptivity and embryo implantation." Histol Histopathol **25**(9): 1215-1228.

Panigel, M., et al. (1993). "Fast scan magnetic resonance imaging and Doppler ultrasonography of uteroplacental hemodynamics in the rhesus monkey (Macaca mulatta)." J Med Primatol **22**(7-8): 393-399.

Papageorghiou, A. T., et al. (2001). "Multicenter screening for pre-eclampsia and fetal growth restriction by transvaginal uterine artery Doppler at 23

weeks of gestation." Ultrasound Obstet Gynecol **18**(5): 441-449.
Papastefanou, I., et al. (2011). "First trimester prediction of small and large for gestation neonates by an integrated model incorporating ultrasound parameters, biochemical indices and maternal characteristics." Acta obstetricia et gynecologica Scandinavica: Epub ahead of print.
Pathak, S., et al. (2010). "Cord coiling, umbilical cord insertion and placental shape in an unselected cohort delivering at term: relationship with common obstetric outcomes." Placenta **31**(11): 963-968.
Pathak, S., et al. (2011). "Relationship between placental morphology and histological findings in an unselected population near term." Virchows Archiv Epub ahead of print.
Pijnenborg, R., et al. (1991). "Placental bed spiral arteries in the hypertensive disorders of pregnancy." Br J Obstet Gynaecol **98**(7): 648-655.
Pijnenborg, R., et al. (1983). "Uteroplacental arterial changes related to interstitial trophoblast migration in early human pregnancy." Placenta **4**(4): 397-413.
Pijnenborg, R., et al. (2006). "The uterine spiral arteries in human pregnancy: facts and controversies." Placenta **27**(9-10): 939-958.
Pinto, S. M., et al. (2010). "Substance abuse during pregnancy: effect on pregnancy outcomes." Eur J Obstet Gynecol Reprod Biol **150**(2): 137-141.
Plasencia, W., et al. (2011). "Placental Volume at 11-13 Weeks' Gestation in the Prediction of Birth Weight Percentile." Fetal Diagn Ther.
Pomorski, M., et al. (2011). "Comparative analysis of placental vasculature and placental volume in normal and IUGR pregnancies with the use of three-dimensional Power Doppler." Arch Gynecol Obstet: Epub ahead of print.
Potter, K., et al. (2008). "Ultrasound settings significantly alter arterial lumen and wall thickness measurements." Cardiovasc Ultrasound **6**: 6.
Proctor, L. K., et al. (2010). "Pathologic basis of echogenic cystic lesions in the human placenta: role of ultrasound-guided wire localization." Placenta **31**(12): 1111-1115.
Raine-Fenning, N. J., et al. (2008a). "Determining the relationship between three-dimensional power Doppler data and true blood flow characteristics: an in-vitro flow phantom experiment." Ultrasound Obstet Gynecol **32**(4): 540-550.
Raine-Fenning, N. J., et al. (2008b). "Evaluation of the effect of machine settings on quantitative three-dimensional power Doppler angiography: an in-vitro flow phantom experiment." Ultrasound Obstet Gynecol **32**(4): 551-559.
Raine-Fenning, N. J., et al. (2008c). "Methodological considerations for the correct application of quantitative three-dimensional power Doppler angiography." Ultrasound Obstet Gynecol **32**(1): 115-117.
Rampling, M. W., et al. (1989). "A comparison of the rheologic properties of

neonatal and adult blood." Ped Res **25**(5): 457-460.
Ramsey, E. M., et al. (1963). "Serial and cineradioangiographic visualization of maternal circulation in the primate (hemochorial) placenta." Am J Obstet Gynecol **86**(2): 213-225.
Ramsey, E. M., et al. (1960). "Radioangiographic studies of circulation in the maternal placenta of the rhesus monkey: preliminary report " Proc Natl Acad Sci U S A **46**(7): 1003-1008.
Ramsey, E. M., et al. (1967). "Fetal and maternal placental circulations. Simultaneous visualization in monkeys by radiography." Am J Obstet Gynecol **98**(3): 419-423.
Rasmussen, K. (1987a). "Methodological problems related to measurement of quantitative blood flow with the ultrasound Doppler technique." Scand J Clin Lab Invest **47**(4): 303-309.
Rasmussen, K. (1987b). "Precision and accuracy of Doppler flow measurements. In vitro and in vivo study of the applicability of the method in human fetuses." Scand J Clin Lab Invest **47**(4): 311-318.
Redman, C. W. (2011). "Preeclampsia: a multi-stress disorder." Revue Medecine Inter **32 Suppl 1**: S41-44.
Reis, N. S., et al. (2005). "Placental lakes on sonographic examination: correlation with obstetric outcome and pathologic findings." J Clin Ultrasound **33**(2): 67-71.
Resnik, R. (2007). "One size does not fit all." Am J Obstet Gynecol **197**(3): 221-222.
Reynolds, O. (1883). "An Experimental Investigation of the Circumstances Which Determine Whether the Motion of Water Shall Be Direct or Sinuous, and of the Law of Resistance in Parallel Channels." Philosoph Trans Royal Soc London **174**: 935-982.
Riccabona, M., et al. (1996). "Three-dimensional ultrasound: accuracy of distance and volume measurements." Ultrasound Obstet Gynecol **7**(6): 429-434.
Riccabona, M., et al. (1995). "Distance and volume measurement using three-dimensional ultrasonography." J Ultrasound Med **14**(12): 881-886.
Rizzo, G., et al. (2008). "First trimester uterine Doppler and three-dimensional ultrasound placental volume calculation in predicting pre-eclampsia." Eur J Obstet Gynecol Reprod Biol **138**(2): 147-151.
Robertson, W. B., et al. (1986). "The placental bed biopsy: review from three European centers." Am J Obstet Gynecol **155**(2): 401-412.
Robson, S. C., et al. (2001). "Endovascular trophoblast invasion and spiral artery transformation: the "two-wave" theory revisited." Placenta **22**: A25.
Romero, R., et al. (2011). "Placental bed disorders in preterm labor, preterm PROM, spontaneous abortion and abruptio placentae." Best Pract Res Clin Obstet Gynaecol: Epub ahead of print.
Ross, G. R., et al. (2010). "Adrenomedullin relaxes rat uterine artery: mechanisms and influence of

pregnancy and estradiol." Endocrinology **151**(9): 4485-4493.
Rott, N. (1990). "Note on the history of the Reynolds number." Ann Rev Fluid Mech **22**: 1-11.
Rowan, J. A., et al. (2009). "Customised birthweight centiles are useful for identifying small-for-gestational-age babies in women with type 2 diabetes." Aust N Z J Obstet Gynaecol **49**(2): 180-184.
Rubens, D. J., et al. (2006). "Doppler artifacts and pitfalls." Radiol Clin North Am **44**(6): 805-835.
Rubin, J. M., et al. (1995). "Fractional moving blood volume: estimation with power Doppler US." Radiology **197**(1): 183-190.
Rubin, J. M., et al. (1994). "Power Doppler US: a potentially useful alternative to mean frequency-based color Doppler US." Radiology **190**(3): 853-856.
Rupnow, H. L., et al. (2001). "Endothelial vasodilator production by uterine and systemic arteries. VII. Estrogen and progesterone effects on eNOS." Am J Physiol **280**(4): H1699-1705.
Salafia, C. M., et al. (2010). "Placental surface shape, function, and effects of maternal and fetal vascular pathology." Placenta **31**(11): 958-962.
Sanderson, D. A., et al. (1994). "The individualised birthweight ratio: a new method of identifying intrauterine growth retardation." Br J Obstet Gynaecol **101**(4): 310-314.
Sankaran, S., et al. (2009). "Aetiology and pathogenesis of IUGR." Best Pract Res Clin Obstet Gynaecol **23**(6): 765-777.
Schaaps, J. P., et al. (2005). "Shunting the intervillous space: new concepts in human uteroplacental vascularization." Am J Obstet Gynecol **192**(1): 323-332.
Schemmer, G., et al. (1997). "First-trimester growth patterns of aneuploid fetuses." Prenat Diagn **17**(2): 155-159.
Schuchter, K., et al. (2001). "Uterine artery Doppler and placental volume in the first trimester in the prediction of pregnancy complications." Ultrasound Obstet Gynecol **18**(6): 590-592.
Schwartz, N., et al. (2010). "Novel 3-dimensional placental measurements in early pregnancy as predictors of adverse pregnancy outcomes." J Ultrasound Med **29**(8): 1203-1212.
Sebire, N. J., et al. (2001). "Is maternal underweight really a risk factor for adverse pregnancy outcome? A population-based study in London." Br J Obstet Gynaecol **108**(1): 61-66.
Severi, F. M., et al. (2002). "Uterine and fetal cerebral Doppler predict the outcome of third-trimester small-for-gestational age fetuses with normal umbilical artery Doppler." Ultrasound Obstet Gynecol **19**(3): 225-228.
Sheppard, B. L., et al. (1976). "The ultrastructure of the arterial supply of the human placenta in pregnancy complicated by fetal growth retardation." Br J Obstet Gynaecol **83**(12): 948-959.
Simpson, N. A., et al. (1997). "Determination of intervillous flow in early pregnancy." Placenta **18**(4): 287-293.

Sinclair, J. G. (1948). "Placental-fetal weight ratios." Texas Reports Bio Med **6**(2): 168-175.

Smith, G. C., et al. (2004). "First-trimester placentation and the risk of antepartum stillbirth." J Am Med Assoc **292**(18): 2249-2254.

Smith, G. C., et al. (2002). "Early-pregnancy origins of low birth weight." Nature **417**(6892): 916.

Sonin, A. A. (2004). "A generalization of the Pi-theorem and dimensional analysis." Proc Nat Acad Sci **101**(23): 8525-8526.

Soothill, P. W., et al. (1999). "Small for gestational age is not a diagnosis." Ultrasound Obstet Gynecol **13**(4): 225-228.

Spencer, K., et al. (2008). "ADAM12s in maternal serum as a potential marker of pre-eclampsia." Prenat Diagn **28**(3): 212-216.

Steer, C. V., et al. (1990). "Transvaginal colour flow imaging of the uterine arteries during the ovarian and menstrual cycles." Hum Reprod **5**(4): 391-395.

Stevenson, G. N. (2011). Towards functional imaging of the placenta. D. Phil., University of Oxford.

Stevenson, G. N., et al. (2010). "OP10.09: A novel semi-automated (SA) technique for 3D ultrasound measurement of placental volume." Ultrasound Obstet Gynecol **36**: 82.

Stratton, J. F., et al. (1995). "Are babies of normal birth weight who fail to reach their growth potential as diagnosed by ultrasound at increased risk?" Ultrasound Obstet Gynecol **5**(2): 114-118.

Thame, M., et al. (2001). "Second-trimester placental volume and infant size at birth." Obstet Gynecol **98**(2): 279-283.

Thilaganathan, B., et al. (2009). "Raised maternal serum cystatin C: an early pregnancy marker for preeclampsia." Reprod Sci **16**(8): 788-793.

Thompson, M. O., et al. (2002). "Are placental lakes of any clinical significance?" Placenta **23**(8-9): 685-690.

Tikkanen, M. (2010). "Etiology, clinical manifestations, and prediction of placental abruption." Acta Obstet Gynecol Scand **89**(6): 732-740.

Toal, M., et al. (2008). "Ultrasound detection of placental insufficiency in women with elevated second trimester serum alpha-fetoprotein or human chorionic gonadotropin." J Obstet Gynaecol Can **30**(3): 198-206.

Toal, M., et al. (2007). "Usefulness of a placental profile in high-risk pregnancies." Am J Obstet Gynecol **196**(4): 363 e361-367.

Valcamonico, A., et al. (1994). "Absent end-diastolic velocity in umbilical artery: risk of neonatal morbidity and brain damage." Am J Obstet Gynecol **170**(3): 796-801.

van Zalen-Sprock, M. M., et al. (1994). "First-trimester uteroplacental and fetal blood flow velocity waveforms in normally developing fetuses: a longitudinal study." Ultrasound Obstet Gynecol **4**(4): 284-288.

Vergani, P., et al. (2008). "Identifying the causes of stillbirth: a comparison of four

classification systems." Am J Obstet Gynecol **199**(3): 319 e311-314.
Viero, S., et al. (2004). "Prognostic value of placental ultrasound in pregnancies complicated by absent end-diastolic flow velocity in the umbilical arteries." Placenta **25**(8-9): 735-741.
Villar, J., et al. (2010). "Conceptual issues related to the construction of prescriptive standards for the evaluation of postnatal growth of preterm infants." Arch Dis Child **95**(12): 1034-1038.
Wadell, H. (1935). "Volume, shape and roundness of quartz particles." J Geology **43**: 250-280.
Welsh, A. (2004). "Quantification of power Doppler and the index 'fractional moving blood volume' (FMBV)." Ultrasound Obstet Gynecol **23**(4): 323-326.
Welsh, A. (2010). "The questionable value of VOCAL indices of perfusion." Ultrasound Obstet Gynecol **36**(1): 126-127; author reply 127-128.
Welsh, A. W., et al. (2005). "Standardization of power Doppler quantification of blood flow in the human fetus using the aorta and inferior vena cava." Ultrasound Obstet Gynecol **26**(1): 33-43.
Wolf, H., et al. (1989). "Second-trimester placental volume measurement by ultrasound: prediction of fetal outcome." Am J Obstet Gynecol **160**(1): 121-126.
Xiao, D., et al. (2009). "Direct chronic effect of steroid hormones in attenuating uterine arterial myogenic tone: role of protein kinase c/extracellular signal-regulated kinase 1/2." Hypertension **54**(2): 352-358.
Yampolsky, M., et al. (2009). "Centrality of the umbilical cord insertion in a human placenta influences the placental efficiency." Placenta **30**(12): 1058-1064.
Yu, C. H., et al. (2003). "Assessment of placental fractional moving blood volume using quantitative three-dimensional power doppler ultrasound." Ultrasound Med Biol **29**(1): 19-23.
Zeitlin, J., et al. (2000). "The relationship between intrauterine growth restriction and preterm delivery: an empirical approach using data from a European case-control study." Br J Obstet Gynaecol **107**(6): 750-758.
Zhang, J., et al. (1995). "Birth-weight-for-gestational-age patterns by race, sex, and parity in the United States population." Obstet Gynecol **86**(2): 200-208.
Zhang, J., et al. (2010). "Defining normal and abnormal fetal growth: promises and challenges." Am J Obstet Gynecol **202**(6): 522-528.

# 8 Appendices

## 8.1 Patient information leaflet provided

Oxford Fetal Medicine Unit

Oxford Radcliffe Hospitals NHS
NHS Trust

### *Patient information Leaflet*

**An investigation of potential new markers for impaired placentation in early pregnancy (REC Ref: 08/H0604/163)**

We would like to invite you to take part in a research study. Before you decide, you need to understand why the research is being done and what it will involve for you. Please take the time to read the following information. Talk to others about the study if you wish, perhaps your GP or midwife. Ask us if there is anything that is not clear, or if you would like more information.

**Why have I been invited?**
You have been invited because you are pregnant and living in the Oxford area. We intend to study between 150 and 200 women, the vast majority of who will be 'low risk' and have entirely normal pregnancies.

**What is the purpose of the study?**
Every baby is believed to have an inherent growth potential which under ideal conditions should produce a healthy baby the appropriate size. In a few pregnancies the placenta does not work as well as it should and as a result the baby may not grow as well as it should. This problem is called intrauterine growth restriction (IUGR). The consequences of IUGR include an increased risk of still-birth (the baby dying before it is born), problems occurring around the time of birth and the child developing cerebral palsy. Early recognition of babies developing IUGR, leading to appropriate monitoring and timely delivery may potentially improve the outcome for the baby.

With the advent of three dimensional (3-D) ultrasound scanning it has become possible to safely look at the placenta early in pregnancy. This should be able to give an indication of whether the placenta is functioning properly long before the baby starts showing signs that the placenta is not working well.

We want to assess the effectiveness of 3-D ultrasound in identifying those babies at risk of IUGR in early pregnancy. This will hopefully lead to development of a simple, non-invasive screening test which could be offered to all women to identify those babies at risk of IUGR. This will allow us to start monitoring these babies earlier and improve the outcome of that pregnancy. We also hope that it would prevent the medicalisation of other pregnancies which were always destined to have a normal outcome.

**Do I have to take part?**
It is up to you to decide whether or not to take part. Your decision will not affect the standard of care you receive. This information sheet describes the study. If you have further questions Dr Sally Collins or Mr Lawrence Impey will be happy to answer them for you. If you do decide to help us with the study, we will ask you to sign a consent form to show you have agreed to take part. You are free to withdraw from the study at any time, without giving a reason.

Oxford Fetal Medicine Unit

Oxford Radcliffe Hospitals NHS
NHS Trust

**What will happen to me if I take part?**
You will be offered an initial appointment about 12 weeks into the pregnancy. If you have decided to have the screening test for Down syndrome, the 'Nuchal' scan, we will do our best to see you the same day to avoid extra visits to the hospital. Don't worry if you have decided not to have that scan as you can still be included in our study.

At that first meeting we will ask you a few questions about your health and the pregnancy, explain the study in detail and answer any questions which you may have. If you chose to continue we will ask you to read and sign a consent form then we will proceed with the ultrasound scan which will look at your baby in the traditional two-dimensions and the placenta in three-dimensions. We will also generate a growth chart which is specific to your baby which we will use to monitor your baby's growth at future visits.

The next 4 visits will take place when you are around 14, 16, 18 and 23 weeks pregnant. These will involve 2-D ultrasound measurement of your baby's growth and 3-D ultrasound measurement of the placenta.

The last two visits will be at 28 and 33 weeks and will just involve 2-D ultrasound measurement of your baby's growth.

During no part of your pregnancy will any type of treatment or care be withheld from you because you are taking part in the study. You may find it helpful to look at the flow chart at the end of this leaflet which shows when we would do each scan. The whole study is expected to take three years to complete although your inclusion will be for the duration of your pregnancy. If you take part in the study you will be asked to make four to five additional visits to the hospital during your pregnancy.

**Is it safe and what are the possible disadvantages of taking part?**
We recognise that we are asking you to attend for more ultrasound scans than you would normally have during routine antenatal care. However, ultrasound has no known risks in pregnancy and all our scans will be performed after the most sensitive period of pregnancy is completed. Furthermore, all our 3-D and Doppler studies will be of the placenta, and maternal blood vessels and therefore will not involve your baby. Attending for the scans may be inconvenient, however every effort will be made to minimise this by being as flexible as possible to your timetable.

**What are the possible benefits of taking part?**
Participating in the study will enable you to see your baby more closely and more often than you normally would. Extra growth scans later on in pregnancy as well as identifying IUGR could potentially identify other problems such as breech presentation which, very occasionally, can be missed during routine care. In these circumstances, Dr Sally Collins or Mr Lawrence Impey will discuss the implications with you and appropriate management will be

Oxford Fetal Medicine Unit

Oxford Radcliffe Hospitals NHS
NHS Trust

initiated with your consent. Unfortunately we are unable to offer any expenses to you for taking part in this study but we hope that the extra scans may compensate you for the inconvenience of the extra visits.

**What if there is a problem?**
Compensation for harm arising from an accidental injury and occurring as a consequence of your participation in the study would be covered by the NHS.

If you wish to make a complaint about any aspect of the trial this should be directed to: Mr Lawrence Impey
The Fetal Medicine Unit
Level 6, The Women's Centre
John Radcliffe Hospital
Oxford, OX3 9DU
Tel: 01865 221710

**Will my taking part in the study be kept confidential?**
If you consent to take part in the research, some parts of your medical records and the results of the study will be looked at by members of the research team, authorised persons from the Oxford Radcliffe NHS trust. Regulatory authorities may also look at the results to check that the study is being carried out correctly. All will have a duty of confidentiality to you as a research participant and we will do our best to meet this duty. With your consent, we will inform your GP that you are taking part in the study. The results of your baby's growth scans will be placed in your hand-held notes

Any information about you which leaves the Fetal Medicine Unit would have your name and address removed so that you cannot be recognised from it. Data will be stored on a computer database in the Fetal Medicine Unit. You will be identified in our computers by a number and not by name and all information will be strictly confidential.

**What will happen if I don't want to carry on with the study?**
You may withdraw from the study at any time during your pregnancy. This will not affect the care you get in any way. Information collected before your withdrawal may still be used.

**What will happen to the results of the research study?**
We will tell you the results of your individual scans at the time they are done. Furthermore, results will be written up as manuscripts for submission to scientific journals. If you were interested, we could provide you with a copy of the article after publication. You are not going to be identifiable in any report or publication.

**Who is organising and funding the research?**
The research is being carried out by the Fetal Medicine Unit and the Nuffield Department of Obstetrics and Gynaecology, University of Oxford. The study is

Oxford Fetal Medicine Unit

Oxford Radcliffe Hospitals NHS
NHS Trust

sponsored by the Oxford Radcliffe Hospitals NHS trust and is funded by the Oxford Comprehensive Biomedical Research Centre (which is in turn funded by the National Institute for Health Research). The study will contribute towards the D.Phil thesis (University of Oxford) for Dr Sally Collins.

**Who has reviewed the study?**
Research is reviewed by an independent group of people called a Research Ethics Committee to protect your safety, rights, well being and dignity. This study has been reviewed and given favourable opinion by Oxfordshire Clinical Research Ethics Committee.

**What do I do if I want to take part in the study?**
Please call Dr Sally Collins on **01865 220129** to arrange an appointment at a time to suit. This appointment needs to take place when you are around 12 weeks pregnant. Alternatively, you can mention it to the ultrasound department staff when you come in for your scan and we will do our best to see you at the same time or organise an appointment for as soon as possible.

**Contact for further information**
If you have any further questions please do not hesitate to contact Mr Lawrence Impey or Dr Sally Collins at the address below:

The Fetal Medicine Unit
Level 6, The Women's Centre
John Radcliffe Hospital
Oxford
OX3 9DU

Phone: 01865 220129
E mail: sally.collins@obs-gyn.ox.ac.uk

Oxford Fetal Medicine Unit

Oxford Radcliffe Hospitals NHS
NHS Trust

**Recruitment visit at about 12 weeks pregnant**
- Chat about you and your pregnancy and what the study would involve
- Decide if you wish to participate
- Generate a customised growth chart for your baby
- 3-D Doppler scan of the placenta
- 2-D Doppler assessment of your uterine blood vessels
- 2-D ultrasound measurement of your baby's size

**Visit 2, 3 & 4 at about 14, 16 & 18 weeks pregnant**
- 3-D power Doppler scan of the placenta
- 2-D Doppler assessment of your uterine blood vessels
- 2-D ultrasound measurement of your baby's growth

**Visit 5 at about 23 weeks pregnant**
- 3-D power Doppler scan of the placenta
- 2-D Doppler assessment of your uterine blood vessels
- 2-D ultrasound measurement of your baby's growth

**Visit 6 at about 28 weeks pregnant**
- 2-D ultrasound measurement of baby's growth

**Visit 7 at about 34 weeks pregnant**
- 2-D ultrasound measurement of baby's growth

**After you have had your baby**
We will gather details of what happened when you had the baby, such as how much your baby weighed

## *8.2 Ultrasound machine settings used*

| ***"BRC Research" programme settings* - Main Menus** | | | | | |
|---|---|---|---|---|---|
| **Power Doppler** | Quality | *Norm* | 2D | SRI | *3* |
| | WMF | *Low 1* | | Angle | *60* |
| | PRF | *0.9KHz* | | Dyn Contr | *6* |
| | | | | Focal Zones | *1* |
| | | | | Harm freq | *High* |
| | | | | Gain | *5* |
| ***"BRC Research" programme settings* - Sub Menus** | | | | | |
| **Power Doppler** | PD Map | *5* | 2D | Gray map | 7 |
| | Frequency | *Low* | | Tint | Clear |
| | Flow Res | *Mid 2* | | Line Filter | Off |
| | L Filter | *2* | | Persist | 3 |
| | Artefact | *On* | | Enhance | 3 |
| | Smooth | *Rise 4* | | SRI | 3 |
| | Line Dens | *6* | | Line Density | Normal |
| | Smooth | *Fall5* | | Reject | 15 |
| | Ensemble | *15* | | | |
| | Balance | *150* | | | |

## *8.3 Segmentation Protocol*[25]

1. Load greyscale volume into an appropriate viewer, such as ITK-SNAP.

2. Select the acquired plane, not either of the reconstructed planes, and maximise.

3. Settings:

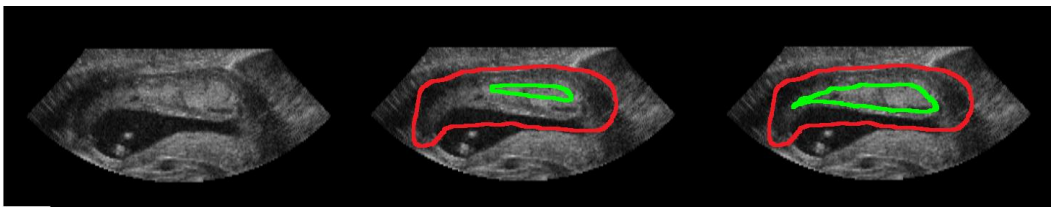
(a) Linear interpolation must be set to 'On'.

(b) Paintbrush should be set to 6-8 pixels in size, square and isotropic.

(c) Different colours should be used to represent background and placental tissue. Figure 50 (page 192) shows a typical colour scheme.

4. Scroll backwards and forwards through the individual 2D images until the user feels confident that they can identify the boundaries of the placenta.

5. Starting from one end of the placenta, seed the first 3 images. Then continue seeding every ten slices until reaching the other end. At this point, seed the last three slices of the placenta. To maximize accuracy, care must be taken to ensure that all the different textures of the placenta have been included in the seeding Figure 50 (page 192).



**i)** **ii)**

**Figure 50: Two different seedings of the same 2D image.**

*i) may result in a falsely small volume, as the cystic areas have not been identified as placental tissue.*

*ii) correct seeding including all the different greyscale textures.*

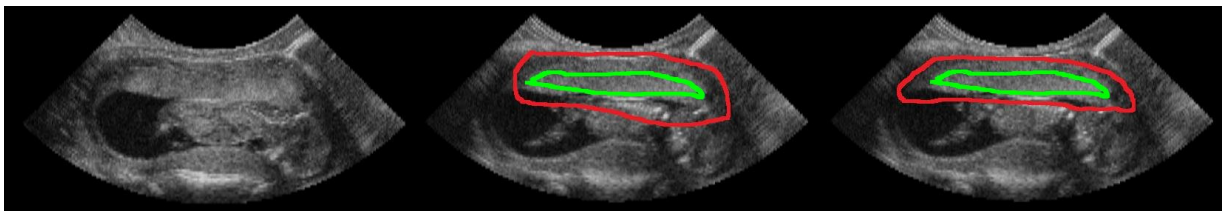
[25] Developed with Gordon Stevenson at the IBME, University of Oxford

6. Seeding of a slice should be done using the steps as outlined below.

**(a)** The lines defining the placenta and the background should be placed close to, but not over, the placental boundary. A closed loop is usually employed for both but where the placenta is very thin the placental label may have to be just a single line. The 'placenta defining' loop is indicating that everything within the loop is placental tissue and the algorithm will recognise it as such. The 'background defining' loop is indicating that everything outside the loop is not placental tissue.

**(b)** Where the placental tissue is hetrogeneous (e.g. cystic) all the different textures must be included within the 'placenta defining' loop. See Figure 50 (page 192).

**(c)** Care must also be taken when the fetus is in close proximity to the placental/amniotic fluid boundary, Figure 51, (page 193). In these situations the gap between the loops may be very small so that the user is nearly delineating the interface.



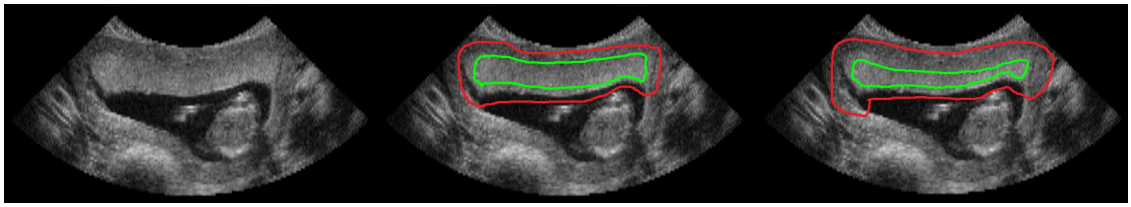
iii) iv)

**Figure 51: Seeding when the fetus is close to the placenta.**

*iii) may result in the fetus being identified as placenta.*

*iv) correct seeding ensuring the feto-placental boundary is demarcated.*

**(d)** In contrast, when the boundary is unclear, scrolling back and forth through the adjacent images should provide extra information as to the perceived location. The gap between the two loops should then be left large enough to allow the algorithm to define the most likely position of the boundary. See Figure 52 (page 194).



v) vi)

**Figure 52: Two different seedings of the same 2D image (poorly demarcated interface).**

*v) may have included some decidual tissue within the area marked as placenta.*

*vi) a sufficient gap has been left to allow the algorithm to define the most likely site of the boundary.*

7. Save the image.

## *8.4 Assessment of Normality*

**Table 19: Results of the normality analysis for the continuous variables explored to predict SGA**

| Variable | Kolmogorov-Smirnov | Histogram & Q-Q plot appear normal? |
|---|---|---|
| Maternal age | 0.2 | Yes |
| Maternal BMI | 0.002 | Skewed to the left |
| PAPP-A (MoMs) | <0.001 | Skewed to the left |
| NT (MoMs) | 0.08 | Yes |
| βhCG (MoMs) | <0.001 | Skewed to the left |
| 1st trimester Ut A PI | 0.2 | Yes |
| 2nd trimester Ut A PI | 0.001 | Skewed to the left |
| Booking mean arterial pressure (MAP) | 0.7 | Yes |
| Placental Volume (PlaV) | 0.02 | Skewed to the right |
| Placental Quotient (PQ) | <0.001 | Skewed to the left |
| Sphericity, **ψ** | 0.2 | Yes |
| Standardised placental volume (*s*PlaV) | 0.2 | Yes |
| Standardised functional area (*s*FA) | 0.008 | Skewed to the left |
| FAQ | 0.2 | Yes |